AN ABSTRACT OF THE THESIS OF

JOHN CHARLES HARLETT for the DOCTOR OF PHILOSOPHY
(Name) (Degree)

in OCEANOGRAPHY presented on 28 July 1972
(Major) (Date)

Title: SEDIMENT TRANSPORT ON THE NORTHERN OREGON CONTINENTAL SHELF

Abstract approved: Redacted for Privacy

The distribution of surface sediments on the northern Oregon continental shelf is characterized by a nearshore sandy facies and an outer shelf muddy facies, separated by a mid-shelf zone of mixed sand and mud. Currents which have been measured at 130 centimeters above the bottom indicate that the distribution of the surface sediment is a reflection of the hydraulic regime.

The strongest bottom currents which were measured were in the nearshore region at a depth of 36 meters. Here currents of over 40 cm/sec generated by surface waves are capable of placing the nearshore sands in suspension, where they are transported shoreward by the wave surge. At mid-shelf, in 90 meters of water, the bottom current veolcity ranges from zero to over 25 cm/sec, although the mean is normally about 10 cm/sec. The strongest currents at this depth are capable of eroding some of the fine sediments, but probably

do not rework the older sediments which have been compacted. Currents which are similar in character to those at mid-shelf were observed at the shelf edge in a depth of 165 meters. A significant departure, however, is the difference in frequency where the most energy is found. At the shelf edge the dominant frequency was about four cpd whereas the dominant frequency at mid-shelf was two cpd or lower. The dominant frequencies indicate that tides are important in the generation of continental shelf bottom currents. The twelve-hour period is that of the semi-diurnal tide; the six-hour period is the second harmonic of the semi-diurnal component. No indication of surface wave influence was found at mid-shelf or shelf -edge depths.

Profiles of turbidity made at four east-west transects of the continental shelf indicate suspended sediment transport occurs principally at three levels in the water column. An upper layer is at the level of the seasonal thermocline, a mid-water layer is located at the level of the permanent pycnocline, and the third layer is at the bottom. The surface layer is important in transporting suspended sediment of the Columbia River plume, although there is also a contribution to the surface layer from the surf zone by the process of diffusion of fine particles.

The mid-water layer thickens vertically and becomes less intense seaward, indicating a nearshore source for the suspended material. This source is diffusion of fine particles from the surf

zone at mid-water depths. The mid-water layer is located at the level of the permanent pycnocline. The layer is sub-parallel to the bottom over the shelf but becomes diffuse at the shelf edge. Sediment transport in the mid-water layer provides a mechanism by which sediment bypasses the outer shelf and upper slope area.

The bottom layer receives its suspended material from erosion of the bottom, from the water column above, and from fine material moving seaward from the surf zone. The amount of eroded material contributed to the bottom layer depends on the bottom current strength and on the bottom roughness characteristics. Over a rough bottom the erosive power of a given bottom current is increased drastically. For this reason, the presence or absence of rippling is important to sediment transport on the shelf. The fine material of the bottom layer may concentrate by settling during quiescent periods, allowing low-density flows to initiate.

Several time-series observations of turbidity indicate that the bottom layer thickens and thins in response to increases and decreases in current velocity. The mid-water layer migrated somewhat in a vertical direction, but its thickness and intensity remained nearly the same. The thickness and intensity of the upper layer responded to changes in the structure of the thermocline, becoming thick and dispersed when the upper part of the water column is mixed.

A model of sediment transport proposes that mid-water and bottom currents transport suspended sediments diagonally across the shelf toward the south-southwest. The sediments of the Columbia River plume are also transported in a southerly direction in the surface waters. Relatively little deposition takes place on the shelf and upper slope, with the bulk of the sediments bypassing the shelf and depositing on the lower slope and continental rise.

Sediment Transport on the Northern Oregon Continental Shelf

by

John Charles Harlett

A THESIS

submitted to

Oregon State University

in partial fulfillment of
the requirements for the
degree of

Doctor of Philosophy

June 1972

APPROVED:

Redacted for Privacy

Associate Professor of Oceanography
in charge of major

Redacted for Privacy

Chairman of Department of Oceanography

Redacted for Privacy

Dean of Graduate School

Date thesis is presented 28 July 1971

Typed by Susie Kozlik for John Charles Harlett

ACKNOWLEDGEMENTS

The successful completion of this study is, to a considerable measure, indicative of the assistance which a large number of persons have given freely. Without such assistance and cooperation, any study would be doomed from the beginning.

I am sincerely grateful to my major professor and advisor, Dr. Vern Kulm, for his initial guidance and continuing advice, and for his encouragement at times when successes were few.

I am indebted to the late Dr. George Beardsley who helped steer the research in a fruitful direction, and to Tom Sholes and Jack Groelle of the Optical Oceanography group, who assisted in the collection of optical data.

A special note of thanks is due two good friends, Rob Buehrig and Mark Halsey, for their unselfish assistance in all phases of the study. Rob was always available for advice or for muscle, and it is now my pleasure to acknowledge his contribution to the study. Mark was called upon, often at short notice, to assist in data collection. I thank him for his good natured assistance when the rewards were few.

Thanks are due to many others who in some way contributed to the study. The personnel of the R/V Cayuse and R/V Yaquina, the staff of the Department of Oceanography, my student compatriots, all give valued assistance. Ken Keeling and Mike Gimperle helped with

the automatic data processing; Gordon Ness was a valued hand at sea as well as being a valued friend. I thank Dr. Paul Komar for initially reading and reviewing the thesis.

Finally, I thank my wife Terry, who was left to hold the fort during many days and weeks when I was at sea, and who offered encouragement when it was needed. To my mother and father I express my unspoken thanks for their years of patience and trust.

The opportunity to undertake this graduate study was made possible by the United States Navy, under its Postgraduate Education Program; personal financial support was also provided by the Navy. The research pertaining to the study was made possible by grants from the Office of Sea Grant to Oregon State University (Contract NSF GH 97) and from Esso Production Research Company. Initial support for the research was provided by the Office of Naval Research (Contract NONR 1286 (10)).

TABLE OF CONTENTS

	Page
INTRODUCTION	1
Background	1
Statement of the Problem	4
INSTRUMENTATION	5
Current Meters	5
Mooring Techniques	9
Beam Transmissometer	12
DATA REDUCTION	15
Currents	15
Optical Data	20
RESULTS	21
Geologic Setting	21
Oceanographic Regime	27
Results of Current Measurements	28
Bottom-current Profile	28
Cruise Y 7002 C	35
Cruise C 7004 C	36
Cruise C 7006 B	39
Cruise C 7008 D	42
Cruise C 7012 D	45
Cruise Y 7102 F	48
Cruise C 7103 F	48
Cruise Y 7104 C	49
Cruise Y 7105 A	57
Results of Optical Measurements	64
Cruise Y 7102 A	64
Cruise Y 7104 C	72
Cruise Y 7105 A	77
DISCUSSION OF DATA	82
Currents	82
Optical Observations	87
The Surface Layer	87
The Mid-water Layer	90
The Bottom Layer	94
Sediment Erosion and Transport	98

		Page
CONCLUSIONS		106
BIBLIOGRAPHY		111
APPENDIX I.	Station locations and weather conditions	117

LIST OF FIGURES

Figure		Page
1	Sample current meter record	8
2	Photograph of moored current meter	10
3	Diagram showing technique for mooring current meter	12
4	Location of stations	23
5	Distribution of surface sediments	25
6	(a) Distribution of phi median diameter values in surface sediments	26
	(b) Distribution of phi deviation values in surface sediment	26
7	Observed current profiles	30
8	(a) Selected current profile	31
	(b) Theoretical current profile in near-bottom region	31
9	Cruise Y 7002 C. Current direction record and frequency of direction	37
10	Cruise C 7004 C. Progressive vector diagram	38
11	Cruise C 7006 B, 100 meters. Current direction record	40
12	Cruise C 7006 B, 175 meters. Current direction record and frequency of direction	41
13	Cruise C 7008 D. Current speed and direction record	43
14	(a) Cruise C 7008 D. Frequency power spectrum	44
	(b) Smoothed record of speed and direction	44
15	Cruise C 7008 D. Progressive vector diagram	46

Figure		Page
16	(a) Cruise C 7012 D. Frequency power spectrum (b) Record of current speed	47
17	Cruise C 7103 F. Current speed record	50
18	(a) Cruise C 7103 F. Frequency power spectrum (b) Smoothed record of speed	51
19	Cruise Y 7104 C, 90 meters. Current speed record	53
20	(a) Cruise Y 7104 C, 90 meters. Frequency power spectrum (b) Smoothed record of current speed	54
21	Cruise Y 7104 C, 165 meters. Current speed and direction record	55
22	(a) Cruise Y 7104 C, 165 meters. Frequency power spectrum (b) Smoothed record of current speed and direction	56
23	Cruise Y 7104 C, 165 meters. Progressive vector diagram	58
24	Cruise Y 7105 A, 90 meters. Current speed and direction record	59
25	(a) Cruise Y 7105 A, 90 meters. Frequency power spectrum (b) Smoothed record of current direction and speed	61
26	Cruise Y 7105 A, 90 meters. Progressive vector diagram	62
27	Cruise Y 7105 A, 165 meters. Current speed and direction record	63
28	(a) Cruise Y 7105 A, 165 meters. Frequency power spectrum (b) Smoothed record of current speed and direction	65
29	Cruise Y 7105 A, 165 meters. Progressive vector diagram	66

Figure		Page
30	Cruise Y 7102 A. Turbidity profiles and bottom currents along latitude 45° 11'N	68
31	Cruise Y 7102 A. Scattering values along latitude 45° 11'N	70
32	Cruise Y 7102 A, 165 meters. Time series of turbidity profiles and bottom currents	71
33	Cruise Y 7102 A, 100 meters. Time series of turbidity profiles and bottom currents	73
34	Cruise Y 7102 A. Turbidity profiles and bottom currents along latitude 44° 11'N	74
35	Cruise Y 7102 A, 165 meters. Scattering values at time-series station	75
36	Cruise Y 7104 C. Turbidity profiles near shelf edge	76
37	Cruise Y 7105 A, May 5. Turbidity profiles along latitude 45° 59'N	78
38	Cruise Y 7105 A, May 7. Turbidity profiles along latitude 45° 59'N	79
39	Cruise Y 7105 A. Time series of turbidity profiles and temperature-depth profiles	81
40	Cruise Y 7104 C. Temperature-depth profiles near shelf edge	89
41	Cruise Y 7105 A. Temperature-depth profiles at selected stations	105
42	Sediment transport model for the northern Oregon continental shelf	107

SEDIMENT TRANSPORT ON THE NORTHERN OREGON CONTINENTAL SHELF

INTRODUCTION

Background

Early studies of continental shelves concentrated on the nature and distribution of sediments. Perhaps because proper instrumentation was not available with which to make observations, only passing attention was paid to the processes of shelf sedimentation. Emery (1952) introduced the term "relict" to describe those sediments which remain from an earlier environment, distinguishing the relict sediments from modern detrital sediments supplied from mainland sources, and residual sediments from in situ weathering. Curray (1960), in his work on the continental shelf of the northwest Gulf of Mexico, considered the importance to shelf sedimentation of alternating transgressions and regressions of the sea. He recognized that fine sediments carried in suspension from the coastal rivers are deposited independently of the sands which remain in the nearshore zone and are redistributed by wave action. Thus, as the sea rose during the retreat of the glaciers, the nearshore sand body migrated inland, forming a blanket of sand across the shelf. Suspended fines were deposited at some distance from the shore to form a mid-shelf mud facies. Anomalous sands at the outer edge of the shelf in some areas (e.g. off

Freeport, Texas) were explained as resulting from variations in the pattern of the shelf current system which was distributing the muds (Curray, 1964).

More recently, attention has been directed toward the hydraulic regime responsible for the sedimentation on the continental shelf. Draper (1967) calculated that in the high-energy environment of the Celtic Sea, west of Ireland, oscillatory speeds of over 43 cm/sec at 152 meters depth result from wave conditions which may be expected once per year. These velocities appeared to be exceptional and such energy is not considered to be generally available, especially on low-energy coastlines. As isolated observations of near-bottom currents became available, it began to appear that sedimentation on continental shelves is a complex process affected by the tides, weather and sea conditions, and other physical factors, not simply by the surface wave conditions.

When Ewing and Thorndyke (1965) brought attention to the "nephaloid layer" in the deep ocean, interest was stimulated regarding the importance of suspended sediments in sedimentation in the ocean. Heezen et al. (1966) postulated that the continental rise of the eastern United States was formed from deposition of sediments transported by geostrophic contour currents. Lyall et al. (1971) attributed turbid layers at the shelf edge to resuspension by internal waves. Costin (1970) made visual observations from a submersible of turbid layers

and near-bottom currents on the continental slope at three sites in the Caribbean Sea. His observations indicated that turbid layers represented eroded sediments which had been concentrated in stable layers in the water column. Pak (1969) noted a similar stratification in the Columbia River plume over the continental shelf of Oregon, though at shallower depths. McManus and Smyth (1970) observed that turbid bottom water on the continental shelf of the Bering Sea appeared to be an important mechanism for transporting silts from coastal rivers. Wolf (1970), in a study of sediment transport in Monterey Bay, recognized the variability of bottom currents and the importance of change in current regime to sediment transport patterns. However, until this present study no comprehensive investigation of sediment transport on the continental shelf, including both suspended and bottom transport, had been conducted.

The continental margin off Oregon has been the subject of many investigations which afford a background upon which a study of sediment transport can be founded. Through the work of Maloney (1965), Runge (1966), and Chambers (1968), the surface sediment distribution on the shelf and upper slope is known in detail, samples having been obtained on a three-mile grid. Spigai (1970) has provided rates of sedimentation on the southern Oregon continental margin. In addition, observations of currents, hydrographic conditions, and biological factors spanning nearly ten years are available from various studies

conducted by personnel at Oregon State University.

Statement of the Problem

The intent of this research is to determine how sediments are transported on and across the northern continental shelf of Oregon. This information, suitably generalized, can be used to provide a model for general shelf sediment transport. Questions which must be answered are:

1. How are suspended sediments transported from their coastal source regions across the continental shelf?
2. How are bottom sediments affected by bottom currents?
3. Which physical factors and processes are important to sediment transport on the shelf?

In an attempt to answer these basic questions, a study of ocean-bottom currents has been conducted in conjunction with measurements of turbidity in the water column. The results of the study have revealed some previously unreported features of sediment transport which may serve to help answer some of the questions above concerning shelf sedimentation processes.

INSTRUMENTATION

Current Meters

An important side benefit from this study has been the development and successful use of a system specifically designed for use in monitoring bottom currents on the continental margin. The current meters which were used in the study have been modified from that described by Korgen (1969). Basically, the instrument utilizes an optical pickup system which monitors movement of a Savonious rotor. The dynamic characteristics of the Savonious rotor have been listed by Gaul et al. (1963). The response time of this type of rotor is about one-half minute, which is considered adequate for this type of study.

Although the response time of the rotor is longer than the period of surface waves, the effects of swell should still appear. Surface waves traveling in the same direction commonly interfere with each other in such a manner that the waves travel in groups. The groups result as the waves alternately reinforce when they are in phase and cancel when they are out of phase. As a train of waves passes a certain point, the reinforced waves appear as a series of high waves separated by intervals of low waves. The groups of large waves are generally of the order of a minute apart. The larger waves will result in a greater disturbance at the bottom, generating stronger orbital bottom currents. Resolution of currents with a period of about a minute

is well within the capabilities of the Savonious rotor.

The threshold veleocity of this system is lower than that of commercial current meters, and has been determined by Korgen (1969) to be 0.47 cm/sec.

A chopper plate with two slots in the periphery is mounted on the base of the Savonious rotor. As the rotor turns, the plate chops a beam of light which is directed at a light-sensing diode. When a slot in the chopper plate passes the light source, light falls on the diode, whose resistance is then sharply reduced, triggering an amplifier in the current recorder. The amplifier drives an event marker on a miniature strip-chart recorder. An event is recorded each time a slot in the chopper plate passes the light beam, in practice, twice per revolution. Thus, the raw data are presented as revolutions of the rotor per unit time. This recording system, because it actually monitors the movement of the rotor, has the advantage of not smoothing the record, an important feature during periods of near-threshold currents when an analog record might mask short-term fluctuations in speed.

A modification to the system described by Korgen (1969) has been the addition of a direction-sensing unit. This unit utilizes a V-shaped plastic vane which is magnetically coupled to a continuous-rotation potentiometer. The potentiometer is part of a voltage-divider network housed in the main pressure case. The relative position of the vane with respect to the current meter body is recorded on an analog section

of the same trip-chart recorder on which the current-speed event marks are recorded (Figure 1). In order to convert the relative direction of the vane to absolute orientation, the relative value is referred to a north reference which is provided by an externally-mounted combination magnetic compass and inclinometer. This device operates in such a way that the compass is free to move until tension on a trigger lanyard is released, at which time the compass is locked in position. A small corrodable link is used to release the lanyard after several hours on the bottom. Because of the method of anchoring the instrument, its orientation on the bottom does not change and the simple "one-shot" compass can be used to determine the absolute orientation for the entire record.

The strip-chart recorder is normally operated at a nominal speed of 12 inches (30.5 cm) per hour. This speed was selected to achieve the maximum duration (63 hours) of continuous record while allowing individual event marks to be resolved. The practical upper limit of current speed which can be measured at the 12 in/hr chart speed is about 30 cm/sec. Above this speed, event marks tend to merge and become indistinguishable. At locations where currents in excess of 30 cm/sec are expected, such as in nearshort regions, the recorder speed can be increased by changing the gear train, but this also shortens the duration of record.

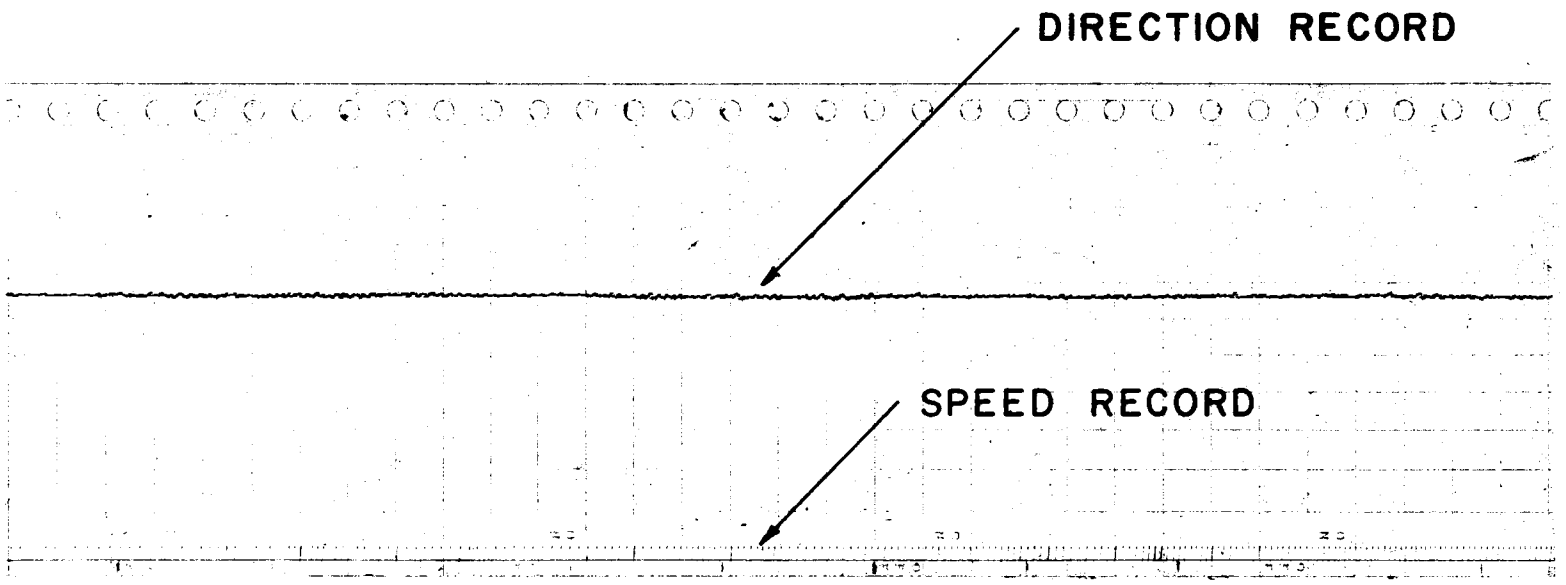

Figure 1. Sample current meter record.

The current meters are equipped with an electronic on-off timer which allows different sampling programs to be used, thereby extending the record duration. A minimum of ten minutes per hour of "on" time is considered necessary to obtain a representative record of currents, especially during periods of low speeds.

The recorder, electronics, and batteries are mounted in a frame which is placed in a cylindrical aluminum pressure case. The pressure case is mounted in an aluminum frame at the end of which are mounted the speed and direction sensors (Figure 2). During initial observations the meter was deployed with the current meter oriented such that the sensor end was at the bottom. However, in this position damage to the vulnerable sensors resulted. Because adequate protection could not be provided for the sensors without additional interference in the flow path resulting, the meters were inverted. This placed the midpoint of the Savonious rotor approximately 130 cm from the bottom, about a meter higher than before.

Mooring Techniques

Several prototype current meters were fitted with timed-release mechanisms which were designed to release the ballast weight which anchored the meter at the bottom. A cluster of glass floats supplied positive buoyancy to return the package to the surface. While this system has obvious advantages, it was decided to defer the development

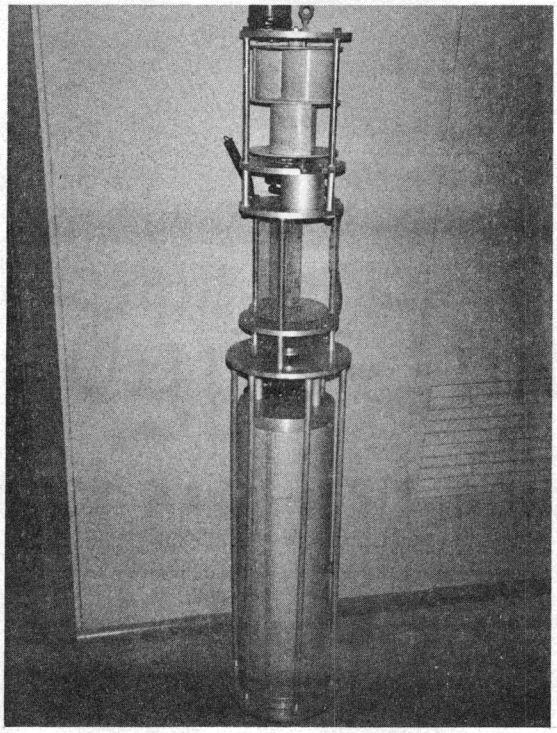

Figure 2. Photograph of moored current meter.

of the free-vehicle system and concentrate on moored systems.

In the moored system (Figure 3), a 70-kilogram anchor is attached at two points to the base of the current meter. By attaching the anchor at two points, the meter is constrained from rotating about the long axis, although it is free to adjust to minor undulations in the ocean floor. A large glass float is tethered to the sensor end of the meter with a 2.5-meter length of 4.8-mm stranded wire. This float, which provides about 22.7 kilograms of positive buoyancy, holds the meter upright. A swivel at the point of attachment prevents transmission of torsional movements from the float to the meter. To place the instrument on the bottom, a length of 4.8-mm hydrographic wire is attached at one of the anchoring points at the base of the meter. The meter is lifted over the side of the ship and lowered to the bottom on this wire. Once the meter is on the bottom, a predetermined length of the wire is payed out while the ship drifts. After this part of wire (whose length is at least twice the water depth) has been laid out, a secondary anchor is attached to the wire and lowered to the bottom. An additional length of wire is then payed out, equal to at least three times the depth, and a large surface marker float is attached. For recovery, the process is simply reversed. The wire used in the operation is payed out and recovered on a small gasoline-powered winch, which provides portability.

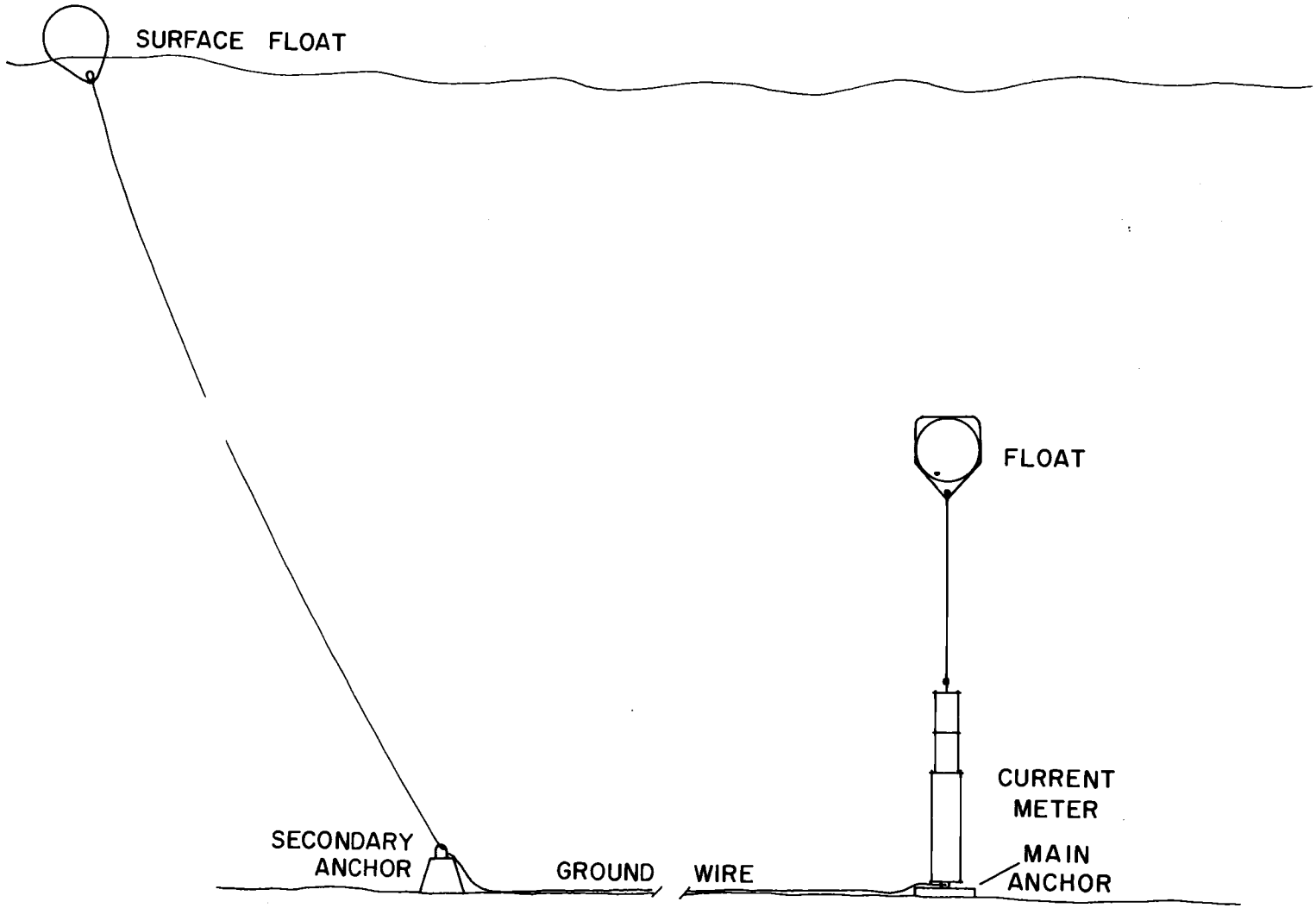

Figure 3. Diagram showing technique for mooring current meter. Depth not to scale.

The advantage of using this mooring system rather than relying on a timed release of ballast is that probability of recovery is much higher than with a free-vehicle meter. Even if the surface marker float is lost, the capability exists for recovery by dragging. The system is depth-limited, however, because of the amount of wire needed for mooring. Even so, this method has been used in depths as great as 1000 meters (Robinson, 1970, personal communication).

Beam Transmissometer

In order to record profiles of turbidity in the water column above the continental shelf, an *in situ* beam transmissometer was employed. Transmittance, simply stated, is a measure of how much transmitted light is received by the sensor. It depends not only on the amount of light which is not absorbed, but also on the light which is scattered in a forward direction by suspended particles. In order to effectively measure only the amount of light which is not absorbed, a narrow collimated beam is used to minimize the amount of forward scattering. In this study we shall actually be more interested in nontransmittance, or turbidity.

The instrument used in this study was designed and constructed by the Optical Oceanography group at Oregon State University. The light source consists of a microscope lamp bulb powered by a regulated power supply. This lamp was chosen because of its stable

characteristics throughout its life. The light is collimated through a system of lenses into a beam about 1.5 cm in diameter. A photomultiplier sensor one meter away senses the incident light from the beam. Use of stabilized power supplies and precision components minimizes drift due to fluctuations in temperature.

The photomultiplier output is amplified and transmitted to the ship via a conducting cable. The output is recorded on a strip-chart recorder or an X-Y plotter.

Turbidity-depth profiles were recorded by lowering the instrument through the water column at a rate of about 30 meters/minute. The instrument was constructed with a rugged frame and consequently can be used to measure turbidity until in contact with the bottom. A green filter was used during most of the measurements to compensate for the coastal water color.

The values obtained from the transmissometer are only relative values and do not represent percent transmittance. The transmissometer has not been calibrated in terms of absolute values of light transmission. Calibration of the transmissometer in terms of sediment concentration is not possible because varying size distributions of suspended sediment affect the transmission of light in different ways, even though the absolute concentrations of the suspensions are the same. However, the output of the photomultiplier sensor is linear, so comparisons of the turbidity at different levels in the same

cast may be made. In the profiles observed in April and May of 1971, a lucite block was used to calibrate the instrument on deck just prior to lowering. Using this reference point, station-to-station comparisons of turbidity values may be made. Unfortunately, the calibration block was not utilized in the earlier cruises so comparisons between data obtained in February and data obtained in April and May cannot be made, nor can station-to-station absolute comparisons of turbidity be made for the February observations.

DATA REDUCTION

Currents

The first step in processing raw current records, an example of which is presented in Figure 1, is to determine the absolute time scale. Because the chart drive motor slows as the battery energy is consumed, the chart advance speed is not constant. However, the discharge curve of the Eveready 520 battery used as the power supply is essentially linear in the voltage range from six to five volts, where the instrument is operated (Union Carbide, 1968). Therefore, the chart speed can also be assumed to be linearly decreasing. The start and stop times of the recorder were marked on the record in order to provide an absolute time reference. The length of the record in inches (L) was determined and the mean chart speed (S_m) was calculated by dividing by the record duration in hours (D). The chart speed with fresh batteries is known, and normally was 12 in/hr (30.5 cm/hr). With this information the chart speed at the end of the record (S_e) was calculated:

$$\frac{12 + S_e}{2} = S_m \qquad (1)$$

$$S_e = 2\,S_m - 12$$

With the beginning and ending chart speeds known, the decrease in chart speed per hour was calculated:

$$\frac{12 - S_e}{D} = \text{rate of decrease (in/hr)} \quad (3)$$

where D is the duration of the record in hours. The record was then divided into one-minute segments. To facilitate marking the records, the speed for each hour was considered constant with the decrease in speed occurring at the end of the hour. Thus, the record as marked shows a step-like approximation to the linear decrease in speed. The rate of decrease is normally of the order 0.07 in/hour. When divided into 60 parts the difference is nearly imperceptible.

This method of calculating chart speeds has proven to be quite accurate. In certain of the observations, an electronic on-off timer was used to vary the sampling program. A typical program might be to sample continuously for 40 minutes, turn the instrument off for 20 minutes, on for 40 minutes, and so on. The times when the instrument switches on are easily recognized as discontinuities in the record. These discontinuities can be treated as time marks and therefore, provide an accurate time base. This time base compares favorably with that calculated by the method outlined above.

With the record marked in one-minute intervals, the next step in data reduction is to count the number of event marks in each one-minute segment. This laborious task is accomplished by viewing the record through a binocular microscope, which is necessary to distinguish the event marks. Resolution of the record using this method is

drastically increased over that using the unaided eye.

Converting events per minute into revolutions per minute is accomplished by simply dividing by two, the number of slots in the chopper plate. Finally, conversion from revolutions per minute to cm/sec is made through calibration curves.

Korgen (1969) calibrated meters of this type at the Instrument Rating Flume of the North Pacific Division, U. S. Army Crops of Engineers, Bonneville, Oregon. He estimated calibration error at $\pm$ 2%. In addition, chart speed was found to vary approximately $\pm$ 1.5%. Finally, the accumulated error from reducing the data is estimated at 2.5% for speeds in excess of 15 cm/sec; below 15 cm/sec, the error is insignificant. This is because for speeds above 15 cm/sec (at 12 in/hr chart speed) the event marks tend to merge and become more difficult to resolve.

The reduced current-meter record represents a sequence of one-minute averages of the raw record. This method of reducing the raw data is satisfactory for the purposes of this study, as no attempt to measure turbulence or very short-term fluctuations in speed was made. Furthermore, the response time of the instrument is about 30 seconds so an attempt to measure instantaneous velocities would be meaningless. Finally, the shortest-term variations in speed which were measured were of the order of several minutes long. Thus, treating

the averaged values of speed as though they are instantaneous values introduces no significant error.

Current direction is recorded as an analog record on the same strip chart, and thus the same time base, as the event marks. In order to convert the relative direction to true direction, the scale value corresponding to north must be determined. This is accomplished after the instrument is recovered by orienting the direction vane parallel to the north-south line of the compass. The deflection of the galvanometer of the recorder then corresponds to a current direction from magnetic north. Full scale deflection (100 microamps) corresponds to 360°. The potentiometer in the direction-measuring circuit is linear; that is, a one degree change of direction always equals 1/360th of full scale on the chart. Therefore, the scale is easily converted to true azimuth directions by offsetting the north mark of the scale 21° counterclockwise from the north reference correcting for the magnetic declination in this area.

Because of the voltage drop of the power supply, 360° corresponds to full-scale deflection only at the start of observations. At the end of the record, after battery voltage has fallen to perhaps 85% of its original value, 85% of full scale deflection then corresponds to 360°. This decrease is again assumed to be linear throughout the record and is handled in a manner similar to that used to correct for the decreasing chart rate. In this case a transparent overlay is

marked in ten-degree increments, with 360° corresponding to full scale. For the first hour of record the scale is perpendicular to the direction of chart travel. At the start of the second hour and for each succeeding hour, the position of the overlay is adjusted at an angle less than 90° to the direction of chart travel so that the 360° mark corresponds to the maximum deflection of the galvanometer at that time. For instance, if after 24 hours the battery voltage had dropped to 5.6 volts, 93% of the starting voltage, the 360° mark would be placed in the 93 microamp line. The zero mark remains at the zero-deflection line. As the overlay is repositioned for each hour, it adjusts the entire scale an amount proportional to the decrease in scale length.

Current direction values to the nearest five degrees were read every ten minutes. This was considered sufficiently frequent for the computation of transport values and for detection of tidal and inertial effects.

Current-speed data were digitized for each minute of record. These data were then placed on punch cards for processing by computer. Program SPECT 1, a conversational program to estimate, output, and plot power spectra, was used to determine dominant frequencies. This program is stored in compiled form at the Computer Center of Oregon State University under the name *SPECT 1C and may be used from any teletype terminal.

In addition to the estimates of power spectra, the current direction and speed records were plotted by hand in analog form and also as progressive-vector diagrams. In certain records where direction only was recorded, histograms of direction have been constructed.

Optical Data

Transmissometer records are presented in their raw form, except that the vertical scales have been adjusted for the sake of comparison.

During cruise Y7102F, water samples were obtained at selected depths at four stations. The intensity of light scattered by these samples was measured using a Brice-Phoenix light scattering photometer. The characteristics and operating procedures for this device are given by Pak (1969). Scattering was measured at angles of 45°, 90°, and 135° from the incident light beam. The raw data were processed using program SCAT 4, also listed by Pak (1969).

RESULTS

Geologic Setting

The continental shelf from Newport, Oregon to the Columbia River ranges in width from 59 kilometers at latitude 46° 00'N. to 24 kilometers at latitude 45° 11'N. The Columbia River at the northern end of the study area (Figure 4) contributes vast quantities of suspended sediment to the waters over the northern shelf (Pak, 1969). South of the Columbia River, the coast is relatively straight, affording no barriers to large-scale offshore circulation. Coastal geomorphology varies from rugged volcanic headlands to extensive beaches and sand dunes. Byrne (1963) estimated that coastal erosion occurs along 67% of the Oregon coast from the Columbia River south to Heceta Bank, and that land-sliding is the principle means of erosion for 54 miles of the coast. Byrne calculated rates of coastal erosion of 0.5 meters per year for Miocene sedimentary rocks and 13.5 meters per year for unlithified Quaternary sediments. Runge (1966) has calculated that the yearly contribution to shelf sediments from coastal erosion of sea cliffs is 598,000 cubic meters. Estimates by Hixson (1960) indicate that the Columbia River contributes over 14 times that amount annually. Estuaries trap most coarse material from coastal streams and from the Columbia River, though fine sediments reach the shelf waters.

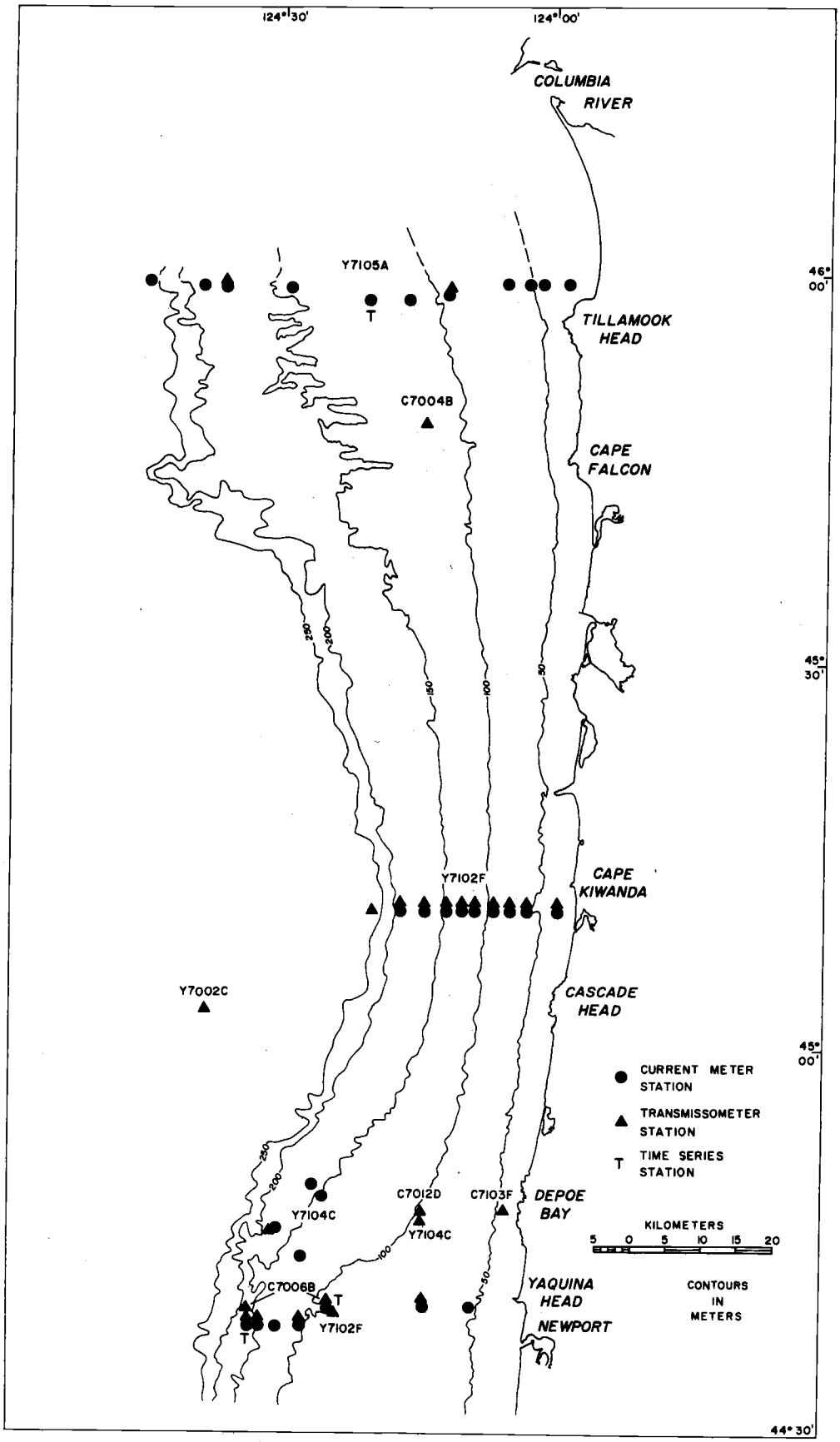

Figure 4. Location of stations.

The distribution of surface sediments on the northern Oregon shelf is shown in Figure 5, prepared from data obtained from Runge (1966). Runge's samples were taken on a three-mile grid using a Dietz-LaFond grab, which has the effect of homogenizing the sample. Nevertheless, Figure 5 presents a sufficiently detailed picture of the top ten centimeters of sediments and is certainly representative of the true distribution of surface sediments.

The average median diameter of sediments on the inner shelf (Figure 6a) increases slightly toward the south, and sorting (Figure 6b) improves in the same direction. The width of the inner sand body, defined as sediment whose median diameter is greater than 3ϕ, is at a minimum at the mouth of the Columbia River, undoubtedly reflecting the large supply of smaller suspended sediments. Elsewhere, the boundary between the inner-shelf sand and the mid-shelf mixed facies (M_d = 3ϕ to 4ϕ) roughly parallels the coastline. Because the shelf itself narrows considerably toward the south, the effect is that sands extend proportionally relatively further across the narrow shelf than on the wide shelf. The average depth of their seaward limit is remarkably constant. Mid-shelf and outer-shelf facies, however, follow the trend of the shelf edge and are narrow where the shelf is narrow and wide where the shelf is wide. A large patch of fine sediment, shaped like an inverted teardrop, represents the only sizeable body of fine sediment on the continental shelf in the study area. Small

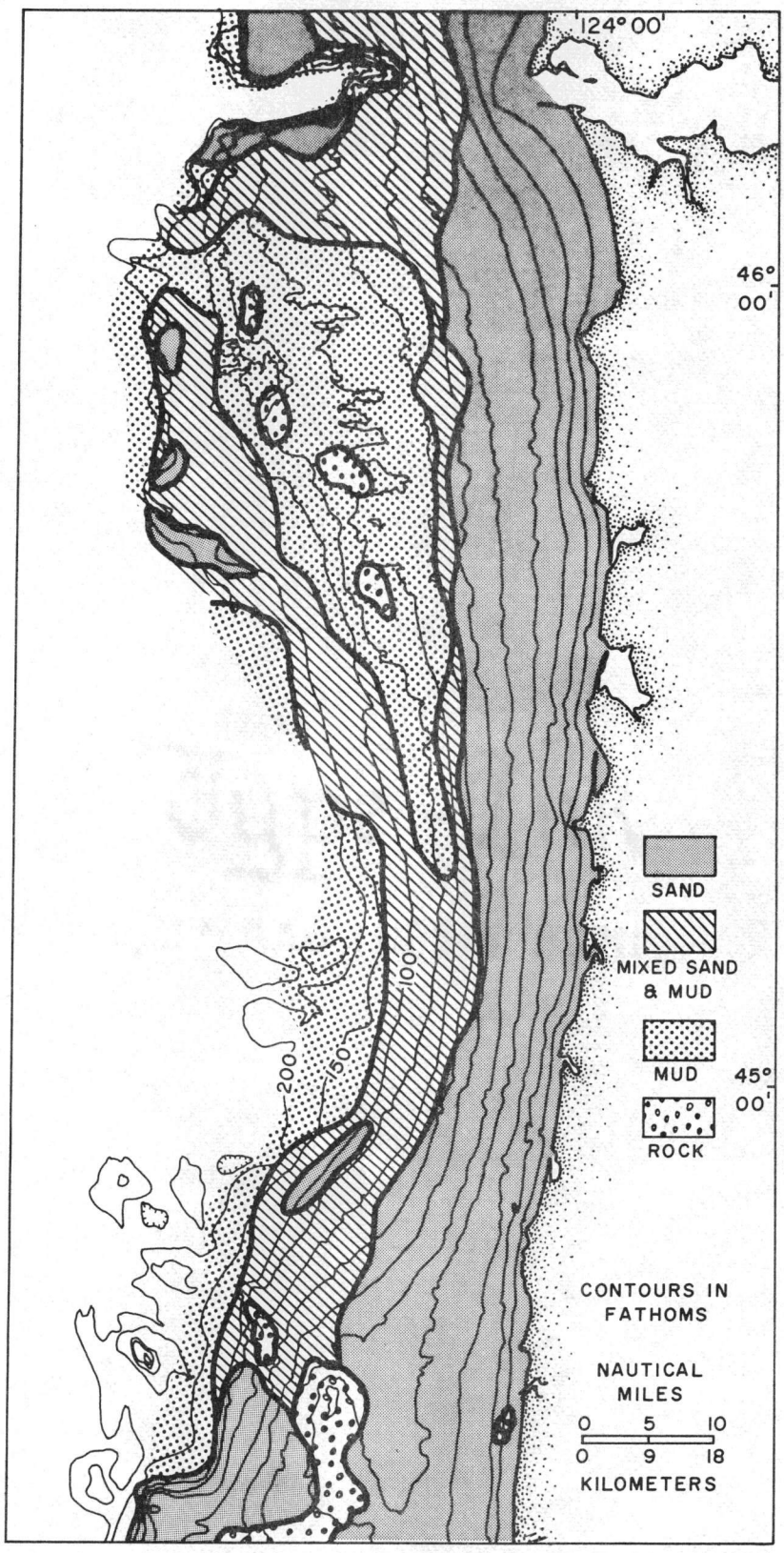

Figure 5. Distribution of surface sediments on the northern Oregon continental margin.

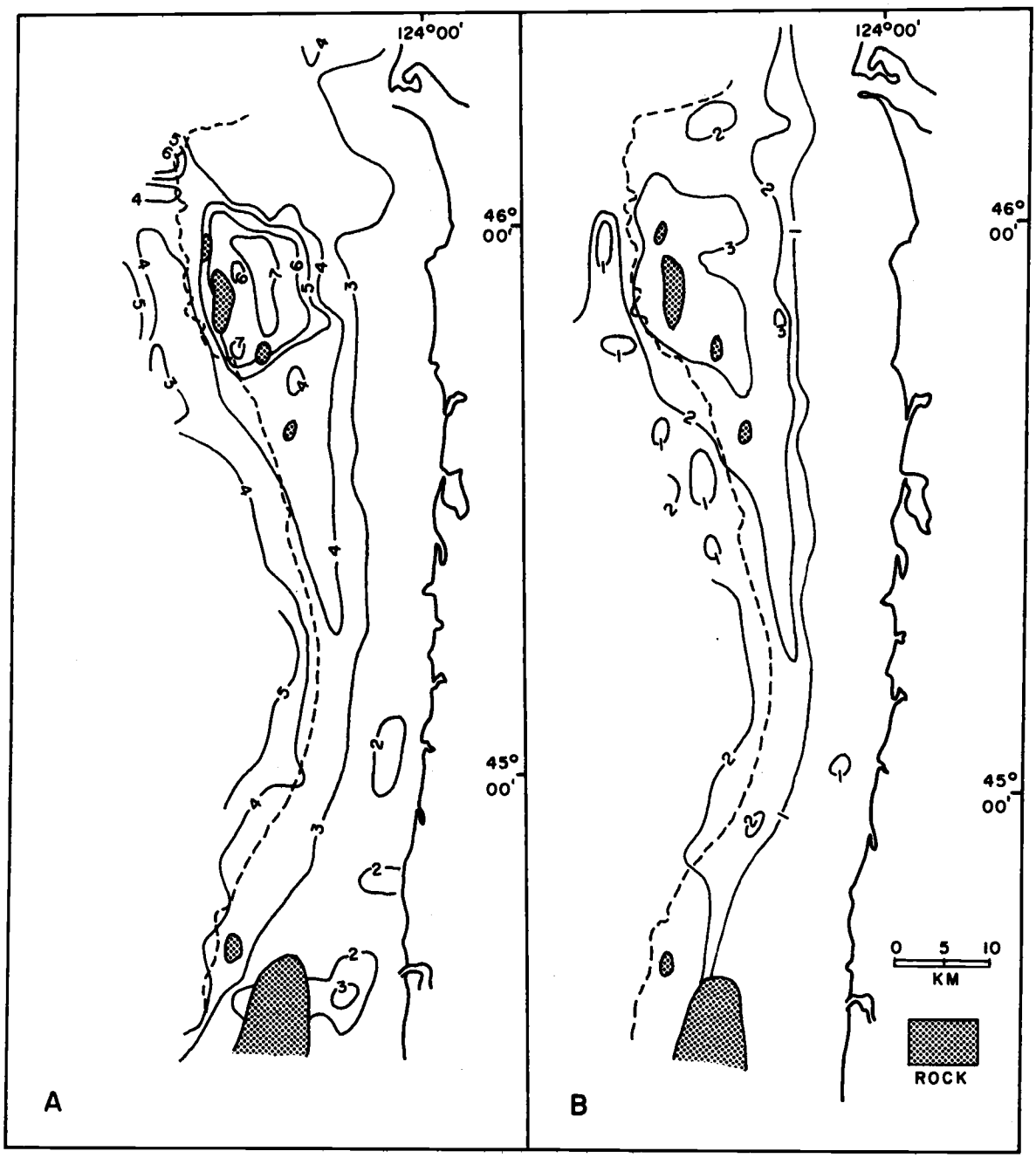

Figure 6. (a) Distribution of phi median diameter values in surface sediments. Less than two phi not contoured.
(b) Distribution of phi deviation (sorting) values in surface sediments. From Runge (1966).

isolated areas of relatively coarse sediments are found in several places at the shelf edge.

Oceanographic Regime

The North Pacific Ocean off the Oregon coast is a region of generally weak southward flowing surface currents. Maughan (1963) noted that inshore surface currents on the central coast are northerly during the winter season (November to March) and southerly during the rest of the year. Burt and Wyatt (1964) noted a similar change in the surface current direction in response to changes in the local wind stress.

During the winter months the winds are normally southerly or southwesterly. It is during this season that the most intense storms develop. The sea is generated in response to the prevailing local wind, but the long period swell which arrives at the coast may be generated in response to circulation around an intense low pressure system in the Gulf of Alaska. Several times during the course of the study, stationary or slowly moving lows in the Gulf of Alaska were oriented such that large waves, generated in the southwest sector of the storm by winds in excess of 40 knots over an unusually long fetch, reached the Oregon coast as long-period, high swells.

In the summer months, winds are most often from the north and northwest. Sea conditions are characteristically much improved over

those during the winter. The northerly winds transport surface water away from the coast causing subsurface water to upwell in the coastal region. The upwelled water provides nutrients to the organisms in the coastal region, resulting in plankton blooms. Beyond this effect, upwelling causes persistant horizontal variations in the physical properties of the ocean which affect physical processes in a complex manner (Smith, 1968).

Results of Current Measurements

Bottom currents were measured intermittently on the northern Oregon continental shelf over a period of 15 months, although the most successful observations were made during the final six months of observations. With the exception of the bottom-current profile measurements, current records will be dealt with chronologically.

Bottom-current Profile

In order to make comparisons between currents which were measured at different distances above the bottom, the bottom-current profile had to be established for extrapolation. A special current meter was built to measure the profile of currents a short distance above the bottom. A frame was constructed with two speed-sensor units at each end of the electronics-package pressure case. The distances from the ocean bottom to the mid-points of the four

Savonious rotors were 48, 180, and 208 centimeters respectively. A four-channel event recorder was used to record currents at each level simultaneously on a single chart. Direction was not measured. The meter was deployed in the manner described earlier.

Currents were measured in depths of 37 meters and 73 meters west of Yaquina Head. The duration of the record at each station was approximately one-half hour. Succeeding short sections of the record at each station were analyzed for speed and are presented as both linear and logarithmic current profiles in Figure 7. The no-slip boundary condition that velocity is equal to zero at the bottom was assumed, and in the linear profiles a smooth curve was drawn through the plotted points. Although the no-slip assumption must be valid, the shape of the curve between the bottom and the first data point above the bottom (48 cm) depends on bottom roughness condition. If the bottom is hydrodynamically rough, as a rippled surface would be, turbulence in the boundary layer will extend all the way to the bottom, and the current profile will look similar to those in Figure 7. On the other hand, if the bottom is hydrodynamically smooth, as an unrippled bottom composed of fine sediment would be, the main turbulent flow will be separated from the bottom by a thin layer of laminar flow. The near-bottom current profile will then resemble Figure 8. .

We can assume a rough boundary and apply the von Kármán-Prandtl equation for boundary currents,

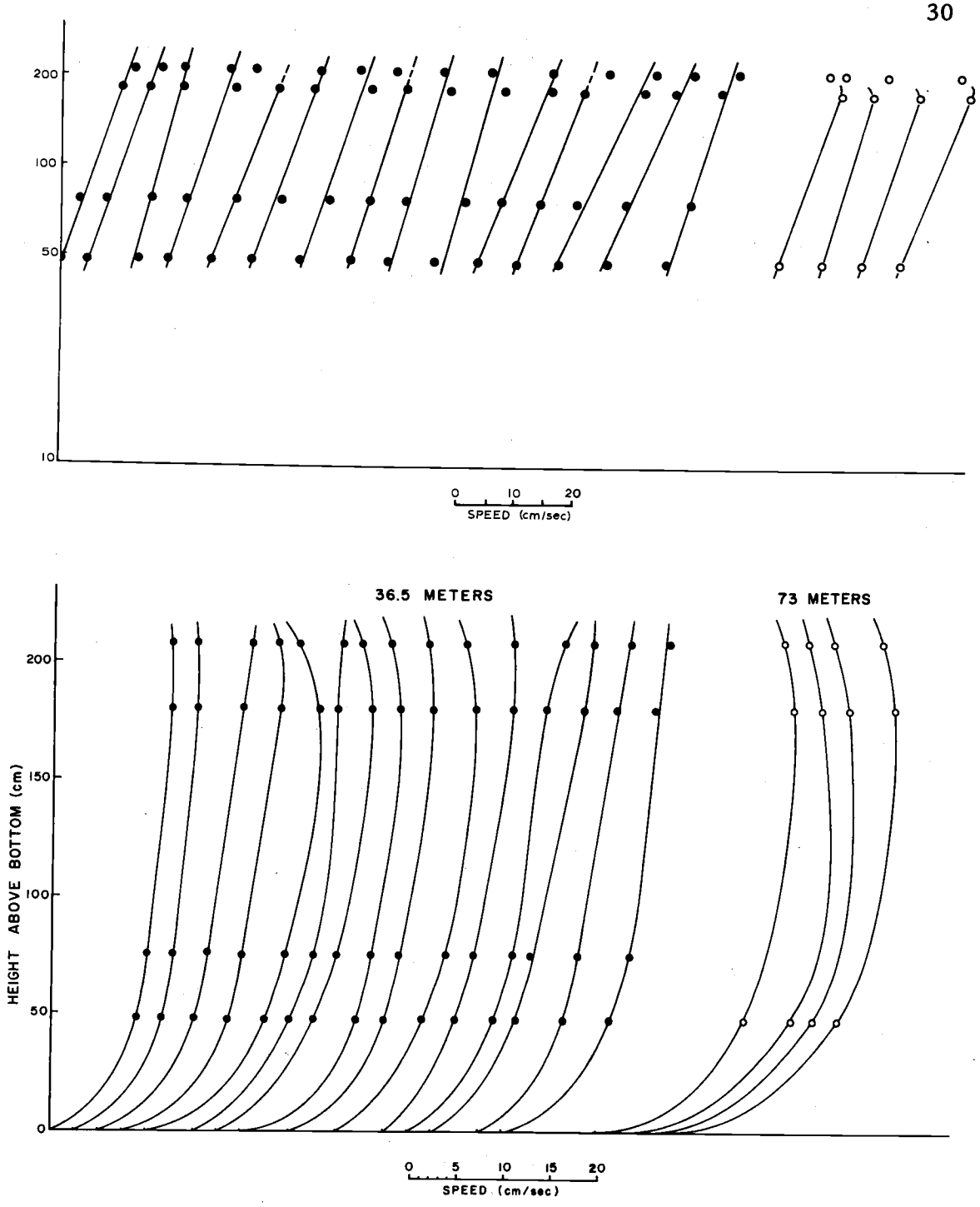

Figure 7. Cruise C 7102 A. Observed profiles of current speed. The profiles have been spaced apart for clarity. In the bottom graph, the bottom points of the curves are assumed to be zero and the speed scale is applied from that point. In the upper graph, which is plotted on a logarithmic vertical scale, the zero points are not shown.

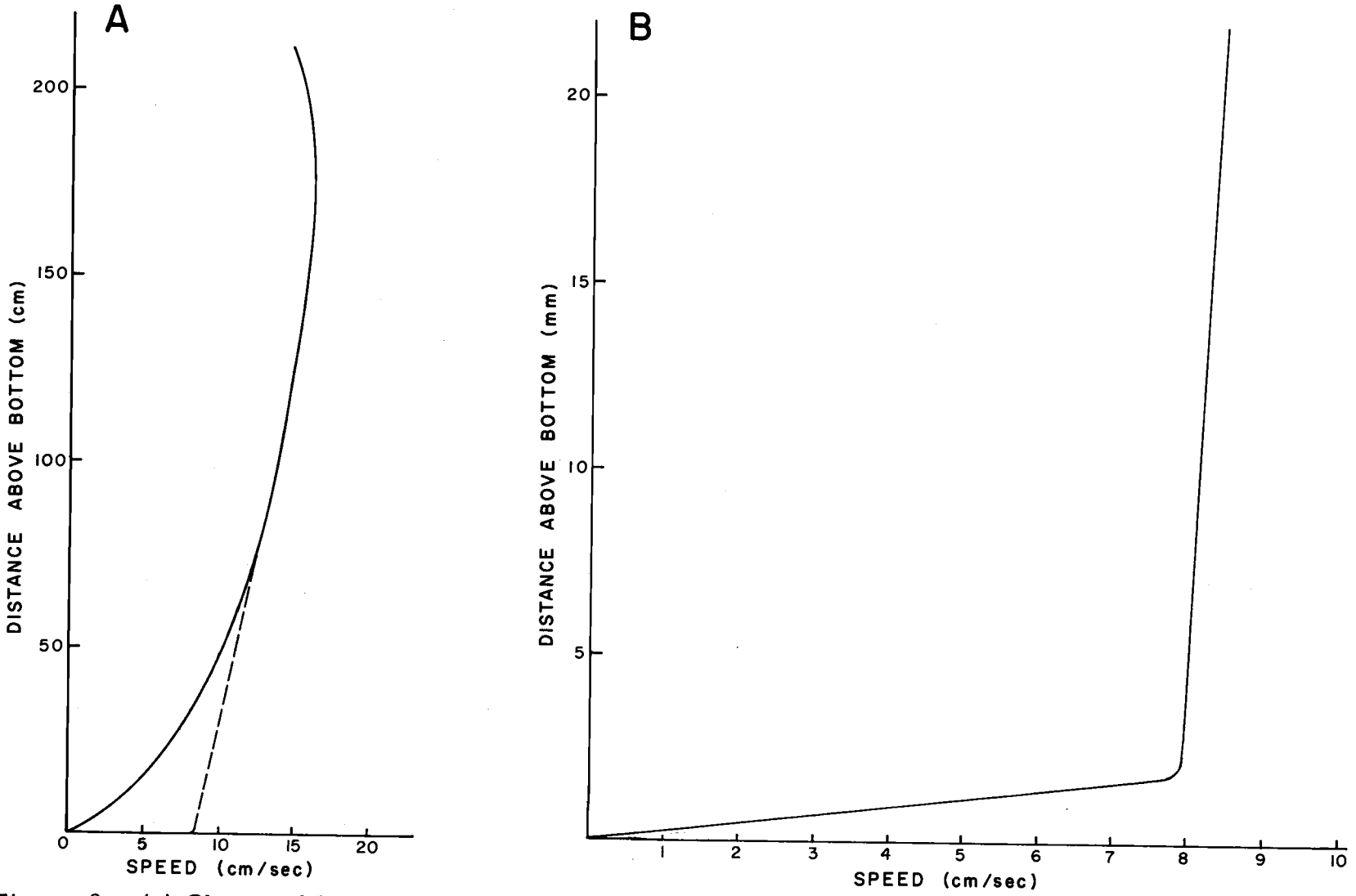

Figure 8. (a) Observed bottom current profile with theoretical lower profile superimposed.
(b) Theoretical current profile in lowermost 20 millimeters of profile.

$$\overline{U} = \frac{U_*}{k_o} \log \frac{z + z_o}{z_o} \quad , \tag{4}$$

where $\overline{U}$ is the average velocity (cm/sec) at a distance z (cm) above the bottom,

U_* is the shear velocity (cm/sec)

k_o is von Kármán's constant, $\doteq 0.4$,

and z_o is the roughness length related to the height of the roughness elements (Inman, 1963).

Inman (1963) has outlined a method by which the value of z_o and U_* can be determined graphically. Equation (4) is rewritten:

$$\log(z + z_o) = \frac{k_o}{U_*} \overline{U} + \log z_o \tag{5}$$

and the logarithm of $(z + z_o)$ is plotted against $\overline{U}$, with z_o assumed to be negligible for the first approximation. The intercept of the plotted line with the ordinate given a first approximation for z_o. This value is used in the next approximation, and so on, until succeeding values of z_o are approximately equal.

Applying this technique and using the average speed obtained at each level for the observations at 37 meters, a value of $z_o = 3.4$ cm is obtained. This probably is an indication that rippling was present, and that the bottom was indeed hydrodynamically rough. However, at a depth of 73 meters, the value for z_o is 0.002 cm. The low value for z_o at the deeper station indicates a hydrodynamically smooth bottom.

In the case of a smooth boundary, Einstein (1950) gives the velocity distribution as:

$$\frac{U_z}{U_*} = 5.75 \log \left(9.05 \frac{U_* z}{\nu}\right) \tag{6}$$

where U_z is the velocity (cm/sec) at z distance above the bottom,

U_* is the shear velocity,

and ν is the kinematic viscosity (cm^2/sec).

Using an observed average value at the deeper station of $U_z = 17.4$ cm/sec at z = 48 cm, and a value of 1.1×10^{-2} cm^2/sec for kinematic viscosity yields a value of $U_* = 0.68$ cm/sec. The thickness of the laminar sub-layer δ, in which the velocity profile is linear, is listed in Chow (1964) as:

$$\delta = \frac{11.6\nu}{U_*}$$

For $U_* = 0.68$ cm/sec, $\delta = 1.9$ mm. The roughness length computed using the von Kármán- Prandtl relationship for rough boundaries was 0.02 mm. The fact that the roughness length is two orders of magnitude smaller than the thickness of the laminar sub-layer indicates that the boundary is hydrodynamically smooth.

The velocity profile within the laminar sub-layer is listed by Chow (1964) as:

$$U_z = z \frac{U_*^2}{\nu} \tag{8}$$

For $z = \delta$,

$$U_z = 11.6\, U_* \tag{9}$$

Using this relation, the velocity at 1.9 mm above the bottom should have been 7.9 cm/sec at the time of the observations (Figure 8).

At the shallower station, where the roughness length was determined to be 3.4 centimeters, if we assume a rough bottom and apply equation (4) using an observed average value of 10 cm/sec at 48 centimeters above the bottom, we obtain $U_* = 3.39$ cm/sec.

The shear velocity is defined as

$$U_* = \frac{\tau_o}{\rho} \tag{10}$$

where τ_o is the boundary shear stress (force/ unit area) and ρ is the density of the fluid. The stations at which the observations were made were spaced closely enough that density can be assumed constant. We can then write

$$\frac{U_{*\,deep}^2}{U_{*\,shallow}^2} = \frac{\tau_{deep}}{\tau_{shallow}} \,. \tag{11}$$

Since U_* at the shallow station was determined to be 3.39 cm/sec and U_* at the deep station was 0.68 cm/sec, it follows that the shear stress at the shallow station is 25 times the shear stress at the deep station. The measured current, on the other hand, was stronger at the deep station. These calculations illustrate the importance of bottom roughness in erosion and transportation of sediments.

The primary purpose for making observations of the bottom-current profile was to relate current observations made at several

distances above the bottom. With one exception, all observations have been made above 48 cm, so the curves of Figure 7 are sufficient for that purpose.

Several of the profiles seem to indicate a velocity maximum at about 170 on above the bottom. Although the number of points on which the curves are based is small, over half of the observations reveal a maximum below two meters. This is slightly nearer the bottom than the velocity maximum observed at 4000 meters depth in the equatorial Atlantic Ocean by Pyrkin (1966), where the maximum was positioned about 250 cm above the bottom. The departure of the uppermost part of the observed profiles from the logarithmic profile may be attributed to shear effects caused by a current direction reversal higher in the water column. Such reversals have been observed between currents near the surface and those 15 meters from the bottom on the continental shelf nine kilometers west of Depoe Bay (Pillsbury et al., 1970).

Cruise Y 7002 C*

The initial attempt to measure bottom currents on the continental margin was made on the upper slope, 52 kilometers west of Cascade Head in February, 1970. (See Figure 4 and Appendix I for locations

* Cruise numbers follow the form: ship, year, month, and sequence. Thus, cruise Y 7002 C was the third cruise aboard R/V Yaquina in February of 1970.

of stations.) A free-vehicle meter was used for this observation, which, at 350 meters, was the deepest of the study. Due to a speed-sensor malfunction, direction only was recorded for the entire 14 hours. Current direction (the direction toward which the current flowed) was generally southerly, with a small westerly component (Figure 9).

Cruise C 7004 C

In April, 1970, a current meter was placed on the mid-shelf (125 meters deep) 26 kilometers southwest of Tillamook Head. Both the speed and direction sensors functioned properly and a 48-hour record was obtained. However, the on-off timer operated sporadically with the result that the absolute time base is uncertain. This uncertainty precluded spectral analysis of the record, although a progressive vector diagram (Figure 10) was drawn using representative current velocities. Currents varied from below threshold speed to 20 cm/sec, measured 25 centimeters from the bottom. Probably the most striking aspect of the record is the nearly constant direction of flow toward the southwest. From 1500 to 2300 on April 29th, current direction did not vary more than five degrees. No tidal or inertial oscillations are apparent in the direction record. There appears to be some systematic periodicity in current speed, although this is uncertain because of the time-base problem.

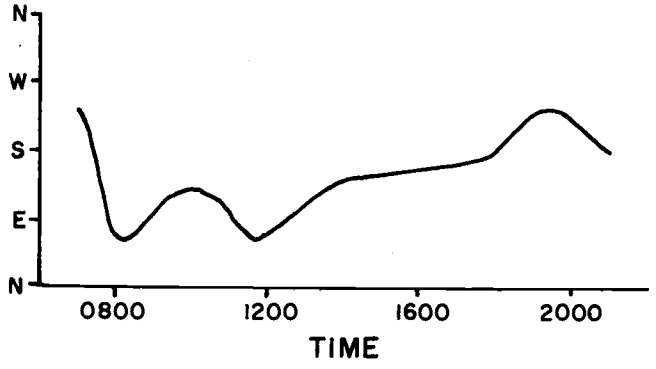

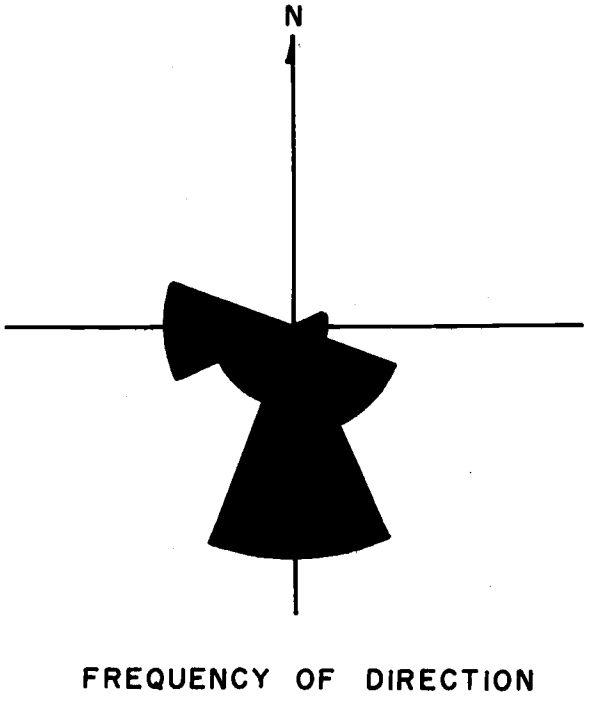

Figure 9. Cruise Y 7002 C. 45° 03.3'N, 124° 38.6'W. Current direction record and frequency of direction.

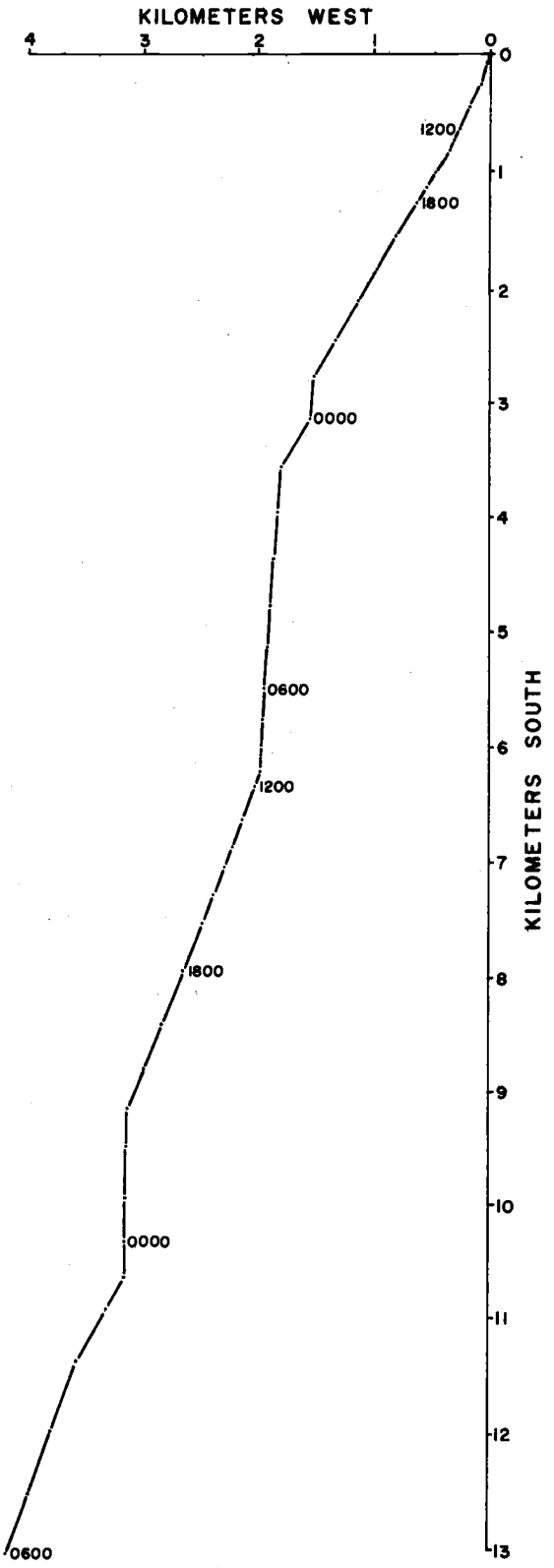

Figure 10. Cruise C 7004 C. 45° 48.5'N, 124° 14.5'W. Progressive vector diagram.

Cruise C 7006 B

Current meters were moored at 100 meters and 175 meters at distances of 30 and 43 kilometers west of Newport during June, 1970. Current speed was recorded for only the first six hours at the 100-meter depth, and not at all at the 175-meter depth. Direction was recorded at both sites for the entire duration of the records, but no north-reference was obtained at the shallow station.

For the first six hours, current speed at 100 meters depth varied from 3.5 cm/sec to 13 cm/sec. Direction, nearly constant for the first 22 hours of the record, became rotary, with a period of about 12 to 13 hours (Figure 11). Although the period is fairly regular, the rate of change in direction is highly variable, and probably indicates the influence of shorter-term processes. The length of the rotational period corresponds with the semi-diurnal period of the tide in this area. Rotation was in a clockwise direction.

Current direction at the deeper station exhibited neither the tidal frequency seen at 100 meters nor the constancy of the currents measured during cruise C 7004 B. As shown in Figure 12, the dominant direction was onshore to the northeast. Unfortunately, the absolute time base of the record at the deeper station is in question, so that comparisons between the two records cannot be made.

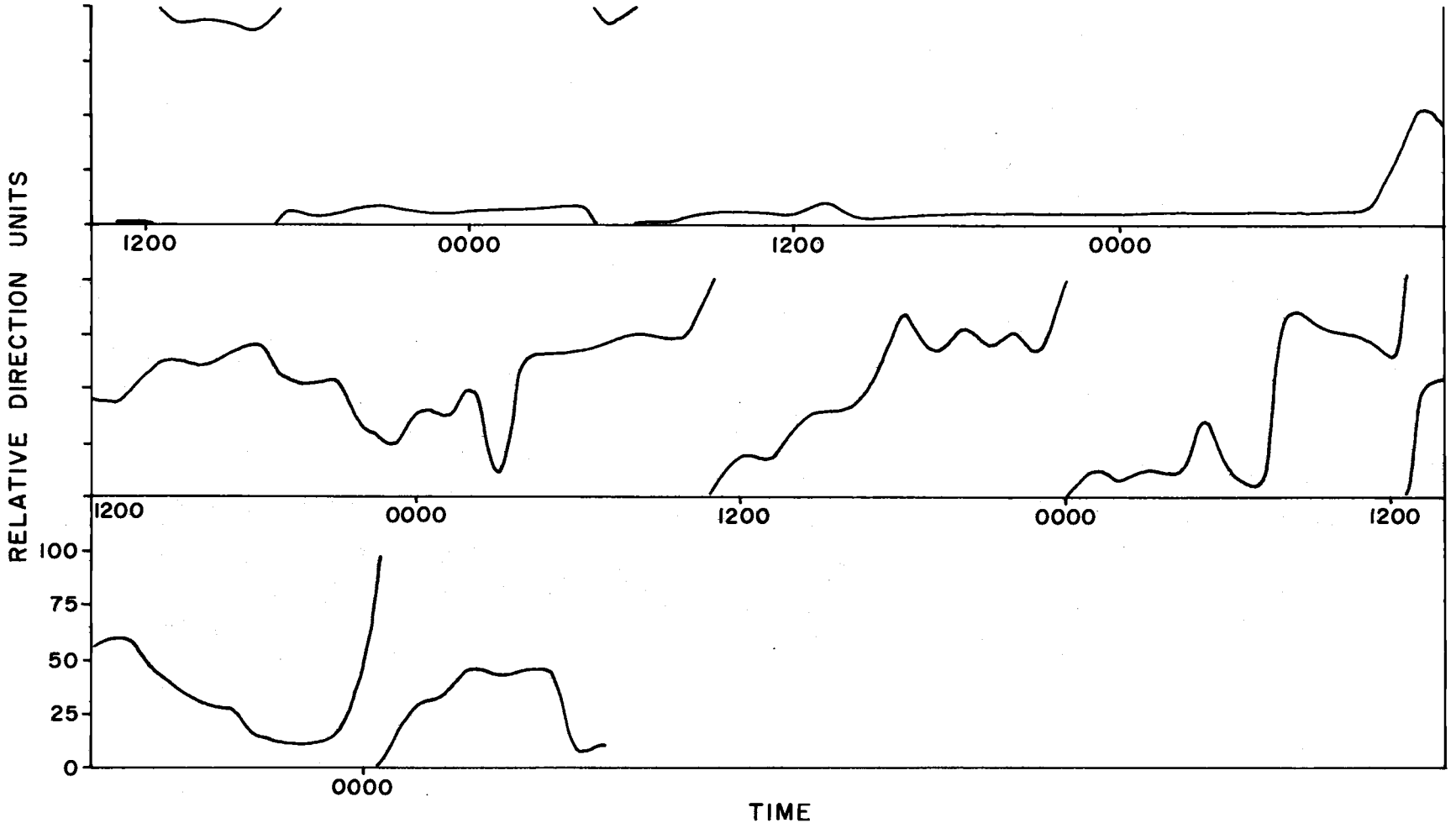

Figure 11. Cruise C 7006 B, 100 meters. 44° 39.9'N, 124° 26.6'W. Relative direction record. No north reference was obtained.

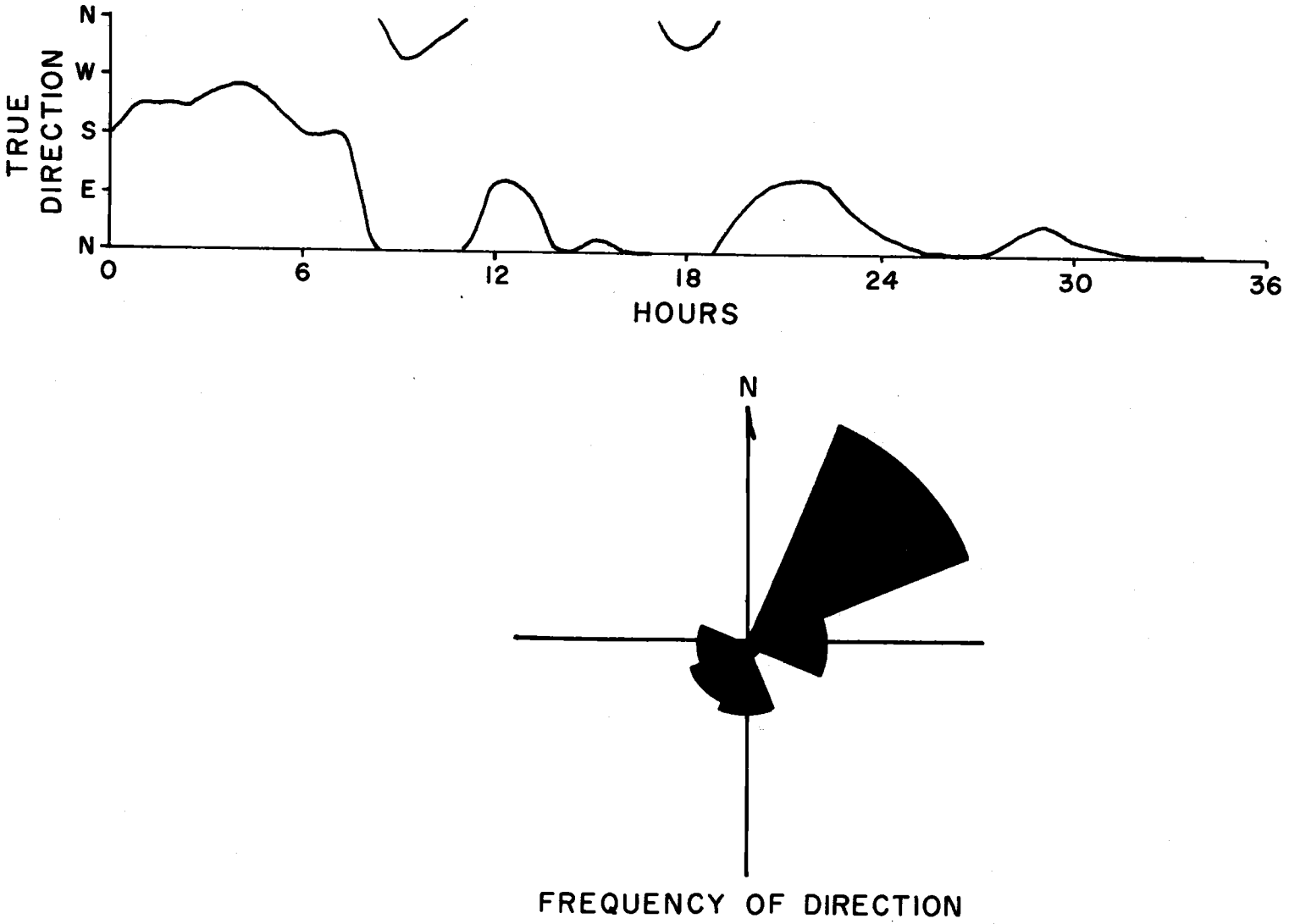

Figure 12. Cruise C 7006 B, 175 meters. 44° 39.8'N, 124° 33.3'W. Current direction record and frequency of direction.

Cruise C 7008 D

Current speed and direction were recorded for 66 hours at 176-meters depth near the shelf edge, 43 kilometers west of Newport. This station was in virtually the same location as the deeper station of the preceding cruise. A detailed picture of the nature of currents 1.3 meters from the bottom is presented in this record (Figure 13). The current meter was programmed to sample 40 minutes continuously, then shut down for 20 minutes. The gaps in Figure 13 represent periods of "off" time.

Speed during most of the record was highly variable, and the magnitude of the variability seemed to increase as the mean speed increased. Large speed increases occurred over short periods of time at several times during the observations, notably from 1355 to 1407 on August 18, an increase of 18 cm/sec, and again from 1501 to 1521 the same day, an increase of 19.5 cm/sec. The mean speed for the record is 8.4 cm/sec, with extremes from below 0.5 cm/sec to 24 cm/sec. The highest sustained speed of 22 cm/sec was recorded from 1522 to 1535 on August 18. In Figure 14b the record has been smoothed by plotting half-hour averages of the measured currents, assuming a linear trend during the gaps in time. From the smoothed record no systematic changes in speed are evident, except that during the latter half of the record the velocity minima are about six hours

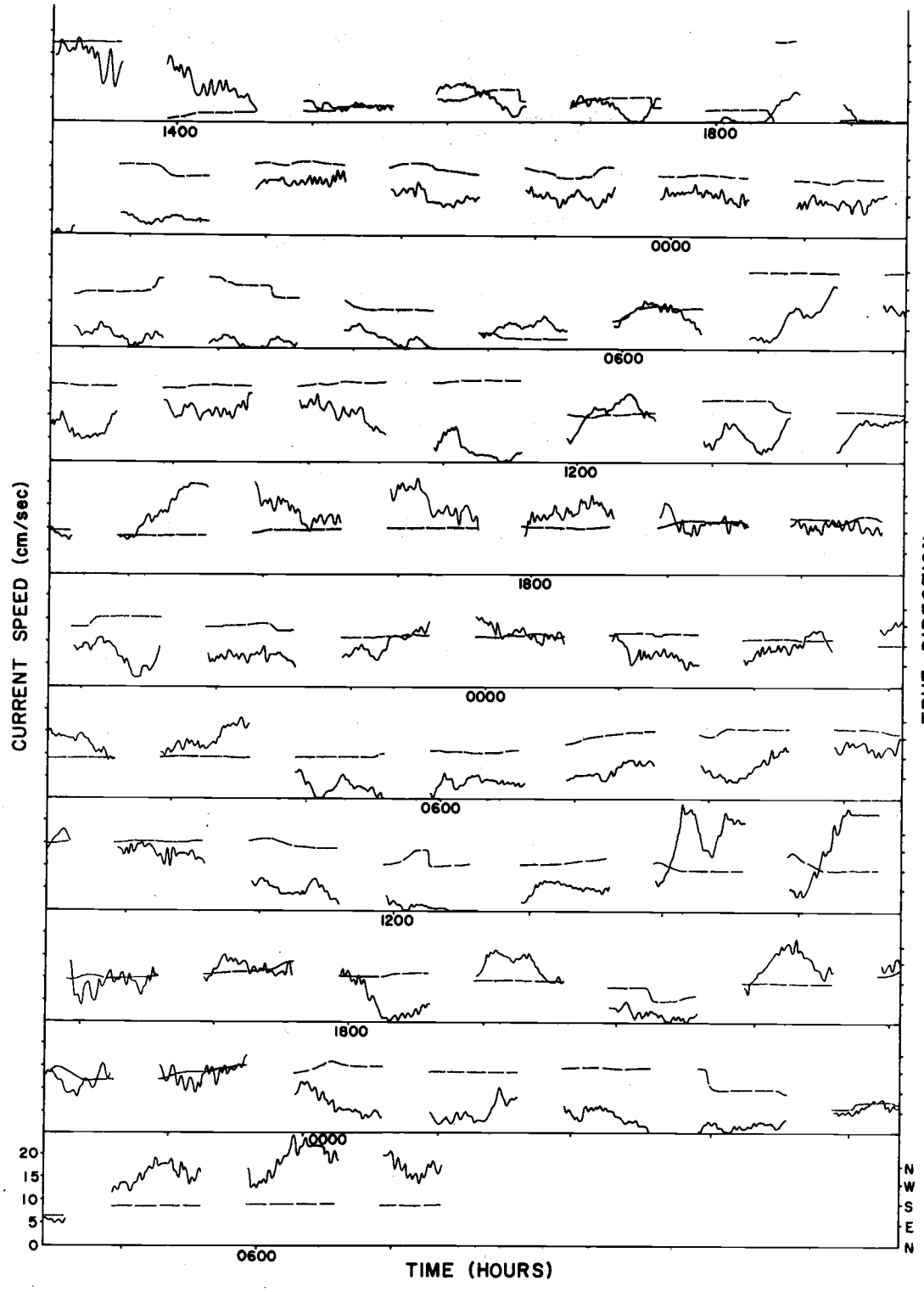

Figure 13. Cruise C 7008 D. 44° 40.9'N, 124° 33.6'W. Current speed (solid line) and direction (dashed line). Caps indicate "off time".

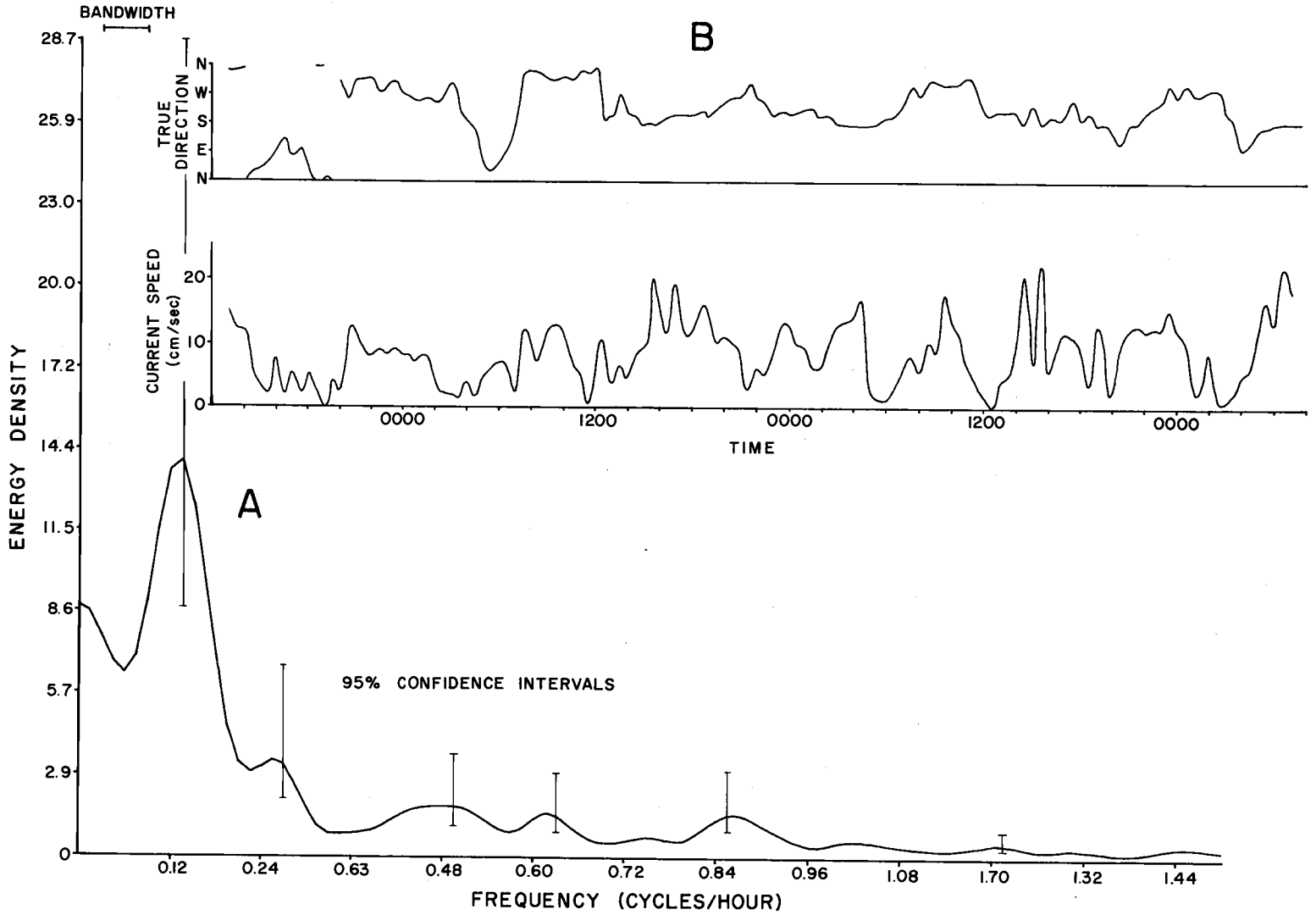

Figure 14. Cruise C 7008 D. 44^{o} 40.9'N, 124^{o} 33.6'W.
(a) Frequency power spectrum. Energy density units are $(cm/sec)^2/3$ cph.
(b) Smoothed record of current speed and direction.

apart. The frequency power spectrum (Figure 14a), however, has peaks at periods of four hours, 2.1 hours, 1.6 hours, and 1.1 hours in addition to the dominant period of about seven hours. The dominant period is close to half that of the semidiurnal component of the tide; later shelf-edge currents also exhibit an energy peak near this period. The meaning of the peaks which occur at shorter periods is not clear, although it is possible that internal waves may be responsible for the higher frequency peaks.

Current direction did not vary with the current speed in any manner which is apparent in the raw record. However, the progressive-vector diagram (Figure 15) shows several "waves" with a "period" of about 12 hours. The net transport, as indicated by Figure 15, is southwest, exactly the opposite of the dominant direction at this site two months earlier.

Cruise C 7012 D

Bottom currents were observed continuously for slightly over two hours at mid-shelf, 135 kilometers west of Depoe Bay. These observations were made using a current meter mounted in a tripod-like frame. The rotor is about 0.5 meters above the bottom in this configuration.

The mean velocity of the current was 8.2 cm/sec, ranging from five cm/sec to 13 cm/sec (Figure 16b). Relative direction was steady

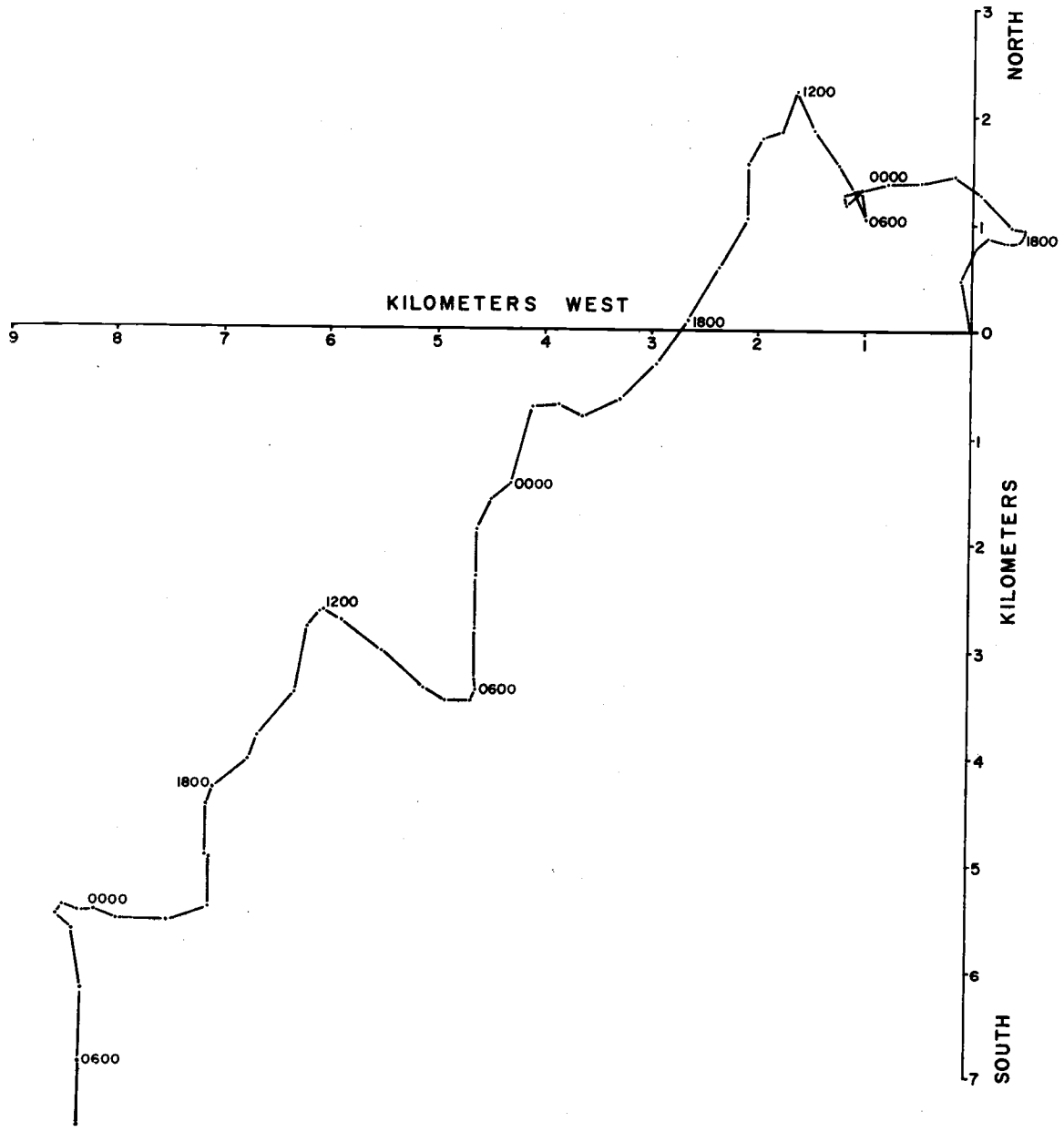

Figure 15. Cruise C 7008 D. 44° 46.9'N, 124° 33.6'W. Progressive vector diagram.

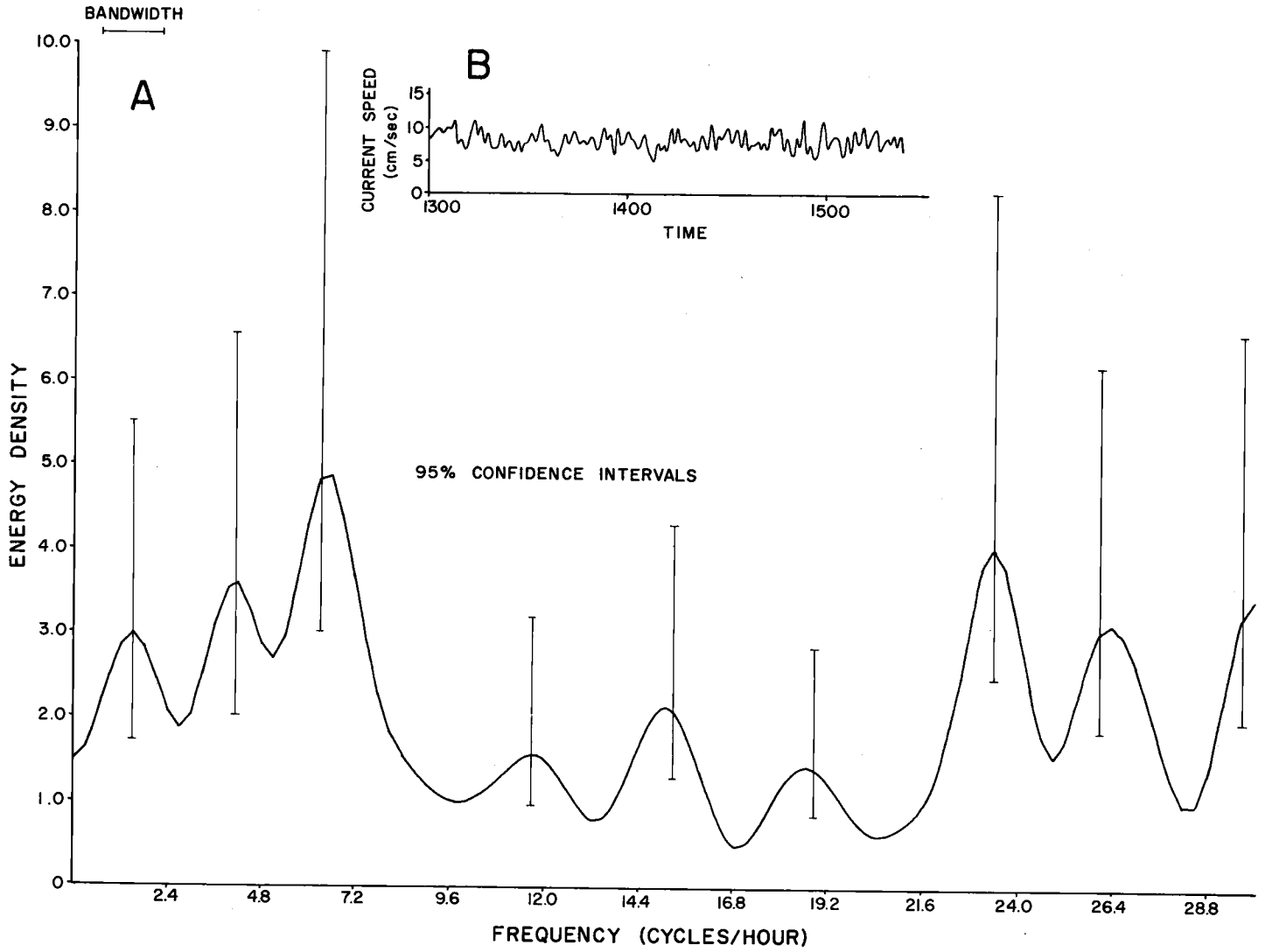

Figure 16. Cruise C 7012 D. 44^{o} 49.0'N, 124^{o} 12.5'W.
(a) Frequency power spectrum. Energy density units are $(cm/sec)^2/cpm$.
(b) Current speed record.

but no north reference was obtained. The frequency power spectrum (Figure 16a) reveals a multitude of peaks with the strongest appearing at periods of 9.5 minutes and 2.5 minutes. A significant part of the energy lies beyond the cutoff frequency of 30 cycles per hour. This record, though short, serves to demonstrate the possible influence of moderate swell (which prevailed during the observations) on bottom currents in relatively deep water.

Cruise Y 7102 F

During February of 1971, short observations of bottom currents were made in conjunction with a series of turbidity-profile stations. These stations were made along transects of the shelf at latitudes 45^{o} 11'N and 44^{o} 40'N (Figure 4), and varied in depth from 275 meters to 25 meters. The record length for each station is about one hour. These records are not presented in analog form. Rather, the average current velocity at each station is presented as a vector in Figures 32, 34, 35, and 36. These observations will be discussed in the section on optical measurements.

Cruise C 7103 F

Bottom currents were measured in relatively shallow water (35 meters), 2.5 kilometers west of Depoe Bay for about 17 hours during March, 1971. The intent of these observations was to determine the

effect of swell on the bottom in the nearshore sand facies.

Figure 17 reveals the strongest currents measured on the continental shelf during the study. Speeds ranged from 13 cm/sec to 48 cm/sec, with a mean speed of 29.6 cm/sec. The rapidly fluctuating current speed indicates the influence of short term surface influences, that is, swell. During the period of measurement, swell nearly doubled in height from about two meters to about four meters. The effect of the increase in the height of the swell is apparent in the increased size of the variations in current speed during the latter half of the record.

The frequency power spectrum (Figure 18a) reveals that energy is distributed throughout the spectrum. Undoubtedly, a significant part of the energy occurs beyond the cutoff frequency of 0.5 cycles per minute. Additionally, tidal effects are to be expected although the record is of insufficient length to allow long period energy peaks to be resolved.

In anticipation of the higher current speeds at this depth, a different type of recorder providing a faster chart speed was utilized. The use of this recorder precluded recording current direction.

Cruise Y 7104 C

Bottom currents were measured simultaneously at mid-shelf and shelf-edge depths, respectively 13.5 and 37 kilometers west of Cape

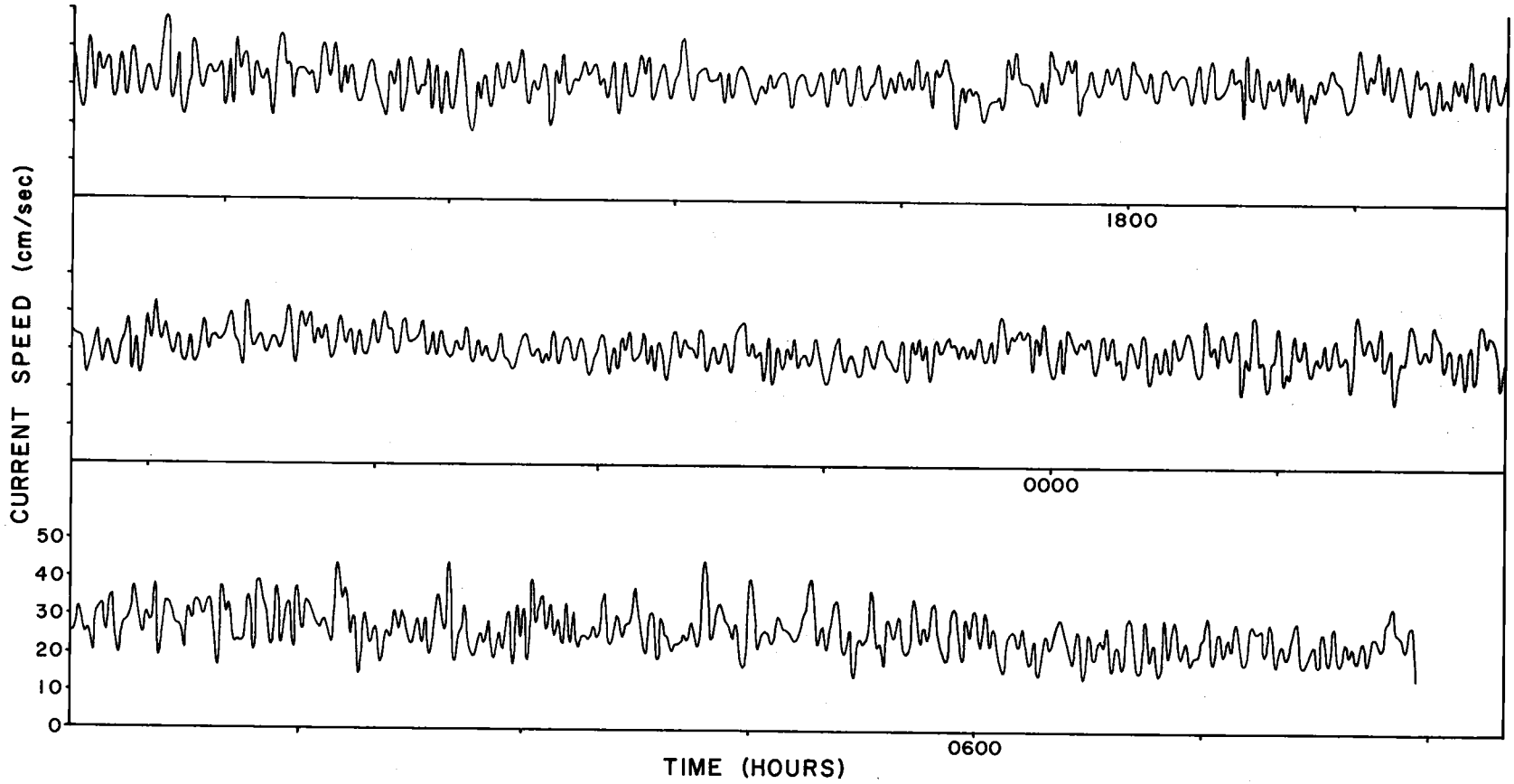

Figure 17. Cruise C 7103 F. 45° 11.0'N, 124° 14.0'W. Current speed record.

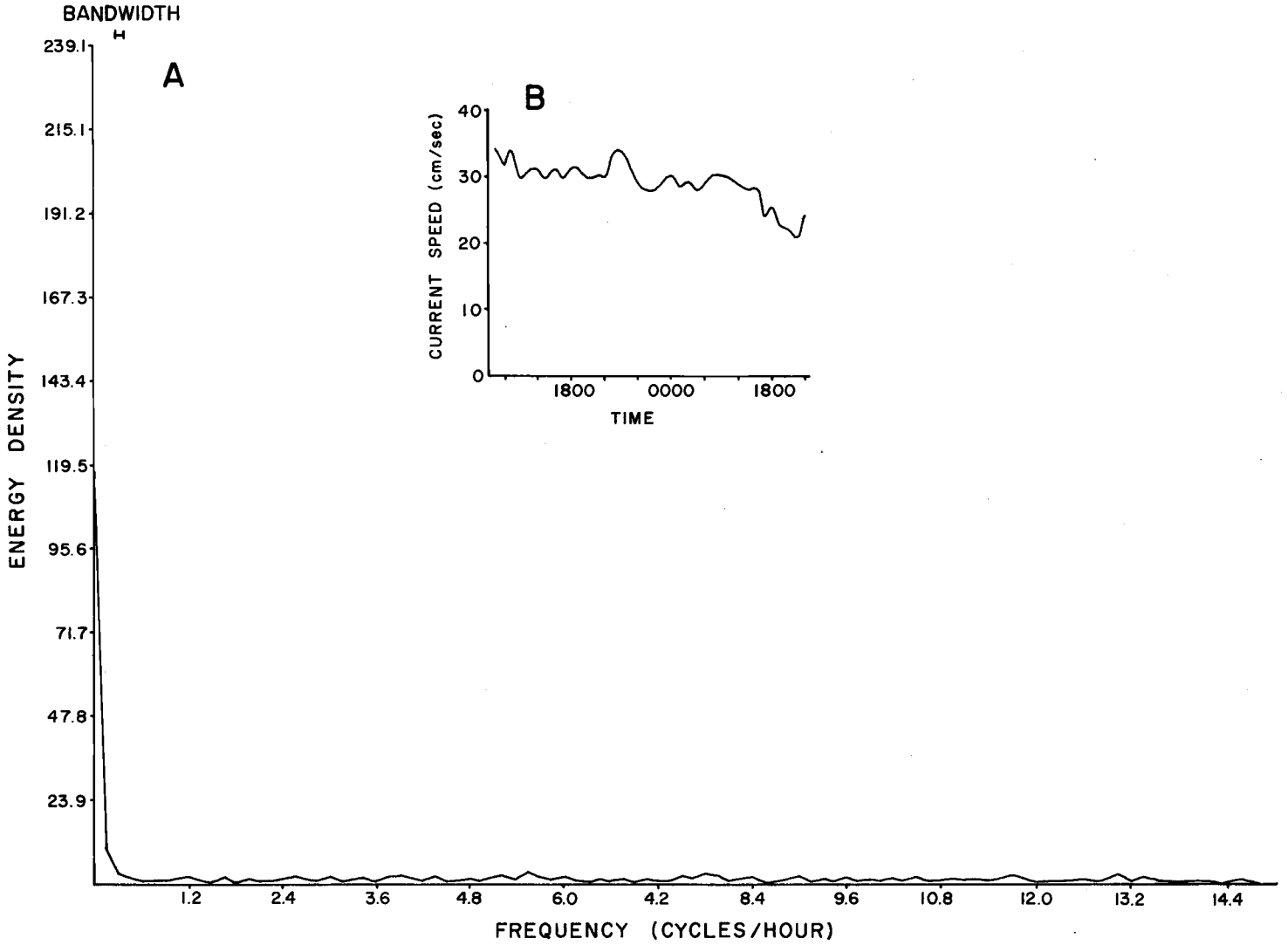

Figure 18. Cruise C 7103 F. 45^{o} 11.0'N, 124^{o} 14.0'W.
(a) Frequency power spectrum. Energy density units are $(cm/sec)^2/0.5$ cpm.
(b) Smoothed record of current speed.

Foulweather. In the vicinity of the deeper station, several observations of turbidity profiles were also made. Bottom photos were taken in this same region in support of a study of pink shrimp (Pandalus jordani).

At the shallow station, the bottom-current speeds ranged from two cm/sec to 34 cm/sec, with a mean of 14.2 cm/sec (Figure 19). For the first time during the study, sustained currents in excess of 25 cm/sec were recorded at relatively large depths. This occurred from 0540 to 0730 on April 27. The current speed in the smoothed record (Figure 20b) appears to vary with a period of 12 to 14 hours. The frequency power spectrum (Figure 20a) indicates that virtually all the energy lies at frequencies lower than 0.3 cycles per hour, with no well-defined energy peaks. Thus, swell apparently did not influence bottom current during these observations. Current direction was not recorded at the shallow station.

At the deeper station, the mean speed was slightly higher at 14.6 cm/sec and the current ranged from below threshold to 32 cm/sec (Figure 21). The sustained strong current observed at 90 meters does not appear in the record at 165 meters, although the current strength during the first 20 minutes of the record is over 25 cm/sec. The smoothed record (Figure 22b) shows the currents at this depth to be somewhat more variable than at 90 meters. Direction records indicate

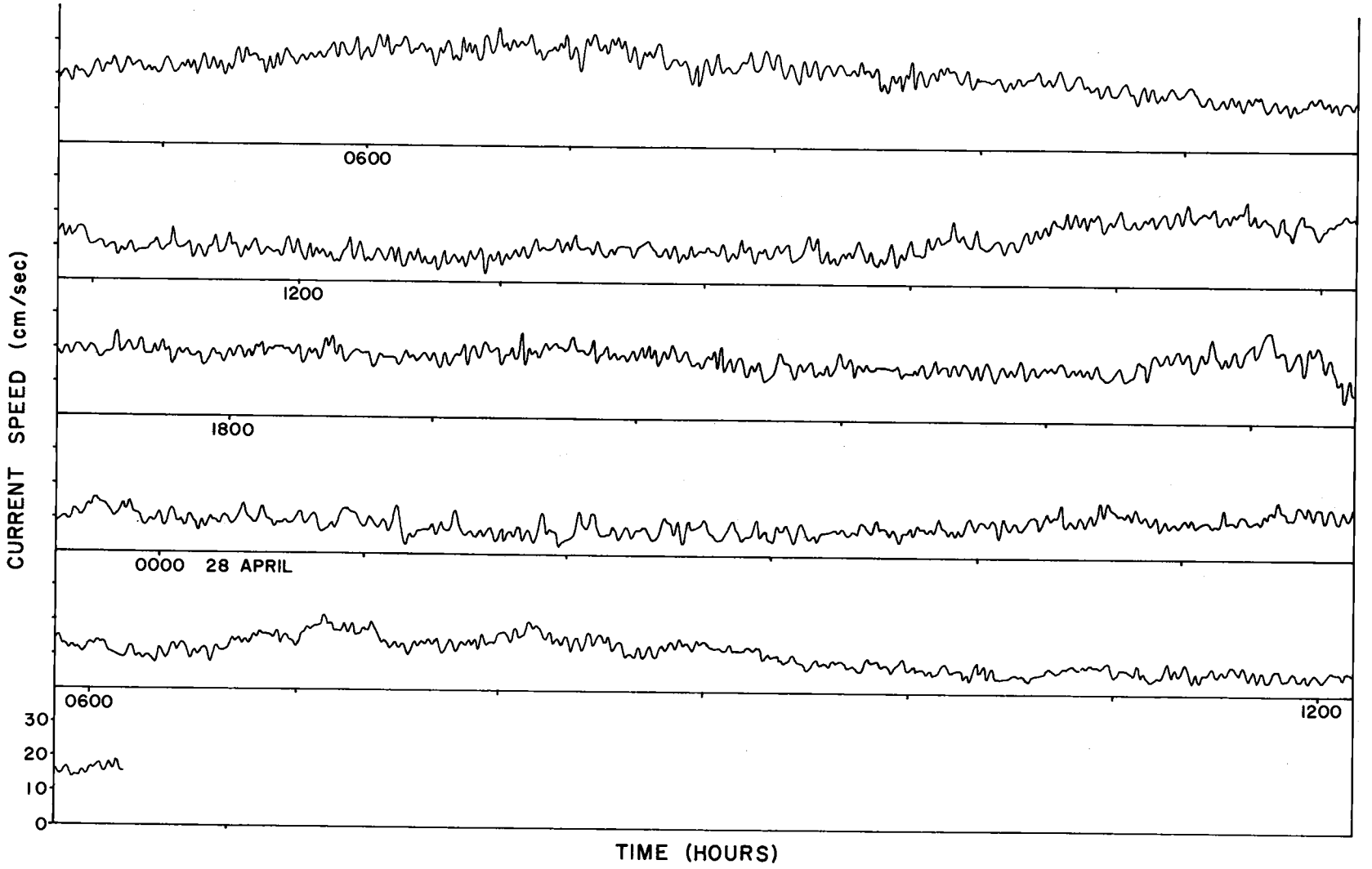

Figure 19. Cruise Y 7104 C, 90 meters. 44° 46.3'N, 124° 14.1'W. Current speed record.

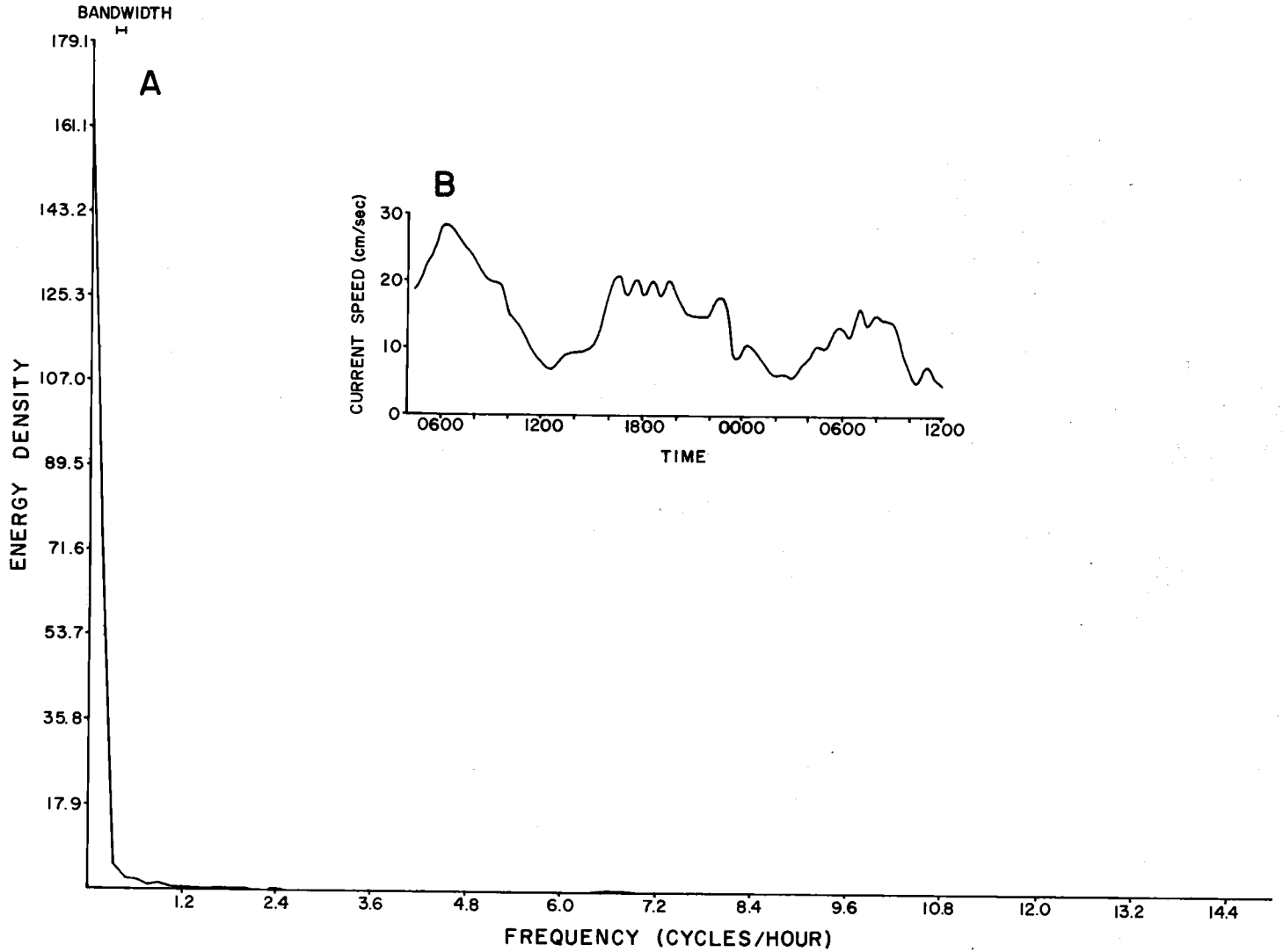

Figure 20. Cruise Y 7104 C, 90 meters. 44^{o} 46.3'N, 124^{o} 14.1'W.
(a) Frequency power spectrum. Energy density units are $(cm/sec)^2/0.5$ cpm.
(b) Smoothed record of current speed.

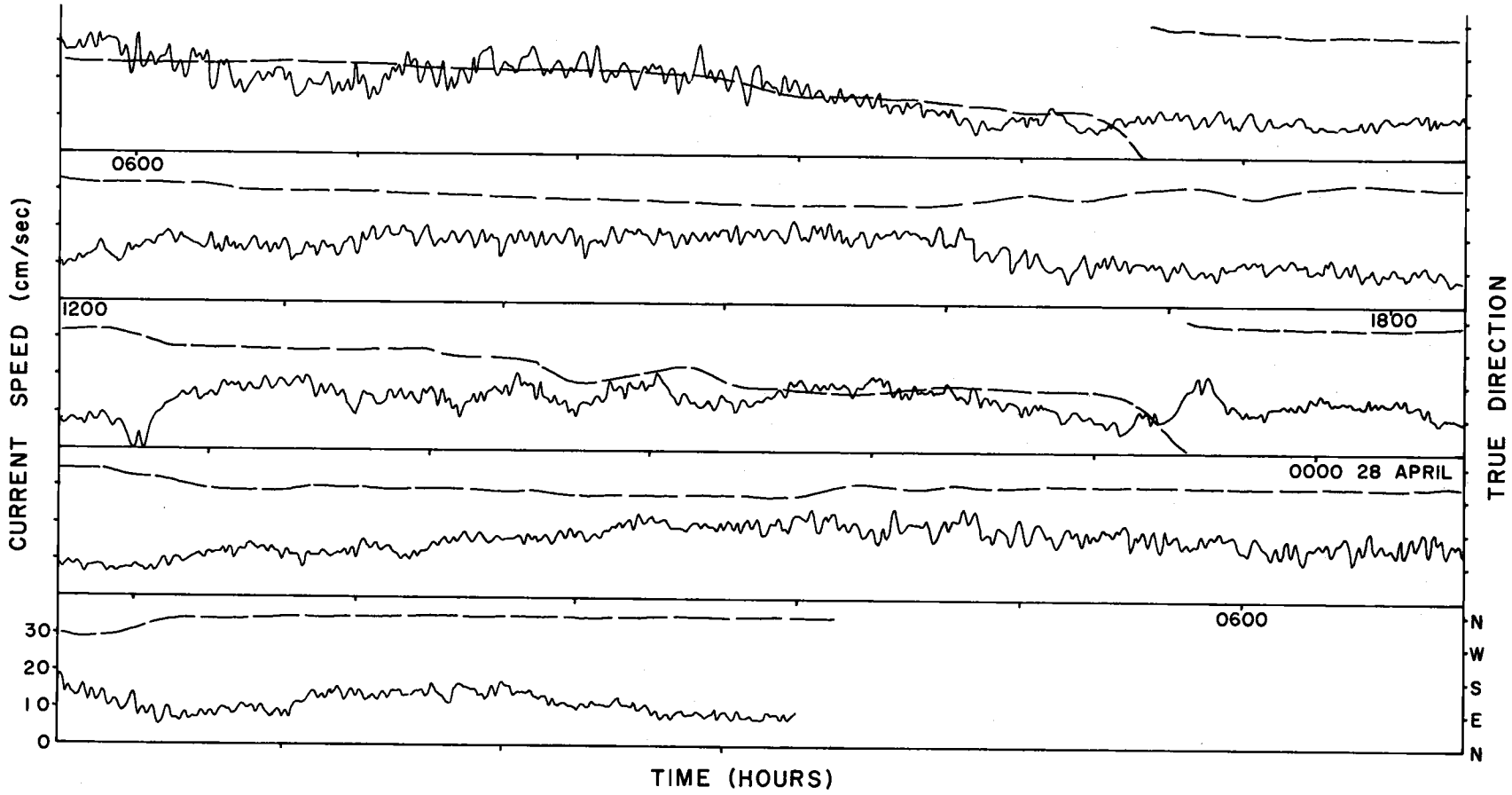

Figure 21. Cruise Y 7104 C, 165 meters. 44° 46.1'N, 124° 31.2'W. Current speed (solid line) and direction (dashed line).

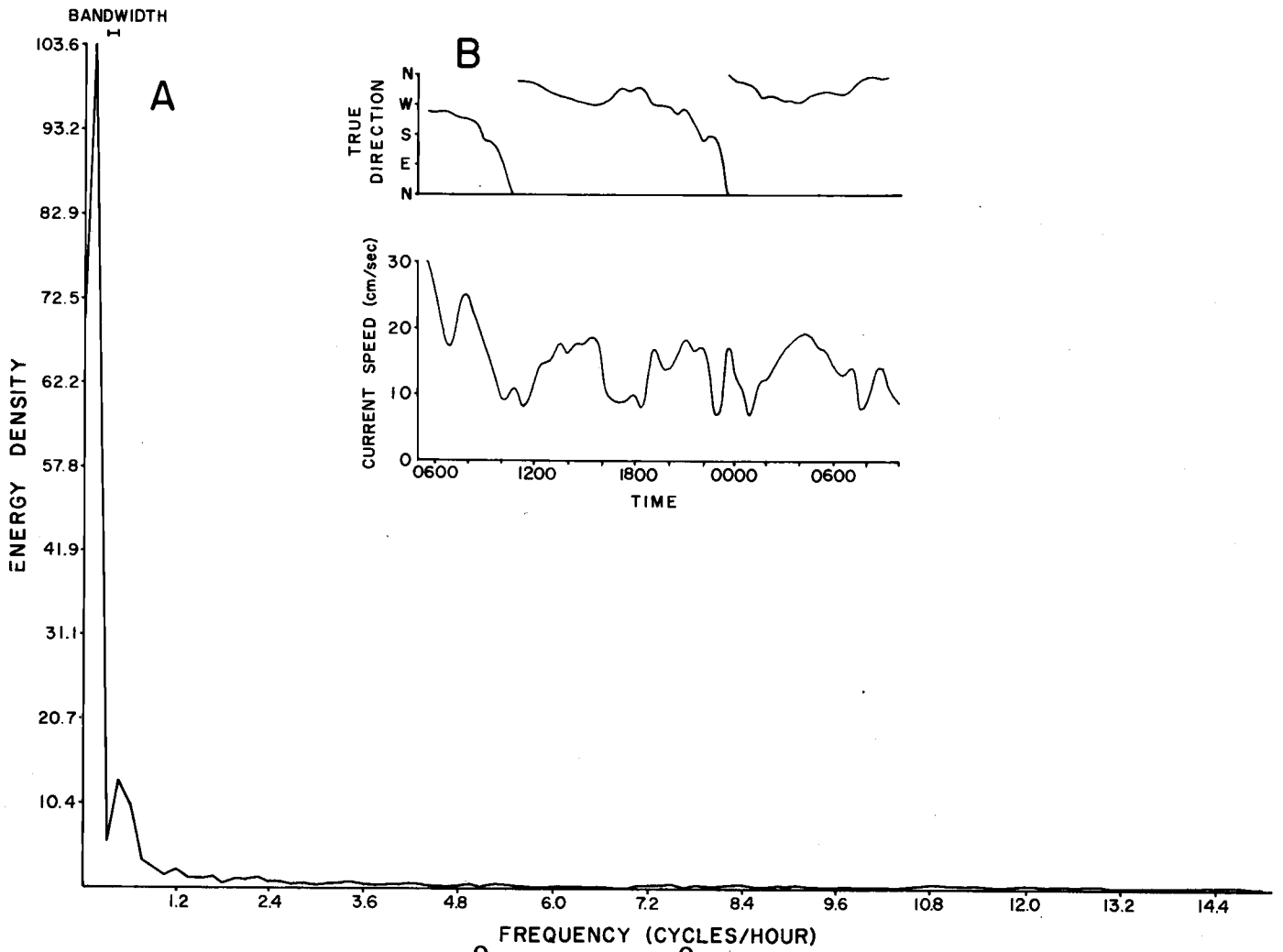

Figure 22. Cruise Y 7104 C, 165 meters. 44^{o} 46.1'N, 124^{o} 31.2'W.
(a) Frequency power spectrum. Energy density units are $(cm/sec)^2/0.5$ cpm.
(b) Smoothed record of current speed and direction.

a distinct counterclockwise rotary motion with an apparent period of about 12 hours.

The frequency power spectrum for the deep station (Figure 22a) has two well-defined peaks corresponding to periods of 6.5 hours and 2.2 hours. As at the shallow station, very little energy is contained at frequencies higher than 0.5 cycles per hour. The 6.5-hour period corresponds roughly to half the semidiurnal period of the tide. The meaning of the peak at 2.2 hours is unclear.

The progressive-vector diagram (Figure 23) displays a general westerly transport during the period of these observations.

Cruise Y 7105 A

Observations of currents were made continuously for two days at depths of 90 and 165 meters west of Tillamook Head in conjunction with measurements of turbidity profiles.

At the mid-shelf station the current speed ranged from below threshold to 28 cm/sec, with a mean of 9.4 cm/sec. The current-speed record (Figure 24) reveals a highly variable flow that seems to be typical of bottom currents in the shelf region. The maximum speed was reached three times in fairly close succession, at 1232, 1323, and 1334 on May 6, after which the current speed fell to a fairly low level.

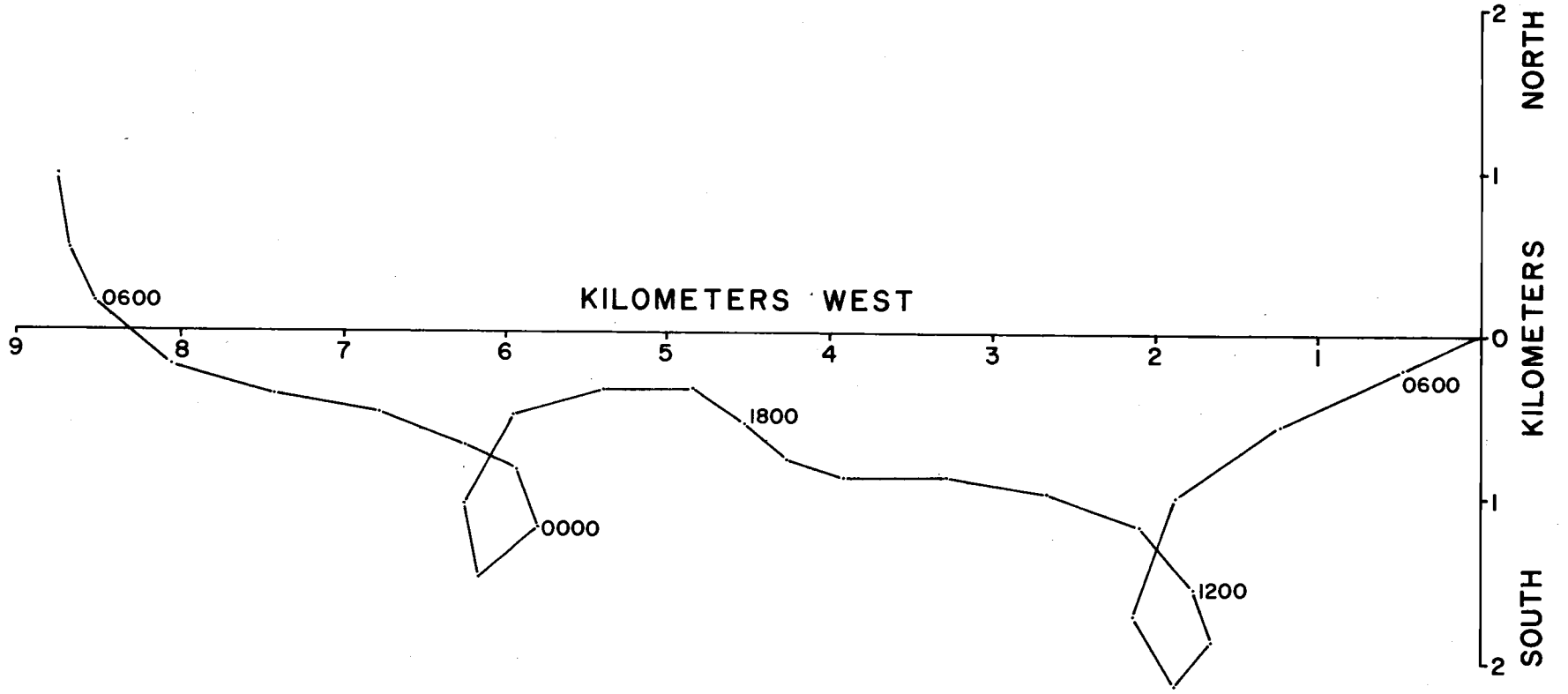

Figure 23. Cruise Y 7104 C, 165 meters. 44° 46.1'N, 124° 31.2'W. Progressive vector diagram.

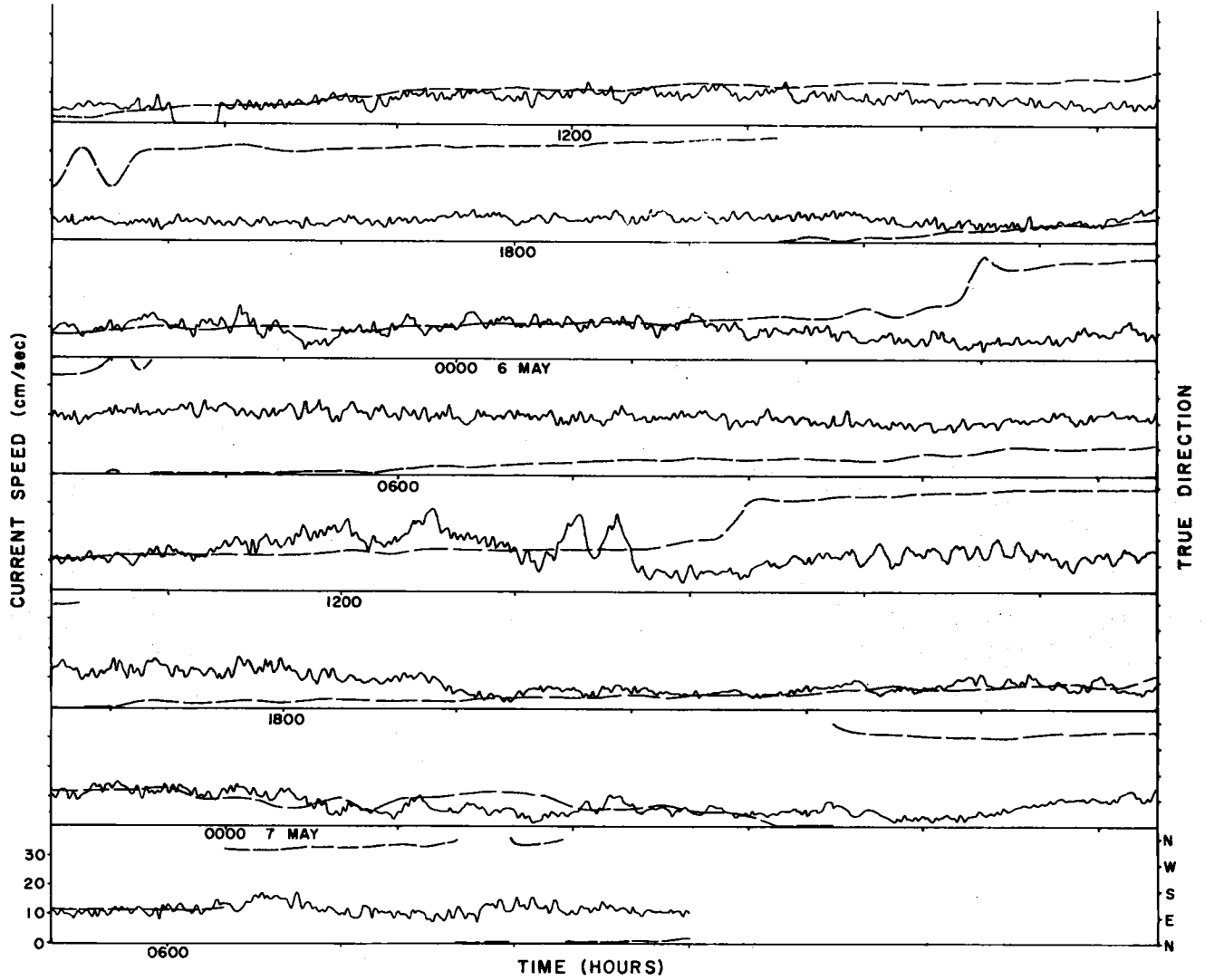

Figure 24. Cruise Y 7105 A, 90 meters. 45° 59.2'N, 124° 11.3'W. Current speed (solid line) and direction (dashed line).

The frequency power spectrum (Figure 25a) shows that most of the energy is contained at frequencies lower than 0.5 cycles per hour. However, minor peaks occur at much higher frequencies, and might indicate the influence of swell, although during the term of observations ocean swell was quite low.

The current direction was strongly rotary in a clockwise direction with a period roughly corresponding to that of the semidiurnal tide. The progressive-vector diagram (Figure 26) indicates an onshore flow of water during the observations.

Again, current measured near the shelf edge at the deeper station (Figure 27) was slightly stronger than at mid-shelf, with a mean of 10.2 cm/sec, although this figure was computed excluding the initial ten hours of record, during which the current was below threshold speed. The record during those ten hours appears to be normal and current direction fluctuates widely, as is normal in a sluggish flow. Several times during the ten-hour period, the raw record shows that the Savonious rotor did turn slightly; furthermore, the current speed increased very slowly after this initial period. Therefore, indications are that this was an extended period of quiescence rather than an instrument malfunction. Nevertheless, such an extended period of quiescence is unprecedented in this study, and is considered to be a rare condition. After the initial ten-hour period, current speed ranged from below threshold to 25 cm/sec.

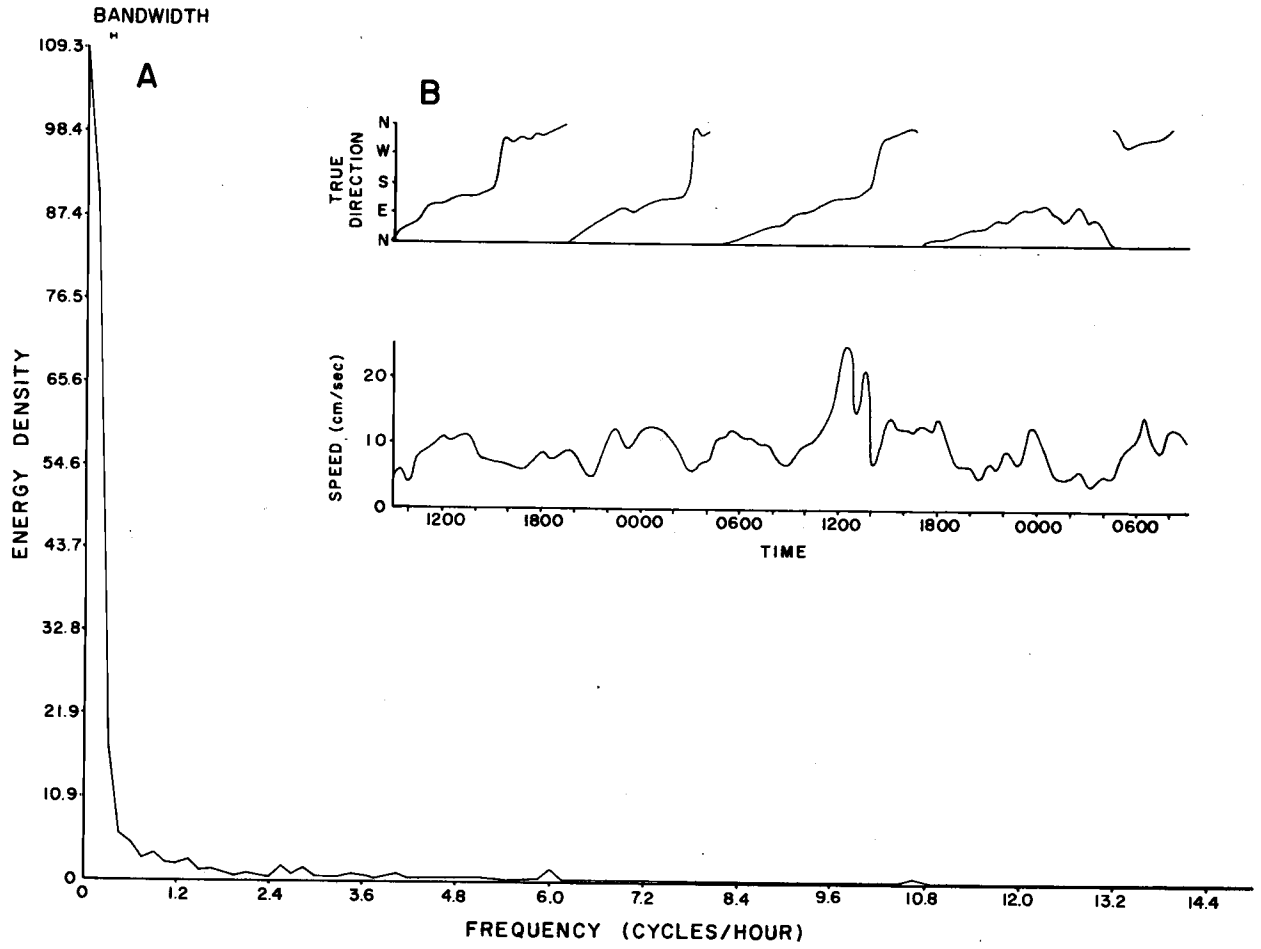

Figure 25. Cruise Y 7105 A, 90 meters. 45^{o} 59.2'N, 124^{o} 11.3'W.
(a) Frequency power spectrum. Energy density units are $(cm/sec)^2/0.5$ cpm.
(b) Smoothed record of current speed and direction.

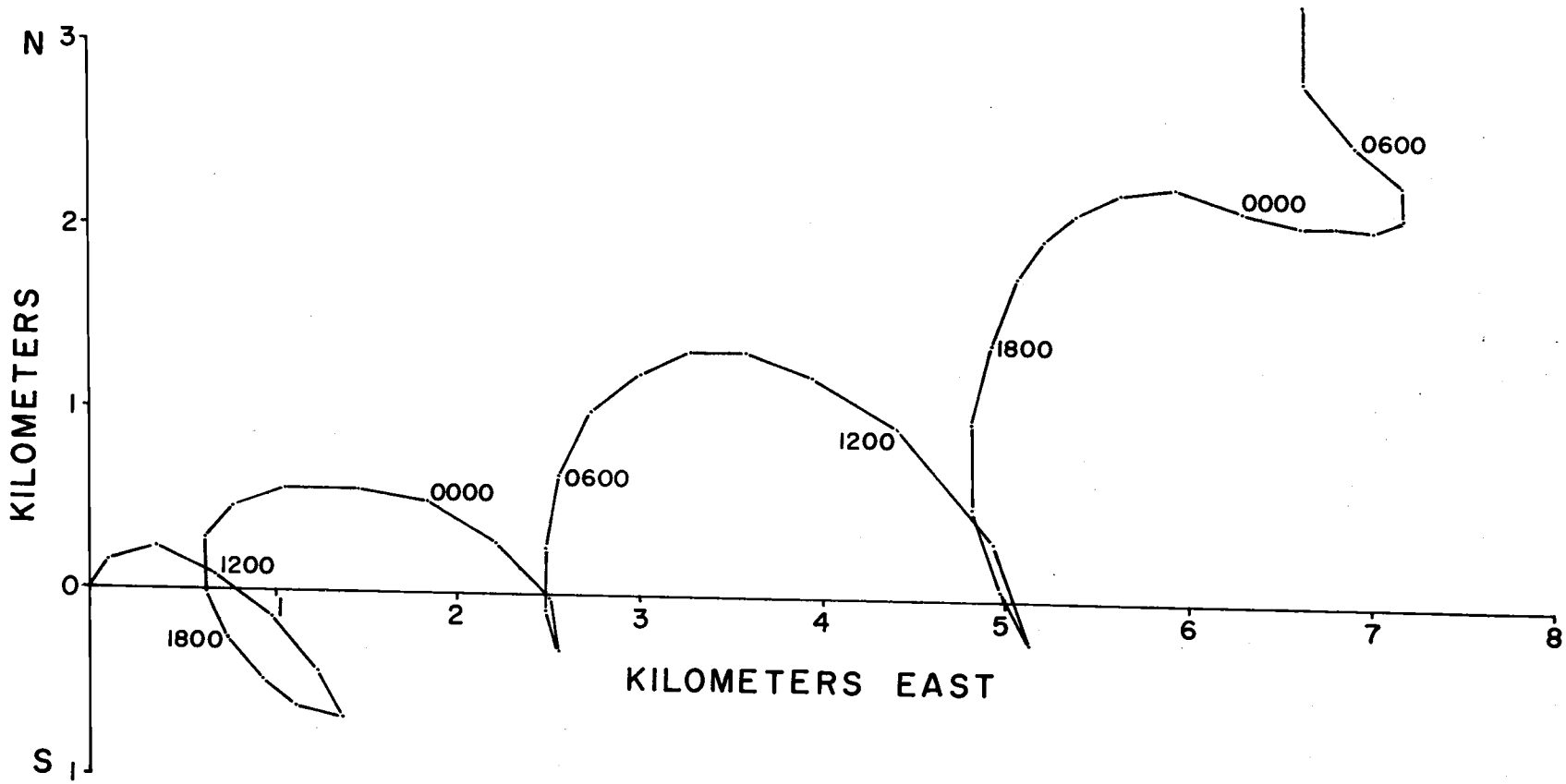

Figure 26. Cruise Y 7105 A, 90 meters. 45° 59.2'N, 124° 11.3'W. Progressive vector diagram.

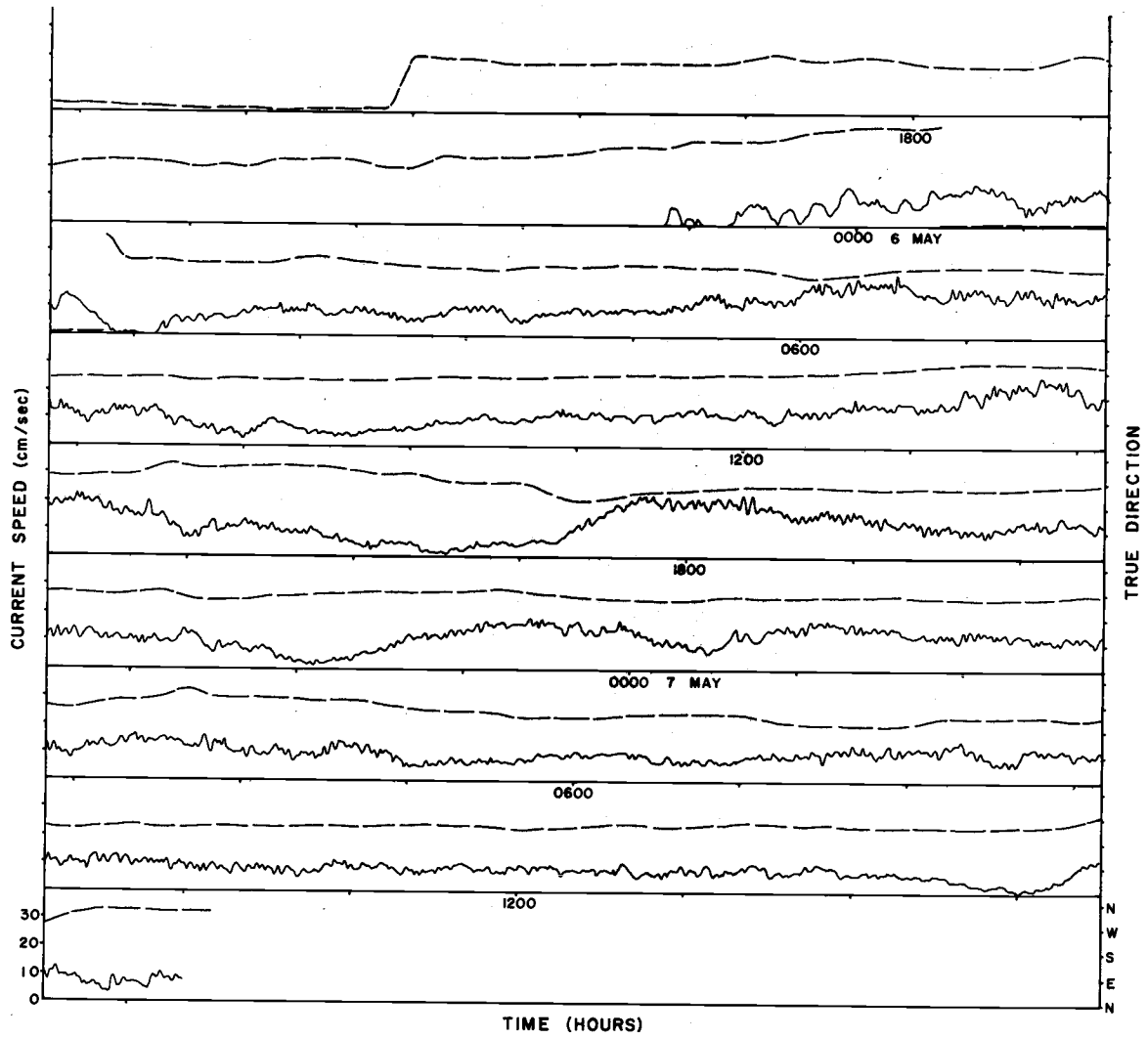

Figure 27. Cruise Y 7105 A, 165 meters. 45° 59.4'N, 124° 36.2'W. Current speed (solid line) and direction (dashed line).

The only significant peak in the frequency power spectrum (Figure 28a) corresponds to a period of 6.5 hours, and virtually no energy is contained at frequencies higher than two cycles per hour. The 2.2-hour period seen at the 165-meter depth for cruise Y 7104 C is not distinct in this spectrum.

The current direction was generally offshore, with no apparent rotation (Figure 29).

Results of Optical Measurements

Continuous transmissometer readings were taken from the surface to the bottom along four transects of the continental shelf. In addition, three time-series stations were occupied for periods of up to 12 hours. Scattered stations in the vicinity of the shelf edge west of Yaquina Head complete the transmissometer data. Complimentary data were obtained at four stations during cruise Y 7102 F by making in-vitro light-scattering measurements using a Brice-Phoenix light scattering photometer. Finally, temperature-depth profiles were observed concurrently with transmissometer readings during cruises Y 7104 C and Y 7105 A. As with the results of the bottom-current observations, the optical data is presented chronologically.

Cruise Y 7102 A

The narrowest part of the continental shelf, along latitude 45°

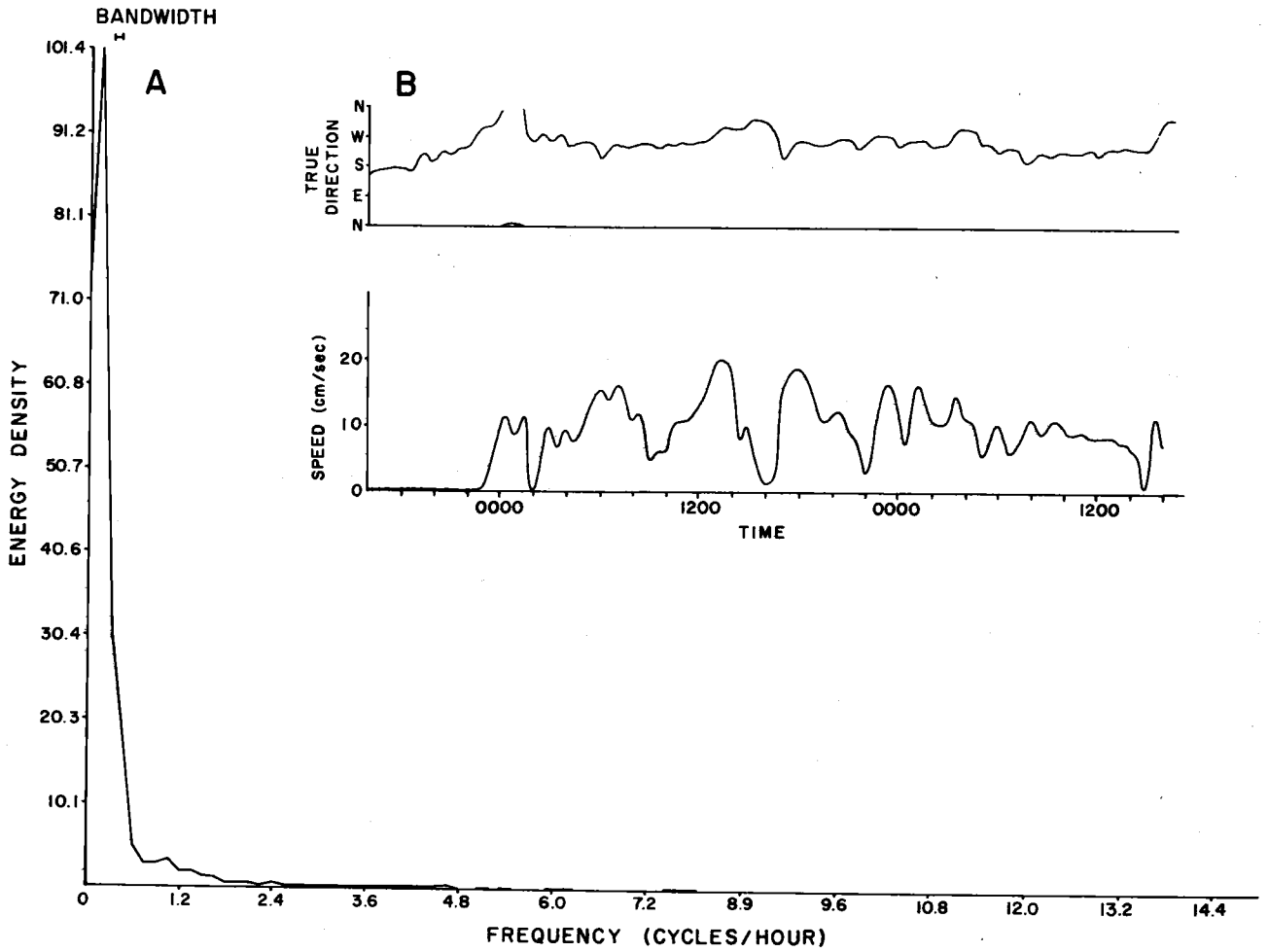

Figure 28. Cruise Y 7105 A, 165 meters. 45° 59.4'N, 124° 36.2'W.
(a) Frequency power spectrum. Energy density units are $(cm/sec)^2/0.5$ cpm.
(b) Smoothed record of current direction and speed.

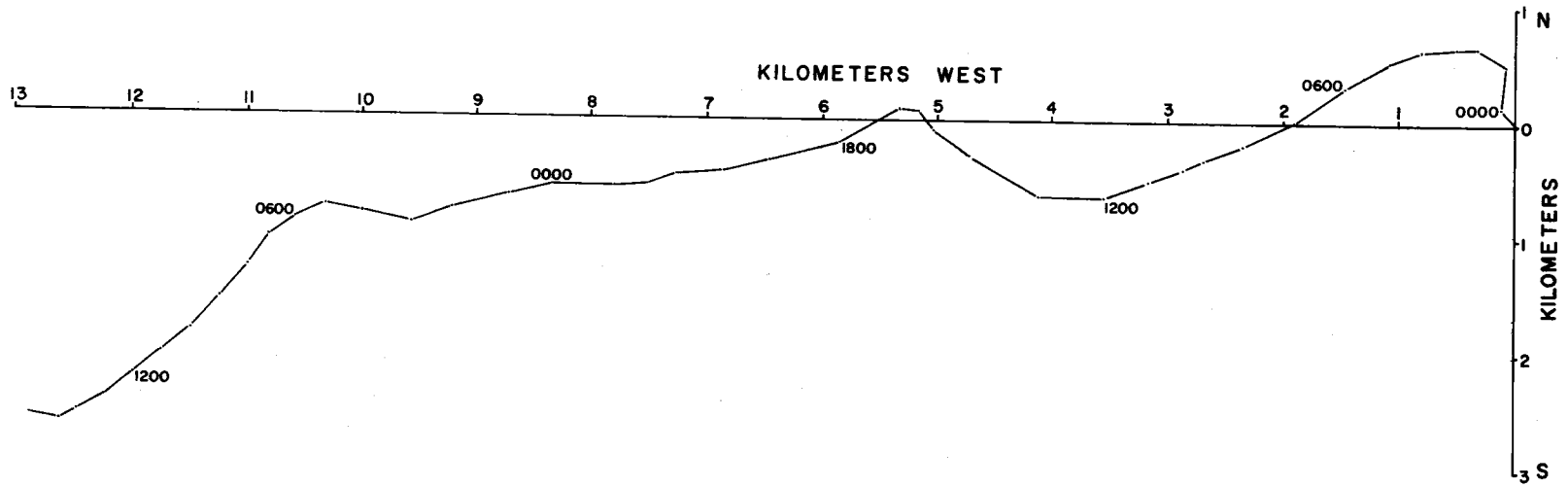

Figure 29. Cruise Y 7105 A, 165 meters. 45° 59.4'N, 124° 36.2'W. Progressive vector diagram.

11'N, was selected as the site of the first observations of turbidity-depth profiles. The shelf gradient at this location is regular, and contours closely parallel the shoreline. Stations were made at 18.3-meter intervals (ten fathoms) from the nearshore region to upper slope depths. Bottom currents were also measured for approximately one hour at each station and additionally on the upper slope at a depth of 275 meters.

The turbidity-depth profiles (Figure 30) reveal a shape which we have found to be characteristic of shelf waters under both winter conditions (which persisted during these observations) and summer conditions. In each profile, three levels exist where light transmission is a minimum. In Figure 30, these layers, which are interpreted as turbid layers, are a surface layer about 15 meters thick, a mid-water layer whose intensity decreases and whose thickness increases from the nearshore station toward the shelf edge, and a bottom layer whose thickness and intensity are variable. At the shallowest station, the mid-water layer is the most intense of the three, but from there to mid-shelf the bottom layer predominates. The surface-turbid zone is strongest of the three from mid-shelf to the shelf edge.

Mean bottom currents for the period of each individual observation are presented vectorially in Figure 30. Currents were highly variable in both direction and speed from station to station, and it is difficult to assess any periodic trend. These mean velocities will be

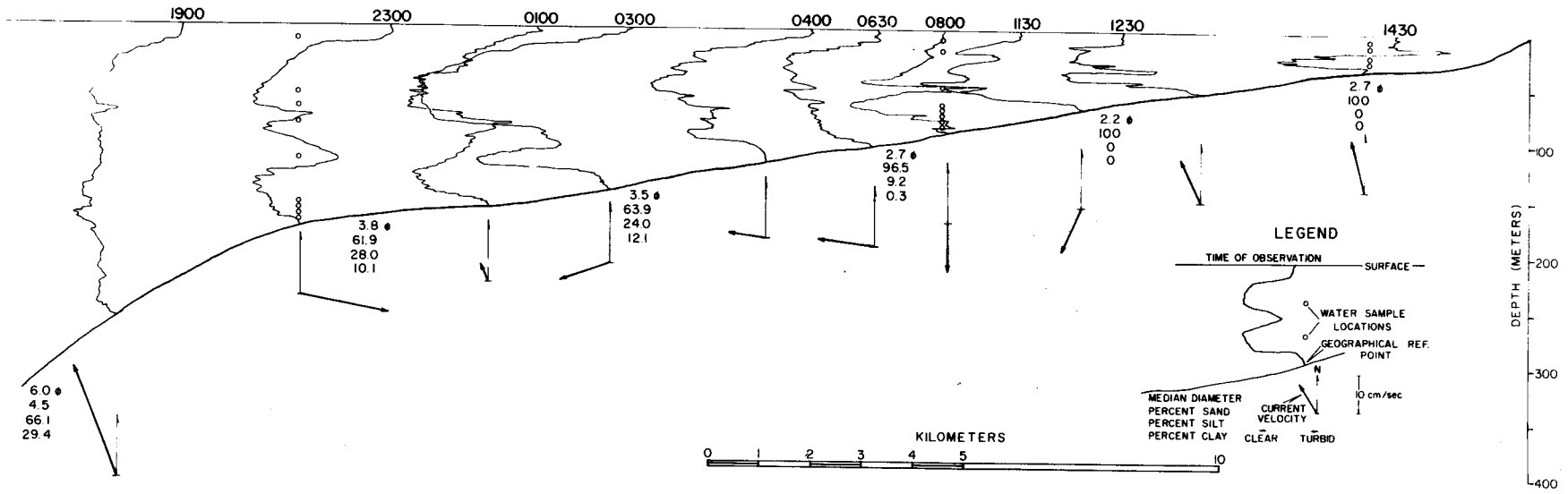

Figure 30. Cruise Y 7102 A. Turbidity profiles and bottom currents along latitude 45° 11'N. Relative values of turbidity can be compared only within the same profile. Absolute comparison of turbidity between stations is not possible.

treated as instantaneous velocities which were present at the time of the light-transmission measurements. This assumption is reasonable since, although the current velocities varied strongly from station to station, the variability was not present at individual sites.

Water samples were obtained at selected depths at four stations. In vitro scattering curves obtained from these samples are presented in Figure 31. The scattering values generally show agreement with the transmissometer data.

A second profile and two time-series stations were made west of Yaquina Head during the latter half of this cruise. In contrast to the first transect, the shelf here is relatively wide and irregular, with a broad mid-shelf region adjacent to Stonewall Bank.

Six profiles of turbidity alternating with five observations of bottom current were obtained during a ten-hour time-series station on February 11, 1971, at 165 meters depth, 40 kilometers west of Newport. These profiles (Figure 32) show the relatively stable light-transmission properties of the waters in the outer shelf region. Again, three turbid layers can be discerned, although the mid-water layer is rather diffuse. The mid-water layer was also diffuse at a comparable depth in the observations along latitude 45° 11'N. The thickness and intensity of the bottom layer vary rather markedly, probably in response to the changing bottom-current strength.

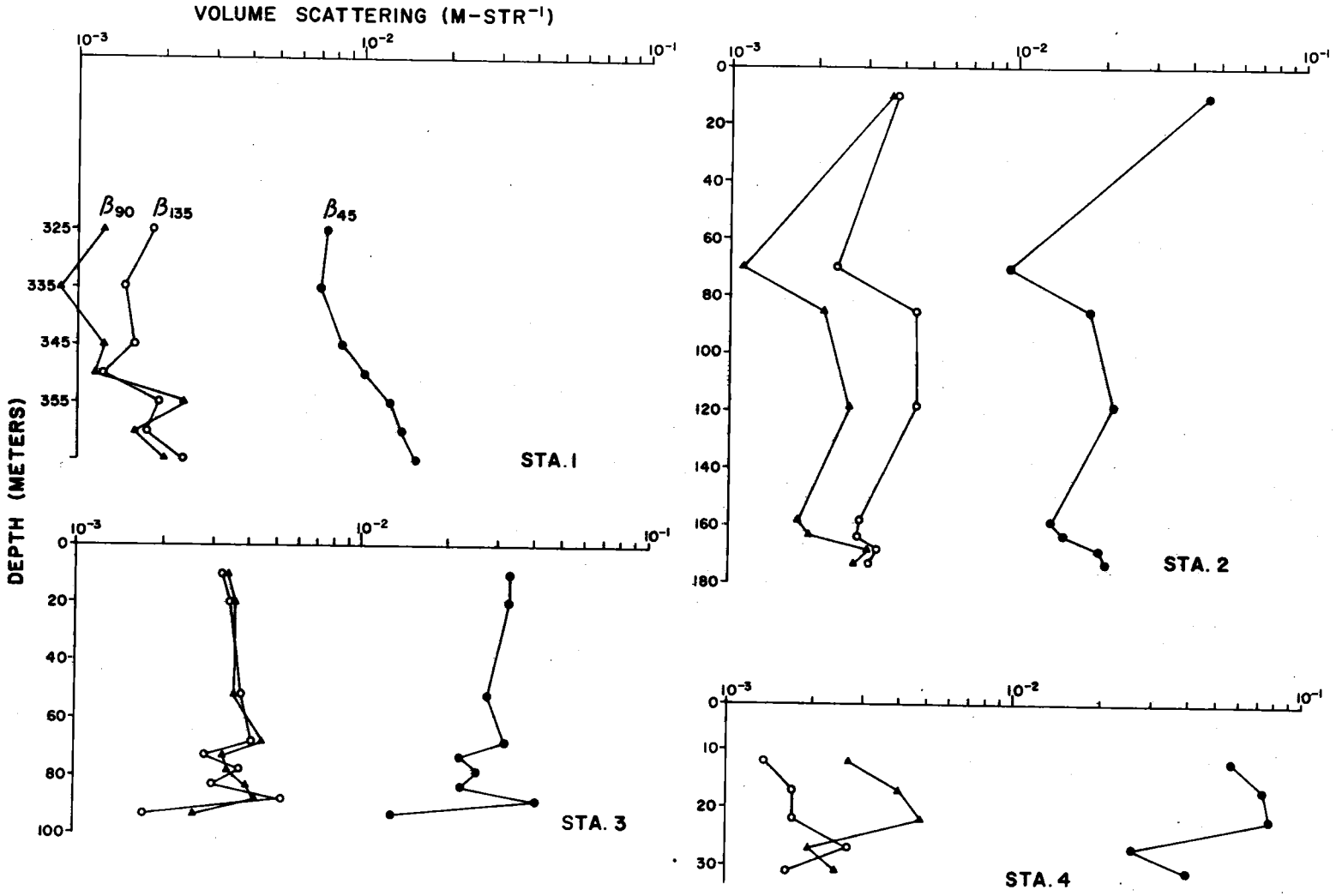

Figure 31. Scattering values for water samples obtained at selected stations along latitude 45° 11'N. Sample locations shown in Figure 33. Scattering units are meters/steradian.

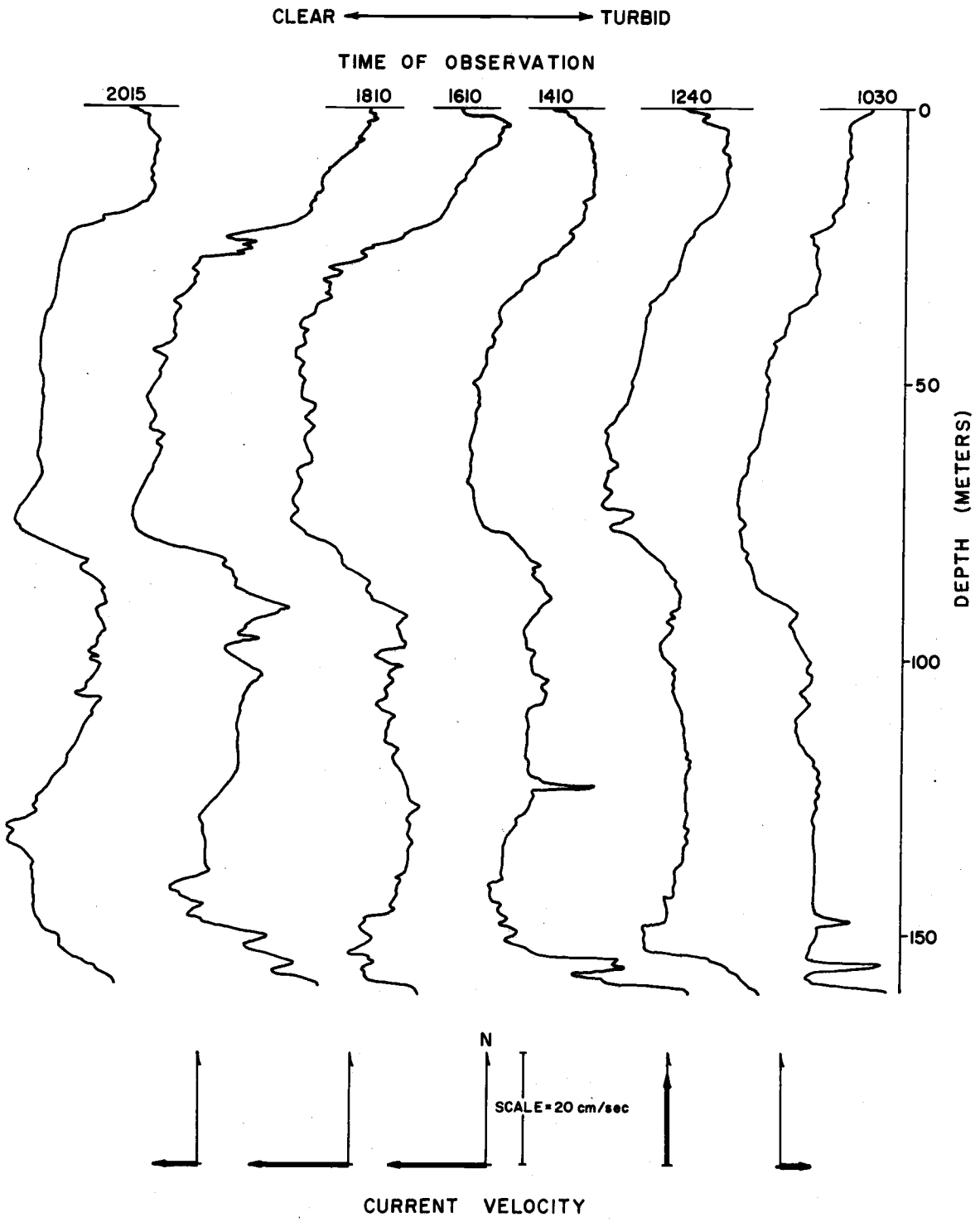

Figure 32. Cruise Y 7102 A, 165 meters. 44° 39.3'N, 124° 33.4'W. Time series of turbidity profiles and bottom currents. Bottom current vectors represent average current between turbidity observations. Relative values of turbidity can be compared only within the same profile. Absolute comparison of turbidity between casts is not possible.

Bottom currents are presented as velocity vectors in Figure 32. Current strength increased from near threshold to over ten cm/sec between the 1030 and 1240 observations of turbidity. Velocities remained at a relatively high level until nearly 1900 when a sharp decrease in strength was recorded. Between the final two turbidity observations, current velocity continued to fall at a decreased rate.

A second time-series station at 91-meters depth again displayed the characteristic three layers of turbidity (Figure 33). Bottom currents were fairly consistent in direction and strength; currents are again represented vectorially.

Turbidity profiles were measured at 18.3 meter (ten fathom) intervals from 37 meters to 165 meters depth in a second transect of the shelf. Along this transect (Figure 34), the thickness and intensity of the bottom turbid layer were somewhat less than had been observed in the earlier transect, although a distinct mid-water layer was observed. Bottom currents were recorded for a short period at four of the stations, and the results are represented vectorially.

In vitro scattering values from water samples obtained at the 165-meter station are presented in Figure 35.

Cruise Y 7104 C

Five profiles of turbidity were recorded at stations near the shelf edge about 32 kilometers west of Depoe Bay (Figure 36). As

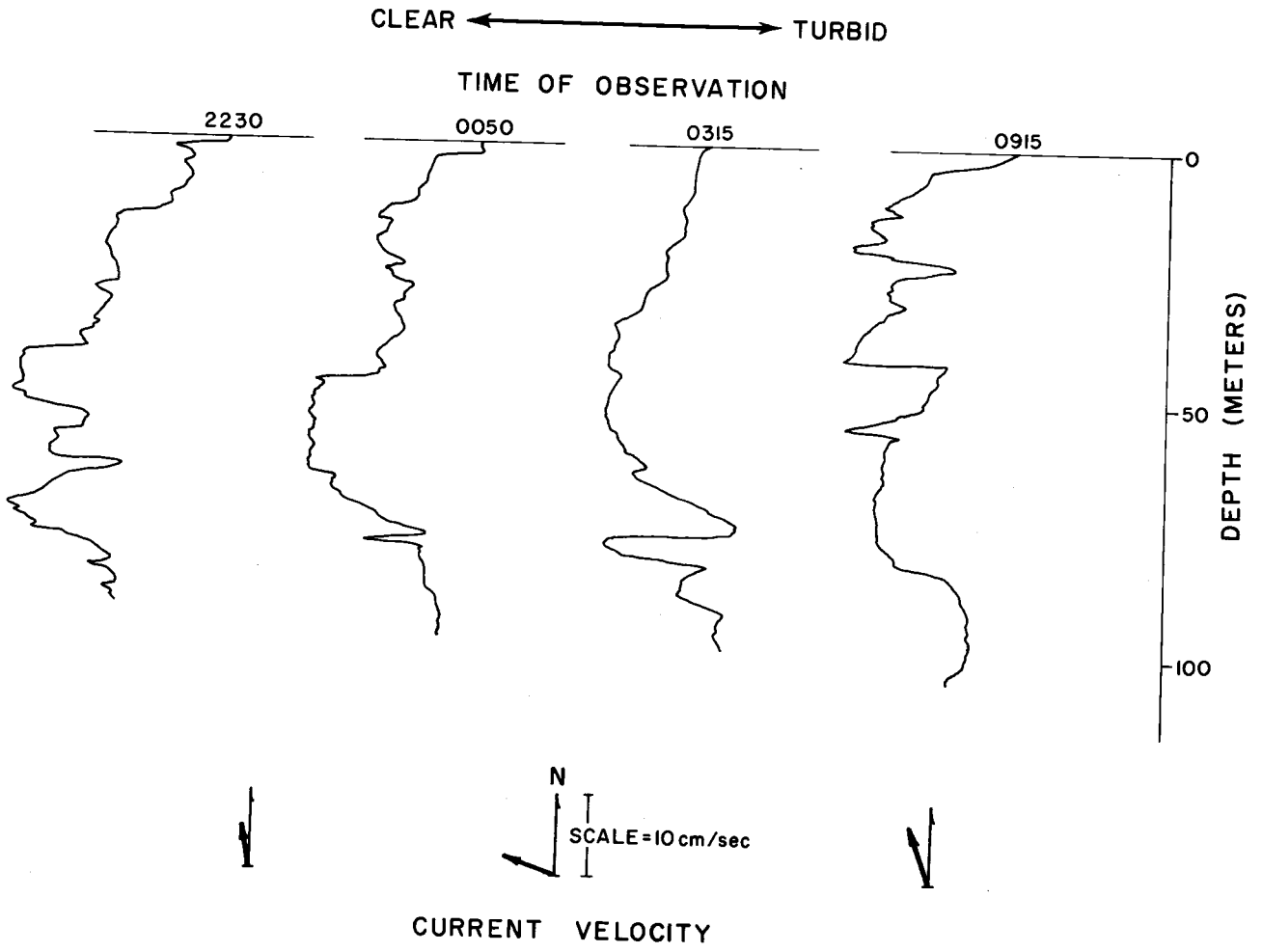

Figure 33. Cruise Y 7102 A, 91 meters. 44° 38.6'N, 124° 76.5'W. Time series of turbidity profiles and bottom current. Bottom current vectors represent average bottom currents between turbidity observations. Relative values of turbidity can be compared only within the same profile. Absolute comparison of turbidity between casts is not possible.

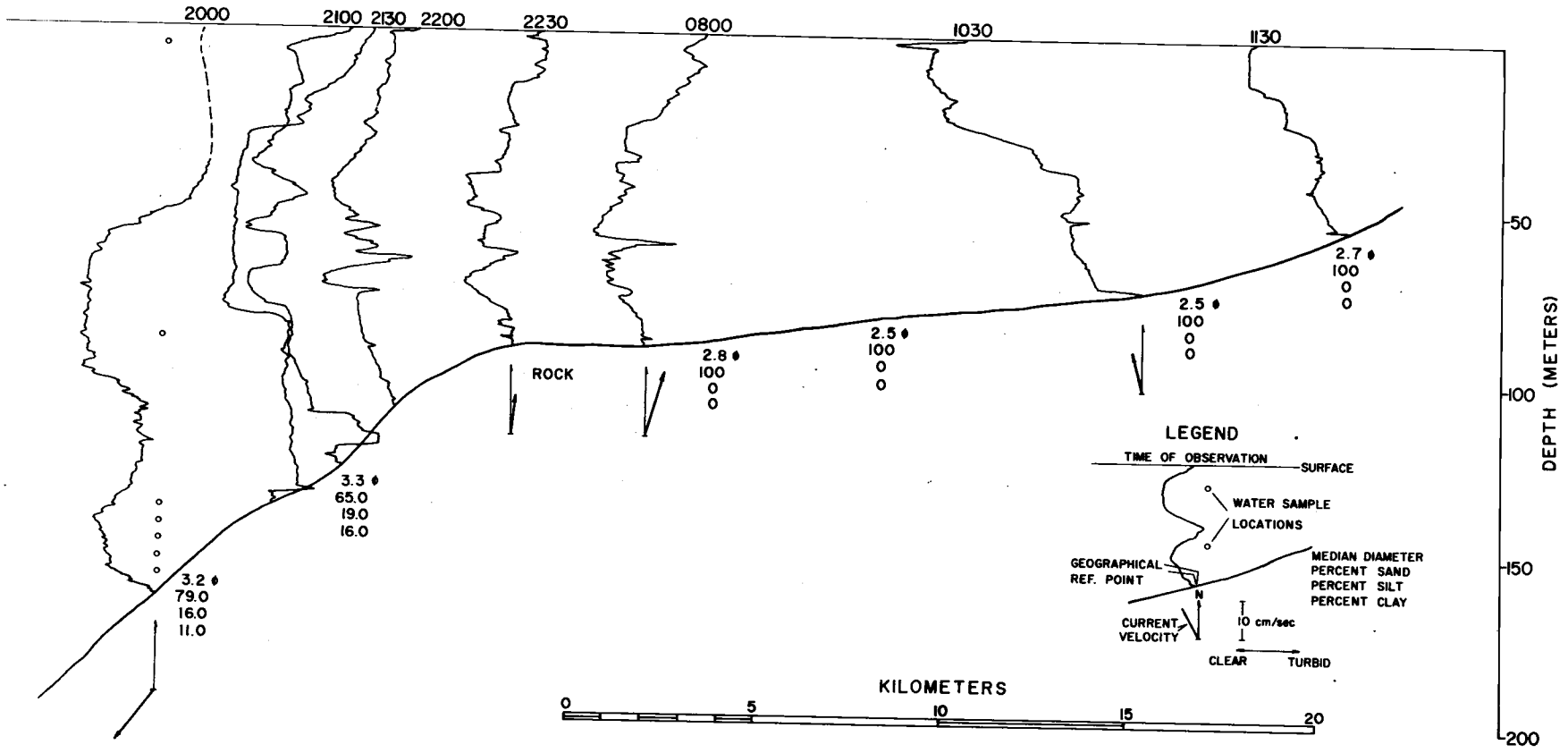

Figure 34. Cruise Y 7102 A. Turbidity profiles and bottom currents along latitude 44° 40'N. Relative values of turbidity can be compared only within the same profile. Absolute comparison of turbidity between stations is not possible.

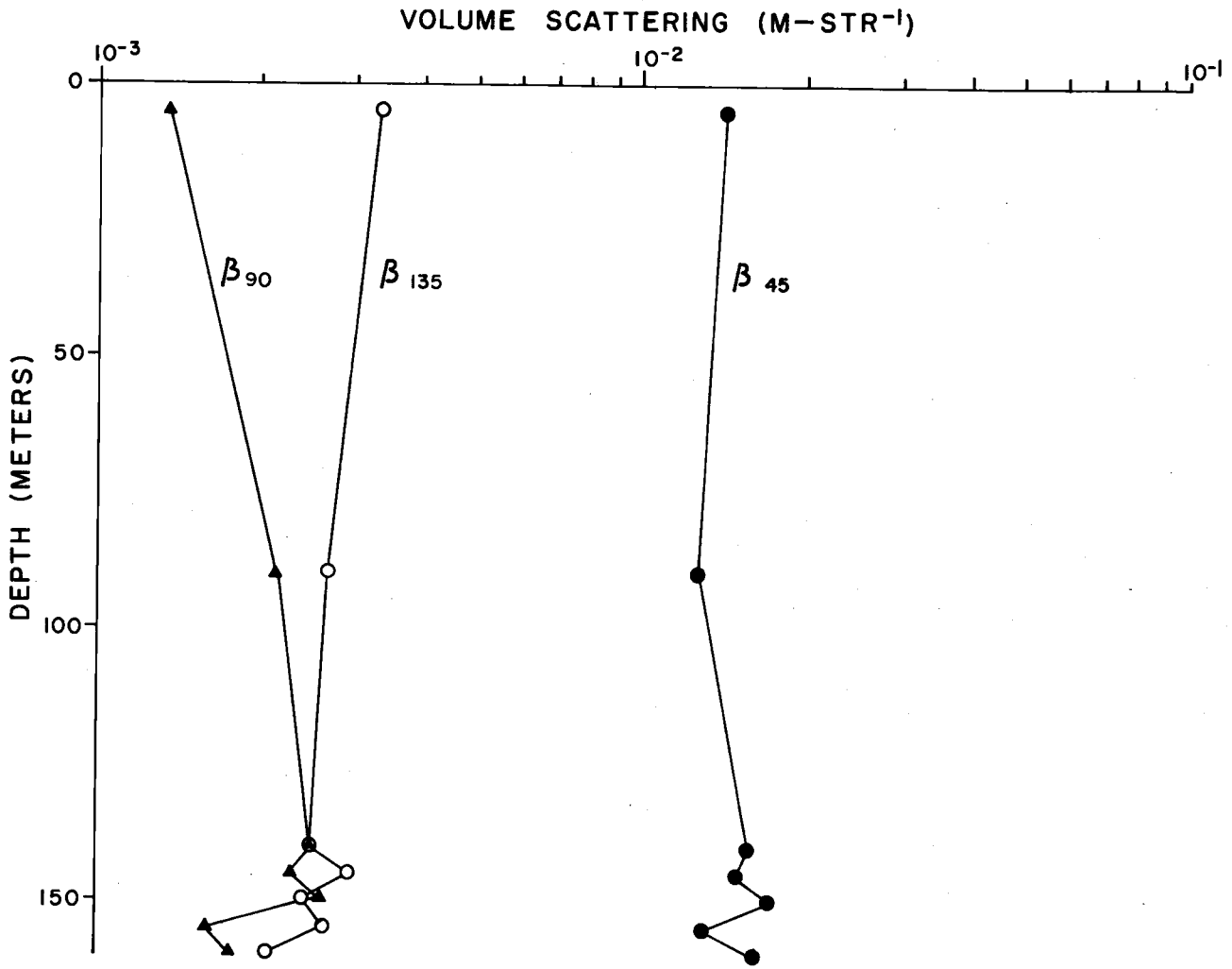

Figure 35. Cruise Y 7102 A, 165 meters. 44° 39.3'N, 124° 33.4'W. Scattering values for water samples obtained near the shelf edge. Sample locations are shown in Figure 34. Units of scattering are meters/steradian.

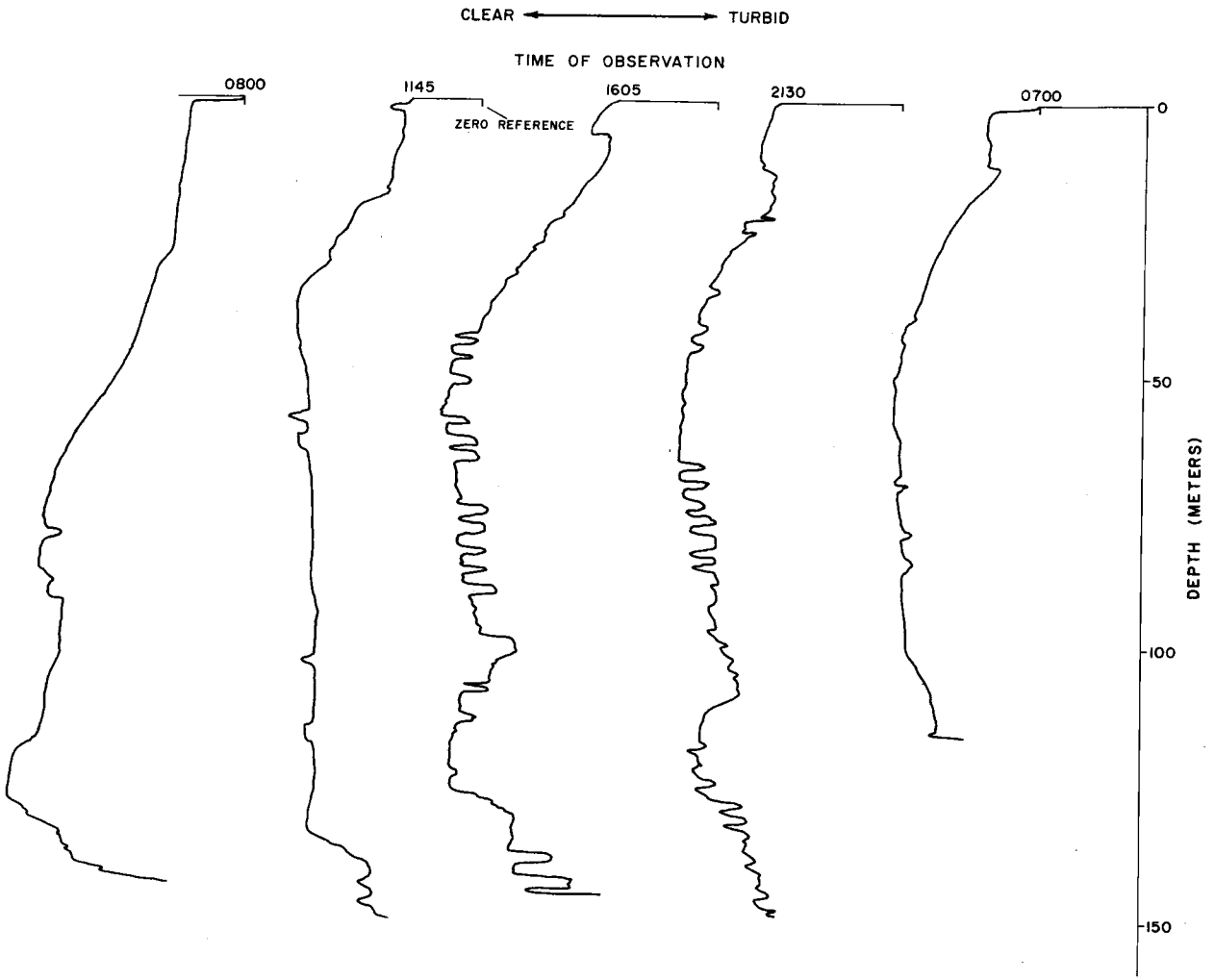

Figure 36. Cruise Y 7104 C. Profiles of turbidity at scattered stations near the shelf edge in the vicinity of 44° 49.0'N, 124° 26.0'W. Comparisons of turbidity between profiles can be made by referring to the zero reference mark for each curve.

in the previous observations made near the shelf edge, these profiles show a relatively weak but easily recognized mid-water layer. Surface and bottom layers are also present, although they, too, are weak.

No bottom-current observations were made in direct support of the turbidity measurements, although a current meter was moored in the vicinity. The current meter records are presented in Figures 19 and 21.

Cruise Y 7105 A

Two transects of the continental shelf and a 12-hour time series of turbidity profiles were made at the widest part of the northern Oregon continental shelf, along latitude 45° 59'N. These observations took place during the summer oceanic regime, with brisk northerly winds prevailing. No hydrographic observations were made, but it is under such conditions that coastal upwelling develops. Shoreward flow observed at mid-shelf may be an indication that upwelling was in progress.

In the May 5th transect, profiles were obtained every 18.3 meters (ten fathoms) from nearshore to shelf-edge depths, with an additional observation on the upper slope (Figure 37). Profiles on the May 7th transect were measured at the same interval but the shallowest station was at 18 meters (Figure 38). Similarity is the rule rather than the

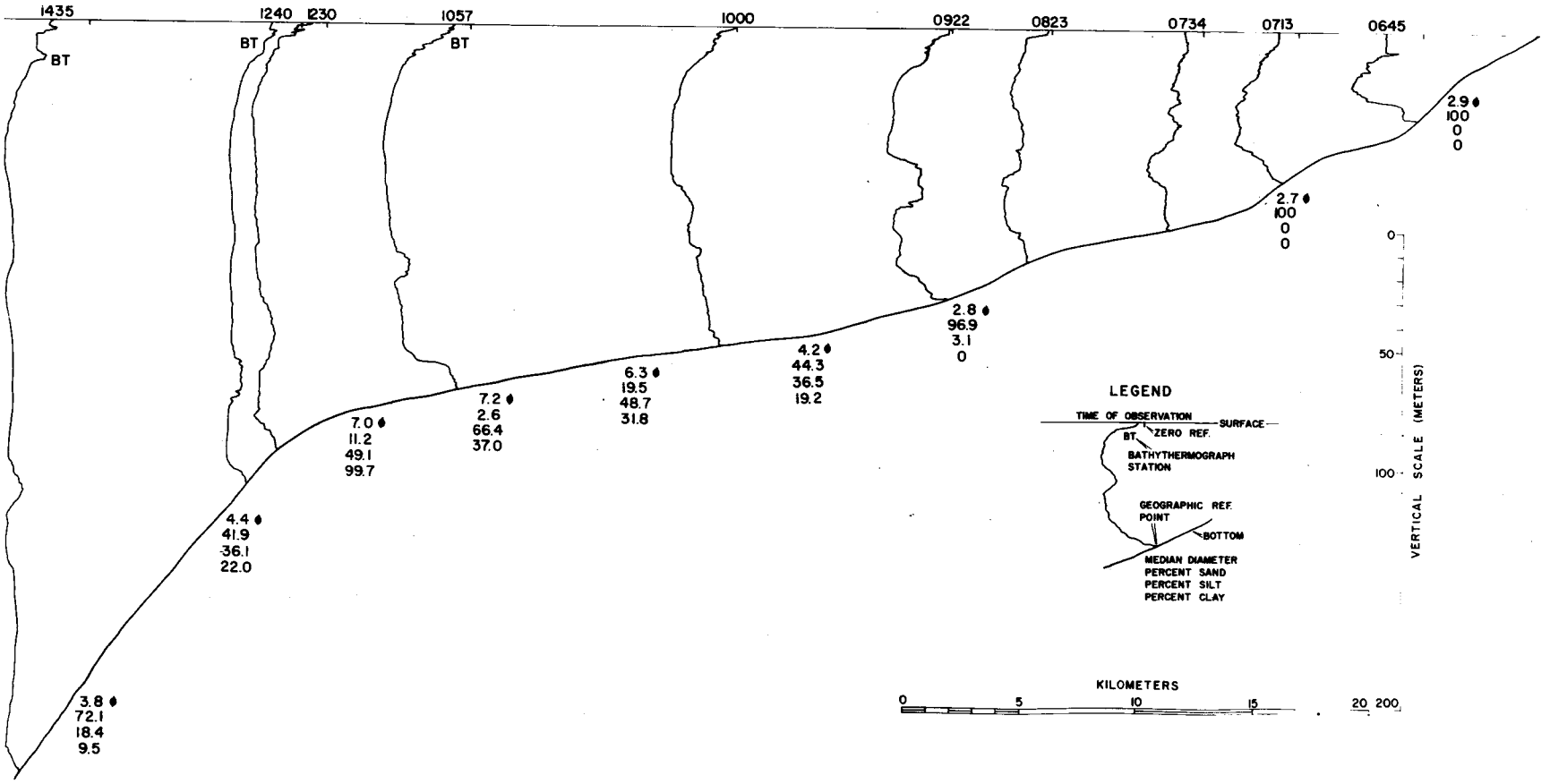

Figure 37. Cruise Y 7105 A, May 5. Turbidity profiles along latitude 45° 59.0'N. Turbidity scale increases to the right. Comparisons of turbidity between profiles can be made by referring to the zero reference points at the right of the tops of the profiles. BT data is shown in Figure 41.

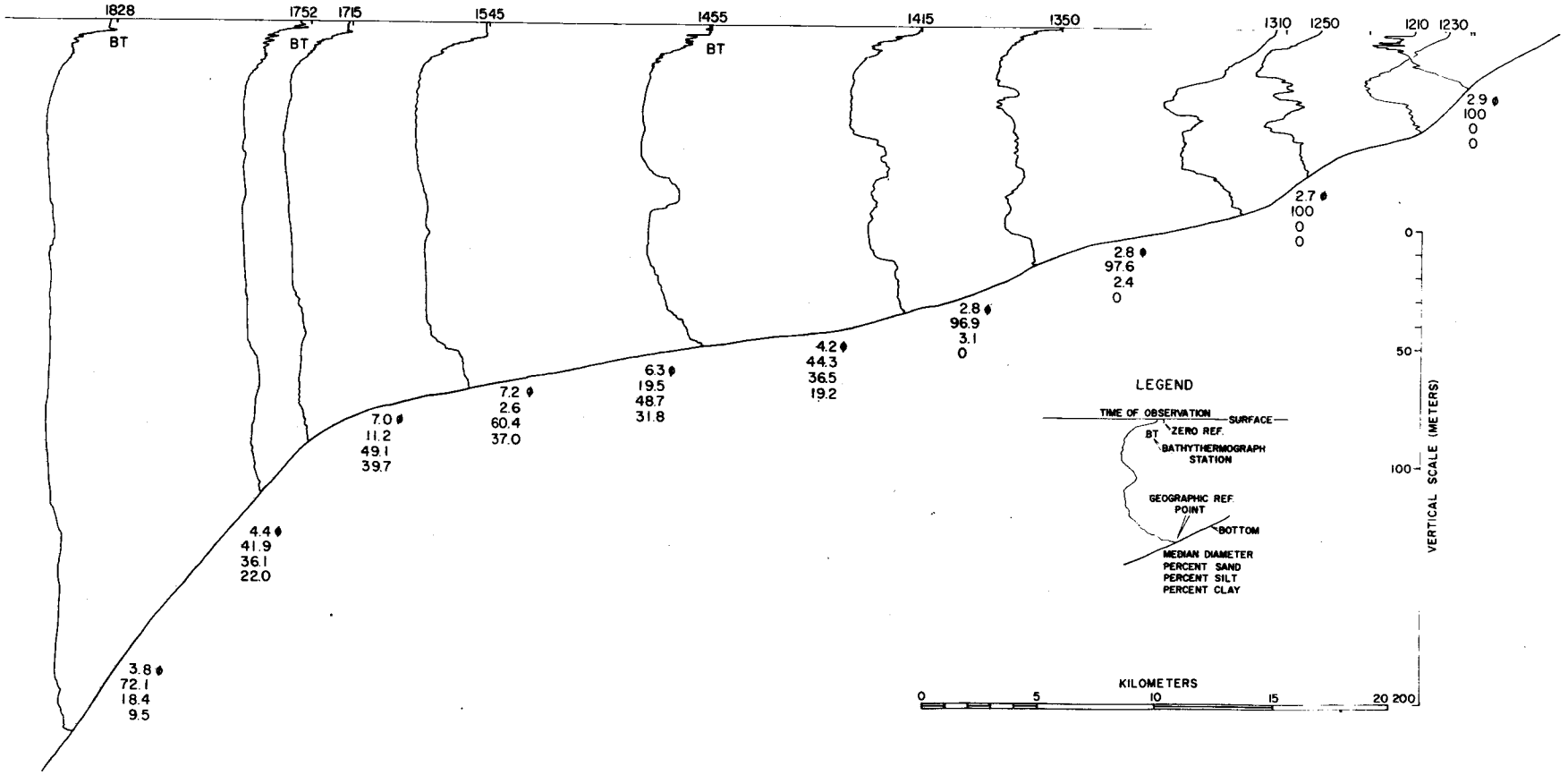

Figure 38. Cruise Y 7105 A, May 7. Turbidity profiles along latitude 45° 59.0'N. Turbidity scale increases to the right. Comparisons of turbidity between profiles can be made by referring to the zero reference points at the right of the tops of the profiles. BT data is shown in Figure 41.

exception when comparing the results from the two days, although minor differences appear. Again, three turbid layers are present though the mid-water layer does not appear to be as intense as in earlier measurements further south. This may be due to the previously noted differences in recording equipment, although the higher background turbidity resulting from the Columbia River effluent may somewhat mask the mid-water turbid layer. Unfortunately, because two different recording systems were used, there is no way to compare absolute values between the February observations and those which were made later.

The time-series station site was chosen to allow turbidity observations over the finest-grained sediment on the northern shelf (Figures 5 and 6a). The bottom layer here was relatively thick and intense(Figure 39), and both parameters increased markedly during the period from 0600 to 1000. The intensity of the mid-water layer was fairly constant although its thickness and distance above the bottom varied slightly.

Bottom currents at 91 and 165 meters on the transect line were recorded during the period May 5 - 7. The records are presented in Figures 24 and 27.

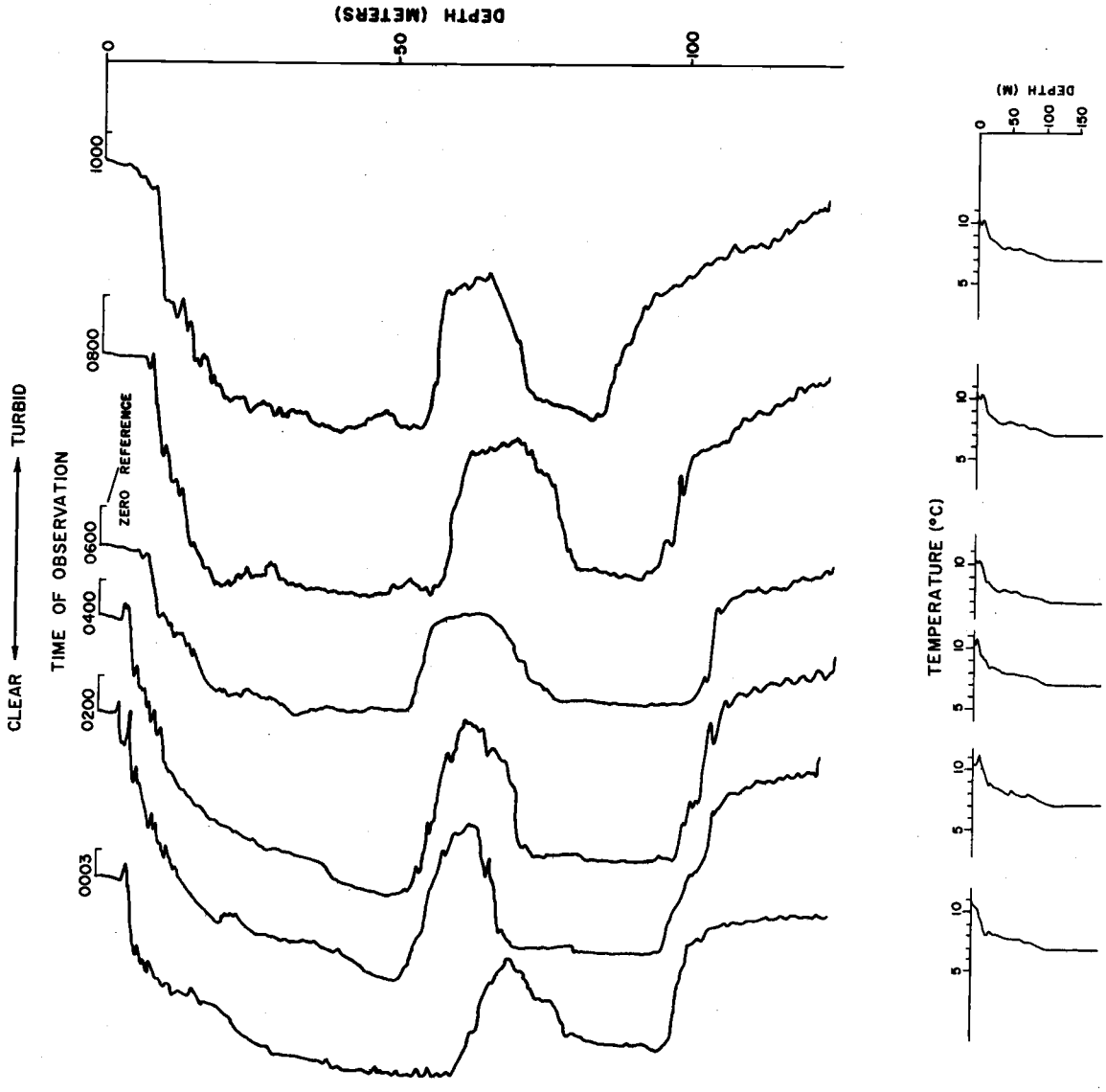

Figure 39. Cruise Y 7105 A. 45° 59.0'N, 124° 20.0'W. Time series of concurrent turbidity and temperature profiles. Comparisons of turbidity between stations can be made by referring to the zero reference points at the right of the tops of the profiles.

DISCUSSION OF DATA

Currents

On the basis of observations of this study and from information available from previous studies, a general picture of sediment transport on the northern Oregon continental shelf can be drawn.

Bottom currents on the northern Oregon continental shelf are generated largely in response to tides. At the mid-shelf stations, the dominant period of the current oscillations is near 12 hours, as shown in the progressive vector diagram for cruise Y 7105 A (Figure 26) and as shown by the rotational period of current direction during cruise C 7006 B (Figure 11) and during cruise Y 7105 A (Figure 25b). Estimates of frequency power spectra indicate that the dominant period is greater than six hours, but because of the relatively short duration of the record the peak cannot be resolved.

Shelf-edge bottom currents have a dominant period of near six hours. In every frequency power spectrum computed for shelf-edge currents, the six-hour period was dominant (Figure 14a, 22a, and 25a). Direction records at the outer shelf show a periodicity of 12 hours also (Figures 22b and 29). Mooers (1970) also noted a periodicity of near six hours in currents over the shelf, and he ascribed this period to the second harmonic of the internal tide.

Based on the observations of this study, short-period oscillations

due to surface waves are apparently significant only in water shallower than 90 meters. This is attested to by the lack of significant amounts of energy associated with frequencies in the range from about five to 30 cph. However, strong influence from short period phenomena was apparent at a depth of 36 meters. According to wave theory, one would expect a greater influence due to surface waves in shallower water. At a depth of 90 meters, for instance, in order for the bottom effects of surface waves to ripple fine sands (2ϕ to 3ϕ), the significant wave period must be in excess of ten seconds; the minimum wave height required with this period is 6.5 meters (Neudeck 1971). Such waves are known to occur an average of 0.5% of the time on the Oregon coast (National Marine Consultants, 1961). Such large waves are probably responsible for the ripple formation noted by Neudeck (1971) near the shelf edge. When viewed over geologic time these relatively infrequent events may be significant. This study indicates that over the shorter time spans surface waves are not an active erosive mechanism on the outer shelf. The importance of surface waves lies in eroding sediments at shoaler depths, and in maintaining them in suspension across the shelf.

No significant amount of energy was apparent in any of the records at frequencies which would indicate short-period (less than 0.5 hours) internal waves. However, Mooers (1970) reported a semi-diurnal internal tide propagating onshore as a progressive wave with

a 30-kilometer wavelength. Internal waves being generated at the shelf edge in response to tidal motion probably are the dominant current generating mechanism.

If short period internal waves do occur on the northern Oregon continental shelf, their main effect would probably be that of placing material in suspension. Cacchione and Southard (1970) performed laboratory studies which show that upslope amplification of bottom shear stress associated with breaking internal waves is strong enough on continental slopes and shelves for sediment motion to occur. Further experiments reported by Southard et al. (1971) indicate that shoaling internal waves act upon the sediment in much the same way as do surface waves, with scour in the swash zone, deposition of a low bar and development of oscillation ripples. If internal waves are responsible for net transport of sediment, and if one can draw an analogy to surface waves, the direction of transport should be onshore in the region of breaking internal waves.

Lower frequencies than those which could be resolved in this study have been reported in several other studies of surface and subsurface currents on the Oregon coast. Mooers and Smith (1968) analyzed tide records and found continental shelf waves with frequencies of 0.1 cycles per day (cpd) moving toward the south and 0.35 cpd moving toward the north. Collins (1968) also noted frequencies of 0.14 cpd, one cpd, two cpd, and 1.4 cpd. Stevenson (1966) found

frequencies of two cpd were most common, although one cpd and 1.4 cpd frequencies were also important. The one and two cpd frequencies are tidal frequencies and the 1.4 cpd frequency corresponds to the inertial frequency at this latitude.

The importance of the low-frequency currents to sediment transport is probably their influence on the current direction. Current direction records reveal none of the short-term oscillations so characteristic of the current speed. While it is variable from site to site, direction of flow changes rather slowly and steadily during most observations. The resulting net transport of water and thus the suspended sediment it contains is clearly shown in the progressive-vector diagrams. Southerly and westerly transport dominates although onshore flow may result from local conditions. The onshore flow observed at 90 meters during cruise Y 7105 A is probably due to coastal upwelling in response to offshore transport of surface water by northerly winds (Smith et al., 1966). The high percentage of onshore direction at 175 meters during cruise C 7006 B does not necessarily indicate onshore transport, since speeds corresponding to the directions are not known.

Pillsbury et al. (1970) observed southerly flow at 18 meters above the bottom on the inner shelf, 13 kilometers west of Depoe Bay. Collins (1967) noted currents in mid-water over the continental shelf were southerly in July but northerly in September and October. Over

the continental slope west of Newport, Stevenson (1966) measured mean southerly transport throughout the water column during the summer with some surface transport to the north occurring in the winter.

The Columbia River is probably the largest contributor of suspended sediment to the northern Oregon continental shelf. In the winter, during periods of low runoff, the northerly current inshore carries the suspended material a relatively short distance to the north (Duxbury, 1965). In the late spring and early summer, however, the southerly current transports the Columbia River plume far to the south. It is during the late spring and early summer months that the Columbia River discharge is the greatest (Morse and McGary, 1965). Thus, based on currents observed in earlier studies, a net southerly transport of sediments from the Columbia River should take place.

Currents observed during the present study reinforce this conclusion. With the exception of the mid-shelf station during cruise Y 7105 A, at which the flow was onshore (Figure 26), all progressive vector diagrams indicate flow was offshore and to the south. Mean bottom-current speeds around 10 cm/sec were the rule at mid-shelf and shelf-edge depths; slightly stronger currents occurred at the shelf edge than were found at mid-shelf. Nearshore bottom currents, on the other hand, were much stronger, with a mean strength nearly three times that of deeper currents. Large fluctuations in speed were

common over very short periods in all records, giving the currents a "gusty" effect. Current speeds greater than 20 cm/sec were not uncommon, although they were seldom sustained. The same is true of slack currents near or below the threshold velocity of the meter.

Optical Observations

Every transmissometer profile shows three distinct layers of turbid water, a surface layer, a mid-water layer, and a bottom layer. Pak (1969) also saw evidence of these layers, although less clearly because his observations were based on discrete samples. Pak et al. (1970) associated a strong mid-water turbid layer three to 13 kilometers west of Depoe Bay with a temperature inversion during coastal upwelling, although they observed that the turbidity maximum persisted after the thermal inversion disappeared. Wildharber (1966), using discrete samples also, found turbid layers at the thermocline and near the bottom off the southern California coast.

The Surface Layer

The turbid layer at the surface closely corresponds to the level of the seasonal thermocline. This relation can best be seen in the time-series profiles from cruise Y 7105 A (Figure 39). The material in the surface layer is hindered in sinking by the relatively denser and more viscous cold water below the thermocline. If such a condition

were to persist for a long period of time, one would expect the surface layer to consist of the finest size fraction and of less dense materials, the larger and denser materials sinking through the seasonal thermocline. Wind mixing and convective mixing would destroy the stratification with the result that all of the material in the surface layer would fall deeper in the water column. This effect can be seen in the profiles from cruise Y 7104 C, where the surface turbid layer is very diffuse. The seasonal thermocline was not well developed during these observations (Figure 40).

In an area where a great volume of suspended sediment is available, such as near the mouth of the Columbia River, the surface turbid layer will be most intense near the source and progressively more diffuse away from the source. This phenomenon is known as the Columbia River plume on the Oregon continental margin, and has been studied in detail by Pak (1969), who traced the plume by measuring particle scattering in the surface layer. The plume extended nearly 240 kilometers south from the river mouth during Pak's observations, covering nearly half of the Oregon continental shelf. In view of the vast amount of sediment supplied by the Columbia River, the importance of this mode of transport to sedimentation on the Oregon shelf is great.

On the central Oregon shelf, where no large river supplies suspended sediment, the surface turbid layer is supplied from the

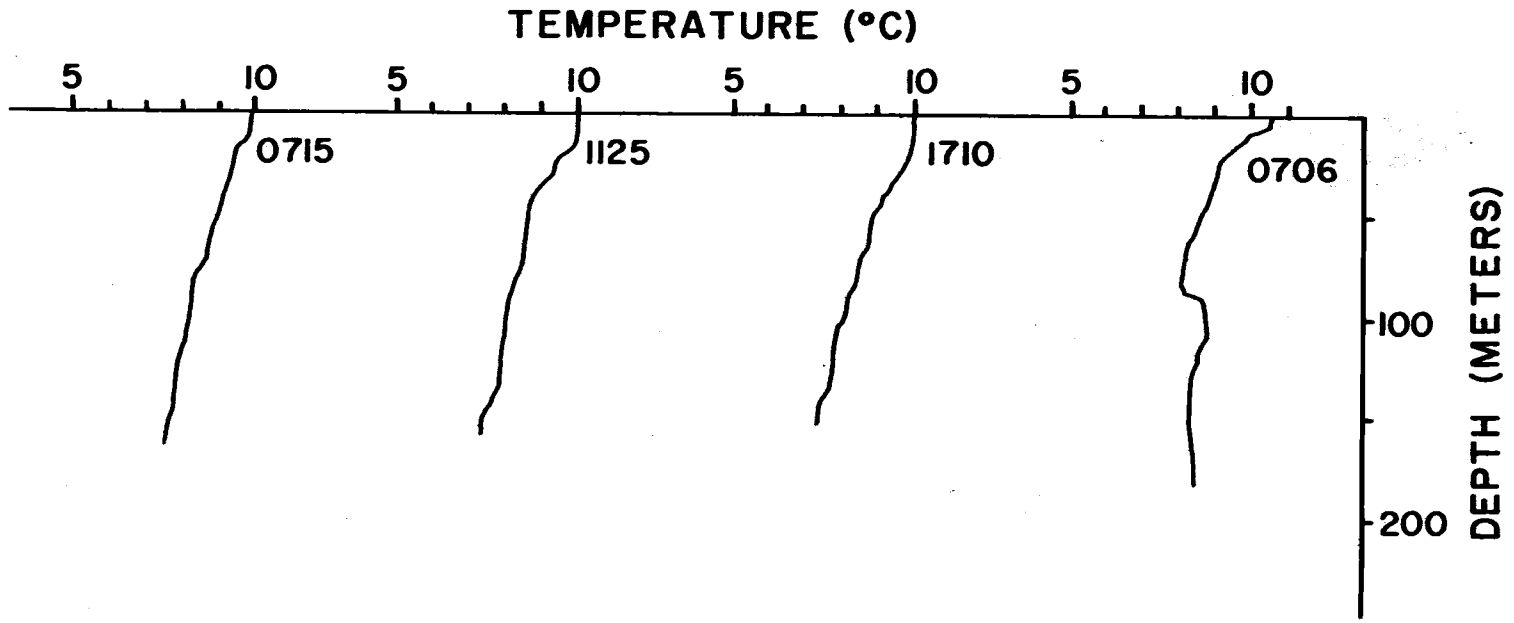

Figure 40. Cruise Y 7104 C. Temperature-depth profiles observed concurrently with turbidity profiles of Figure 39.

nearshore zone. Sediment in the nearshore zone has three major sources: coastal streams, erosion of coastal landforms, and sea bed material transported onshore into the surf zone by wave surge. Coastal streams deposit most of their coarse load in estuaries but the fines make their way to sea by diffusion through the surf zone and via tidal and rip currents. The coarse sediments that find their way into the surf zone are transported by longshore currents. These coarse sediments are constantly being abraided in the high energy environment of the surf zone. As the sediments become finer, some escape seaward from the surf zone, at considerable distances from their original source. Likewise, sediment derived from erosion of coastal landforms and from offshore sources is also distributed by the longshore transport in the surf zone.

The Mid-water Layer

An omnipresent feature of the turbidity profiles in both the summer and winter is the mid-water turbid layer. This feature is evident in every observation of turbidity although the intensity and thickness of the layer vary a great deal. Perhaps the most striking aspect of the profile is seen in the transect along latitude 45^{o} 11'N (Figure 30), made during February, 1971. The mid-water layer nearshore is only about five meters thick but is more intense than either the bottom layer or the surface layer. Moving progressively

seaward, the layer gradually thickens and become relatively less intense when compared to the surface and bottom layers. The layer is sub-parallel to the bottom over the shelf, but becomes very diffuse beyond the shelf-slope break.

In the transect along latitude 44° 40'N (Figure 34), the mid-water layer is neither as intense nor as thick as along 45° 11'N. In the interim between the times when the two transects were made, a rather strong storm of about 24-hours duration passed through the area. The profile along 44° 40'N is taken to be representative of a well-mixed water column. Thus, the mid-water layer along 44° 40'N may be considered youthful, although the characteristics described for the earlier transect still hold true there. The layer closely parallels the shelf gradient while thickening in the seaward direction. At the break in slope seaward of the 2230 observation, the mid-water layer appears to separate somewhat from a path parallel to the bottom. This occurs more distinctly in the profiles made in May, 1971 along latitude 45° 59'N (Figures 37 and 38), where, after it crosses the shelf-slope break, the mid-water layer very plainly continues along much the same gradient as before.

In the time-series profiles, the mid-water layer remains nearly constant in thickness and intensity although some oscillatory vertical migration is apparent in the Y 7105 A series (Figure 39). This migration is also apparent in the permanent thermocline, and

might indicate the influence of internal tides.

The position of the mid-water turbid layer coincides with the position of the permanent pycnocline in coastal waters (Pak et al., 1970). The fact that the layers coincide is not surprising in view of the importance of density stratification in the surface layer. The denser water below the pycnocline can prevent somewhat larger particles from settling than can the surface layer. The intensity of the mid-water layer depends largely on sediment supply. This explains the decreasing intensity with distance from the shore. In the profiles close to the Columbia River, the plume itself acts as a source of particles so the seaward decrease in mid-water turbidity is not as pronounced there. Particles from the surface layer will also continue to sink to the mid-water layer, especially after surface mixing destroys the surface stratification.

The surf zone again acts as a source of suspended sediment for the mid-water layer. Longuet-Higgins (1953) has shown that a significant offshore transport of mass is necessary near mid-water depths for progressive waves. Fine sediments in suspension would be carried seaward in this offshore mass transport. This is graphically illustrated by the geometry of the mid-water layer with a thin, intense layer at the shallow nearshore stations.

Many minor levels of turbid water can be distinguished in the profiles. The discontinuous nature of these layers indicates that

transient conditions exist which are neither persistant in time nor in space.

One might logically raise the question how do we know that the surface turbid layer and the mid-water turbid layer do not result from the primary productivity of phytoplankton. Although no samples were taken to determine the composition of these layers, their terrigeneous origin may be inferred in several ways. In a study of the primary productivity near the edge of the continental shelf west of Newport, Curl and Small (1965) determined that the maximum productivity occurred at depths shallower than 20 meters, and that the euphotic zone extended to depths only as deep as about 50 meters. Thus, the phytoplankton inhabit water above the mid-water layer. Curl and Small also noted that the productivity depth increased in proportion to the amount of sunlight. However, the time-series stations of turbidity indicate no such migration, either in the surface layer or in the mid-water layer. Furthermore, the turbidity profiles observed during cruise Y 7104 C show a poorly defined surface layer at the same time that the BT data show no well-developed thermocline. Mixing of the thermocline would also mix the surface turbid layer; if phytoplankton were present, however, their vertical distribution should not be affected by the presence or absence of a thermocline. Finally, samples taken by Wildharber (1966) in the surface turbid layer off southern California indicate that organic matter provides

only a small contribution to the total amount of suspended material in the surface layer.

The Bottom Layer

The bottom layer is the most widely known and studied (Wildharber, 1966; McManus and Smyth, 1970). Unlike the other turbid layers which were discussed above, the bottom layer is always adjacent to a source of sediment. In addition, sediment is supplied to the bottom layer from nearshore sources and from diffusion through the layers above.

The contribution to the bottom layer of suspended sediment from the nearshore region and from the water column is impossible to judge from the profiles of turbidity. Over the short duration of the measurements these inputs are assumed to remain constant; this assumption should be valid because the environmental conditions under which the observations were made were nearly constant. Any increase in the bottom-layer thickness or intensity is therefore attributed to erosion of the bottom or to mixing of the layer in a vertical direction, while a decrease in thickness or intensity is attributed to deposition, or at least to settling.

At the time-series stations, the sediment characteristics are constant. Any change in bottom-layer thickness or intensity must be due to changes in the bottom current strength. The initial time-series

observation of bottom turbidity was made at 165-meters depth, 41 kilometers west of Newport. The sediment in the vicinity of this station is fine sand with a median diameter of about 3ϕ. About ten percent each silt and clay are also present. The effect of the current is as expected in all but the 1610 profile (Figure 32). Increasing current resulted in a thicker, more intense profile at 1240 and 1410, although because of the relatively coarse sediment the layer is rather thin (about five meters). The current dropped sharply from 23 cm/sec to 13 cm/sec just before the 1610 observation but was 15 cm/sec just afterward. The lack of a bottom layer in this profile is puzzling. Even if the current had stopped altogether, particles with a diameter of 3ϕ sinking at a rate of one cm/sec would require about 8 1/2 minutes to settle to the bottom. It is probable that the suspended sediment is much smaller than 3ϕ and also that some turbulence existed, so 8 1/2 minutes represents a minimum amount of time required for settling. In view of the short time between the end of the current observation and the turbidity measurement, it is considered that the lack of a bottom layer is not due to all the sediment having been deposited.

Rather, it is more likely that the ship had drifted slightly and the measurement was not made over the same type of bottom as those made earlier. Later profiles again reveal a predictable response to the current strength. As the currents decrease, the coarser material

suspended near the bed settles out quickly, with the result that the layer becomes less intense near the bottom, while the total thickness of the layer decreases at a much slower rate. This sequence of changes can be detected in the 1810 and 2015 profiles.

A second time-series station was made in 90 meters depth about 30 kilometers west of Newport. The bottom at this location is rock, so changes in the bottom layer must be attributable to changes in supply from outside sources.

The time-series sequence during cruise Y 7105 A was made over an area of extremely fine (M_d smaller than 6ϕ) sediments, 43 kilometers west of Tillamook Head in 130 meters of water. Although no current meter was placed at this location, current meters at 165 meters and 90 meters bracketed the site. The correlation of the bottom layer thickness (Figure 39) with the current strength measured at 90 meters (Figure 25b) is excellent. Correlation with the current at the deeper station (Figure 28b) is fair.

The surface sediment at this station is dominantly silt and clay with a median diameter of 6.3ϕ. It has been shown by Postma (1967) and others that the velocity necessary to erode sediment in this size range (about 25 cm/sec for freshly deposited sediment) is somewhat larger than the velocities measured concurrently at 90 meters assuming a smooth bottom. If we accept Postma's values erosion must be rules out and the thinning and thickening of the bottom layer

in response to the current strength must be due to near-bottom turbulence. The sediment suspended in the bottom layer is mixed upward, with the result that it now must settle a greater distance before deposition can take place. The turbulent mixing has the effect of increasing the horizontal distance a particle will travel before ultimately coming to rest. On the other hand, if no new sediment is being added to the bottom layer at this location, the layer will become more diffuse because of the mixing, with a resulting decrease in density. If the layer is moving downslope as a low-density flow (Moore, 1970) the rate of movement will be decreased as a result of the decreased effect of gravity, unless the current is acting in a downslope direction also.

Observations made during this study neither confirm nor disprove the existence of such low-density flows. However, this study and the work of Neudeck (1971) do reveal a turbid bottom layer which seems to be present on all parts of the continental shelf. Bottom photographs taken by Neudeck show that the turbid water seems to flow around high areas, indicating the role of gravity in the distribution of the bottom layer. It is likely that during the winter season the bottom layer becomes more dense due to the addition of material from runoff of coastal streams, increased erosion in the surf zone, and stirring of bottom sediments by surface wave effects. Bottom currents measured in this study are capable of maintaining at least

the silt and clay sized sediments in suspension. These suspended sediments settle during periods of quiescence. If such a quiescent period were of several hours duration, the suspension may become dense enough for a low-density flow to be initiated.

Sediment Erosion and Transport

Recent studies by Sternberg (1971) of incipient motion of bottom sediment in a marine environment show that general sediment motion occurs at velocities very close to those predicted by existing theory. The finest sediments observed by Sternberg, however, were medium sands. Sediment this large is not generally present on the northern Oregon continental shelf seaward of the surf zone. Therefore, the value of the reference curves for transport of finer particles in the marine environment is not certain. Using the curves for erosion and transport of sediment from Postma (1967), the velocity at 15 centimeters above a smooth bed which would be required to erode the nearshore sands (M_d = 2ϕ to 3ϕ) is about 30 cm/sec. Assuming a value of 1.1×10^{-2} cm^2/sec for kinematic viscosity, z = 15 cm, and U_z = 30 cm/sec, solving equation (6), $U_* = 1.58$ cm/sec. Using this value and solving equation (6) for U at z = 1.3 meters (the sensor height above the bottom) the current which would have to be measured for erosion of sand to occur in the nearshore zone is 45.5 cm/sec. This is higher than the speeds which were observed in 36 meters of water

west of Depoe Bay (Cruise C 7103F). On the other hand, if we assume a rough bottom with z_o = 3.3 cm, as in the current profile calculations, and apply equation (5) using the mean current of 30 cm/sec measured at 1.3 meters above the bottom during cruise C 7103F, we obtain a shear velocity U_* = 7.5 cm/sec. This shear velocity is easily sufficient for erosion of the nearshore sand facies to occur (Machel and Sternberg, 1971).

Bagnold (1963) points out that sands of open beaches seldom contain sizes smaller than about 3ϕ. If surface waves generate bottom currents of 25 cm/sec at 15 centimeters above the bottom and the bottom slope is three degrees, sediment smaller than 3ϕ should become uniformly distributed in the surf zone and diffuse outward to deeper water (Bagnold, 1963). The previously noted seaward mass transport in mid-water (Longuet-Higgins, 1953) provides a mechanism for this diffusion. Vernon (1966) observed fine sand being placed into suspension at 30 centimeters above the bottom in the nearshore zone, but noted that coarser material moved as bed load. Most of the transport observed by Vernon was shoreward although under certain conditions he observed some transport seaward from the surf zone.

Seaward of the 90 meter depth, if erosion of bottom sediment occurs, it must be accomplished by currents with a mean speed close to 10 cm/sec. It has been previously noted that strong currents of short duration may be a significant mode of transport if the direction

of flow is constant. This may occur in two ways. First, the individual "bursts" of current may be strong enough to erode unconsolidated material for further transport in suspension. Once the material is in suspension, the current strength required to maintain the suspension is much lower. For clay-sized particles ten cm/sec is sufficient to prevent deposition (Postma 1967). The importance of infrequent stirring of sediment by storm-generated surface waves can be seen. Neudeck (1971) notes an apparent seasonal increase of bottom turbidity which he ascribes to seasonal changes in wave conditions.

A less important mode of transport from short-duration currents must be in the form of ripple transport. Neudeck (1971) has observed rippling of bottom sediment as deep as 200 meters though the strongest rippling was found on the inner shelf. Measurements by Kachel and Sternberg (1971) indicate that ripple migration rates are low; ripples in medium sand migrated at rates from nine centimeters per hour to 80 centimeters per hour in a steady current. The current, measured one meter above the bed, ranged from 37 cm/sec to 59 cm/sec. Most of the ripples which Neudeck (1971) observed were symmetrical, indicating formation by oscillatory currents. Such ripples are probably important to the net transport of sediment only as a source of hydrodynamic bottom roughness. As has been previously shown in this study, a rough bottom contributes greatly to the ability of a given current to erode bottom sediments.

The velocity required to erode materials finer than about 3ϕ is also greatly dependent on the water content of the deposit. Postma (1967) shows that recently deposited sediment is most easily eroded. Depositied material tends to lose water with the passage of time, becoming more consolidated and increasingly difficult to erode. Postma found that clay which could be eroded by currents with velocities of 18 cm/sec three hours after deposition required velocities of 90 cm/sec for erosion one month after deposition. Bottom photos taken by the author and by Neudeck (1971) on the Oregon continental shelf reveal the general presence of an unconsolidated blanket of fine material which is probably suspended by currents in excess of about 20 cm/sec. Nevertheless, currents of strength sufficient to erode beyond this surficial layer of unconsolidated material have not been observed on the Oregon shelf. One must conclude that the fine consolidated sediments on the outer shelf are not being actively eroded. This does not preclude reworking of sediments where coarser materials are present, or where the bed has small-scale relief.

Flocculation of clay particles may play an important part in the deposition and erosion of fine sediments. Flocculation of clay particles results when particles collide and adhere to one another. Collisions result from Brownian motion, current shear, and differential rates of settling. The probability of flocculation depends largely on the concentration of particles, and the rate of flocculation decreases

as particles are removed by forming flocs. Therefore, the further away from the source of fine sediment, the less important should be the flocculation process. Concentration of particles in continental shelf waters is normally about one mg/l (Lyall et al., 1970) but near a sediment source such as the Columbia River may be as high as 40 mg/l (McManus and Smyth, 1970). The greater concentration near shore should result in greater amounts of sediment being flocculated and deposited. However, the nearshore environment is one of much higher energy than the outer shelf region. This higher energy may prevent floccules from settling to the bottom. Because of the great amount of water contained in floccules, their density is quite low. As a result, the settling velocity of a clay floccule is much lower than a primary particle of the same size. Einstein and Krone (1962) state that a 5.2μ floccule and a 2μ primary particle have equal settling velocities. Kuenen (1965) states that a current of 0.2 cm/sec generates enough turbulence to retard settling. Costin (1970) points out that settling velocities of fine sediments in still waters can be as much as four orders of magnitude less than the vertical component of turbulence. Thus, it is likely that the greater turbulence in nearshore waters would prevent the floccules from depositing, and might even tear them apart.

As the floccules reach the lower energy environment of the outer shelf, some may settle to the bottom and be depositied.

Partheniades et al. (1969) show that as floccules settle through the laminar sublayer, they are subjected to strong shear forces which tear many of them apart before deposition can take place. Turbulence then injects this deflocculated clay back into the water above the bottom. Thus, even though a particle finally sinks to the bottom, there is no assurance that deposition does take place. Furthermore, when a floccule does contact the bottom, it adheres to the sediment. If erosion of this floccule takes place at a later time, it may take other adhering particles with it (Einstein and Drone, 1962).

Even though the floccules are relatively large, their density is low, about 1.2 g/cc (Einstein and Drone, 1962). The fact that floccules remain suspended in the water column over long distances has been shown by Pak (1969). Undoubtedly many of these same floccules are found in the mid-water turbid layer, although the current shear near the bottom may disintegrate floccules at that level.

Finally, the activity of benthic organisms has been an important agent for reworking older sediments. Box cores taken by Roush (1970) showed an increasing amount of reworking by benthic organisms with increasing distance from the shore. The actions of burrowing organisms undoubtedly place sediment in suspension. Animals which feed at the sediment-water interface are also responsible for stirring sediments; anyone who has observed a flatfish settling itself on the bottom has witnessed a powerful sediment reworking mechanism.

Smaller animals are important when present in large enough numbers. Bottom photos taken during cruise Y 7104 C show a large pink shrimp population on unconsolidated fine sediments. These animals are probably capable of placing a considerable amount of sediment into suspension by their movements.

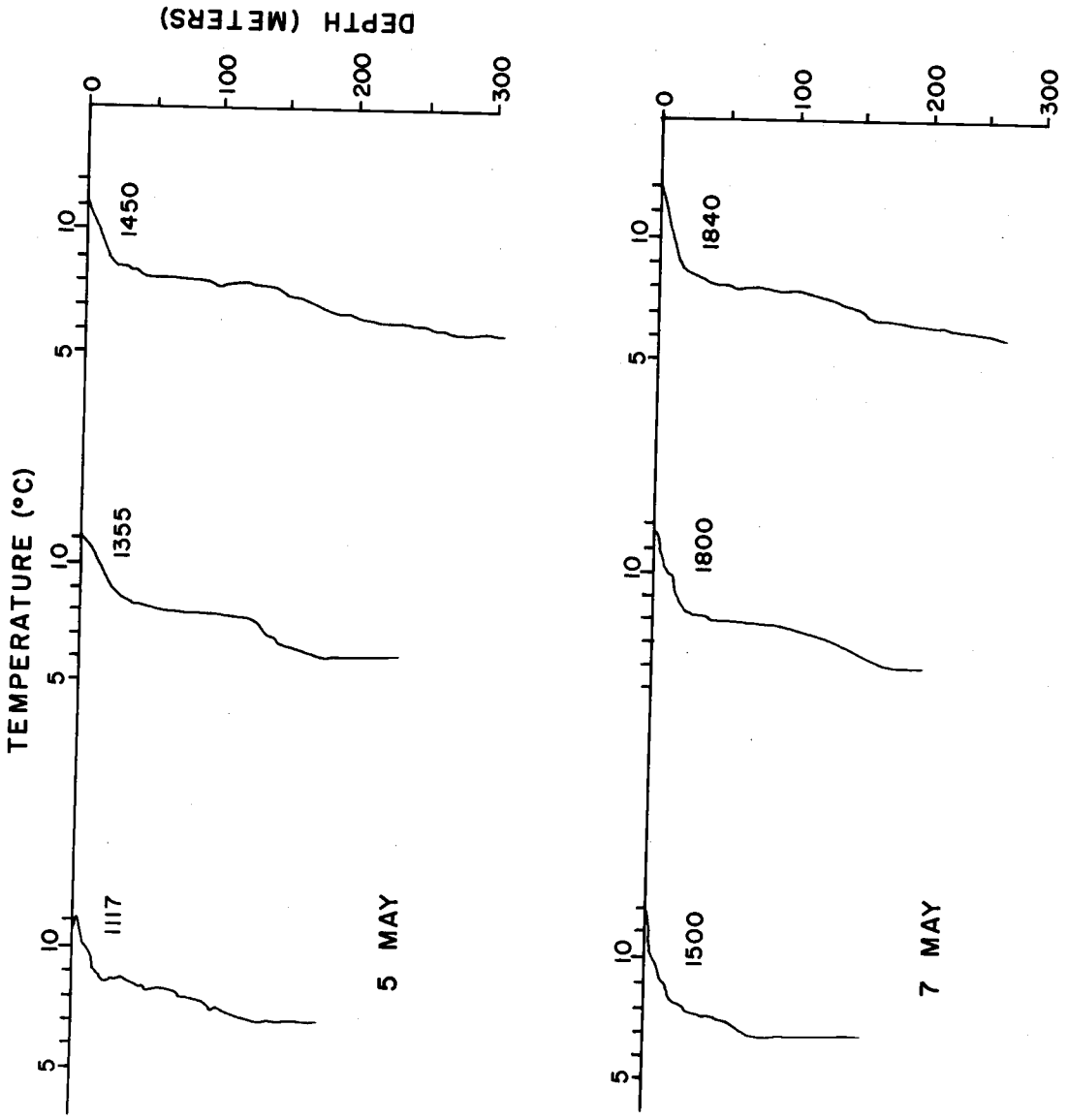

Figure 41. Cruise Y 7105 A. Temperature-depth profiles observed concurrently with indicated turbidity profiles of Figures 40 and 41.

CONCLUSIONS

Modern sediment transport on the northern Oregon continental shelf is a combination of many processes, as shown in Figure 42. The bottom currents are generated in response to internal tides. On the inner shelf, current with a mean speed of 30 cm/sec are sufficiently strong to erode and transport the nearshore sands. At mid-shelf depths, currents are much slower, with a mean speed of about 10 cm/sec. The semi-diurnal component of the tide is reflected in the 12-hour period the current speed and direction. Flow is onshore during upwelling, but otherwise is to the south and west. On the outer shelf, the mean speed is slightly higher than at mid-shelf, but is still near 10 cm/sec. The dominant period of current oscillations at this depth is about six hours, corresponding to the second harmonic of the semi-diurnal tide. Flow is offshore and to the south.

No evidence of high frequency (two to six cph) internal waves was noted in the current records, nor was there any indication of surface wave influence at depths greater than 90 meters. Surface wave influence was strong at 36 meters depth, however.

Suspended sediments move seaward from the shore along three major surfaces, the seasonal thermocline, the permanent pycnocline, and the bottom. Sediments in the upper layer consist of fine materials diffusing seaward at the surface from the surf zone and fine materials contributed by the Columbia River plume. The Columbia River is the

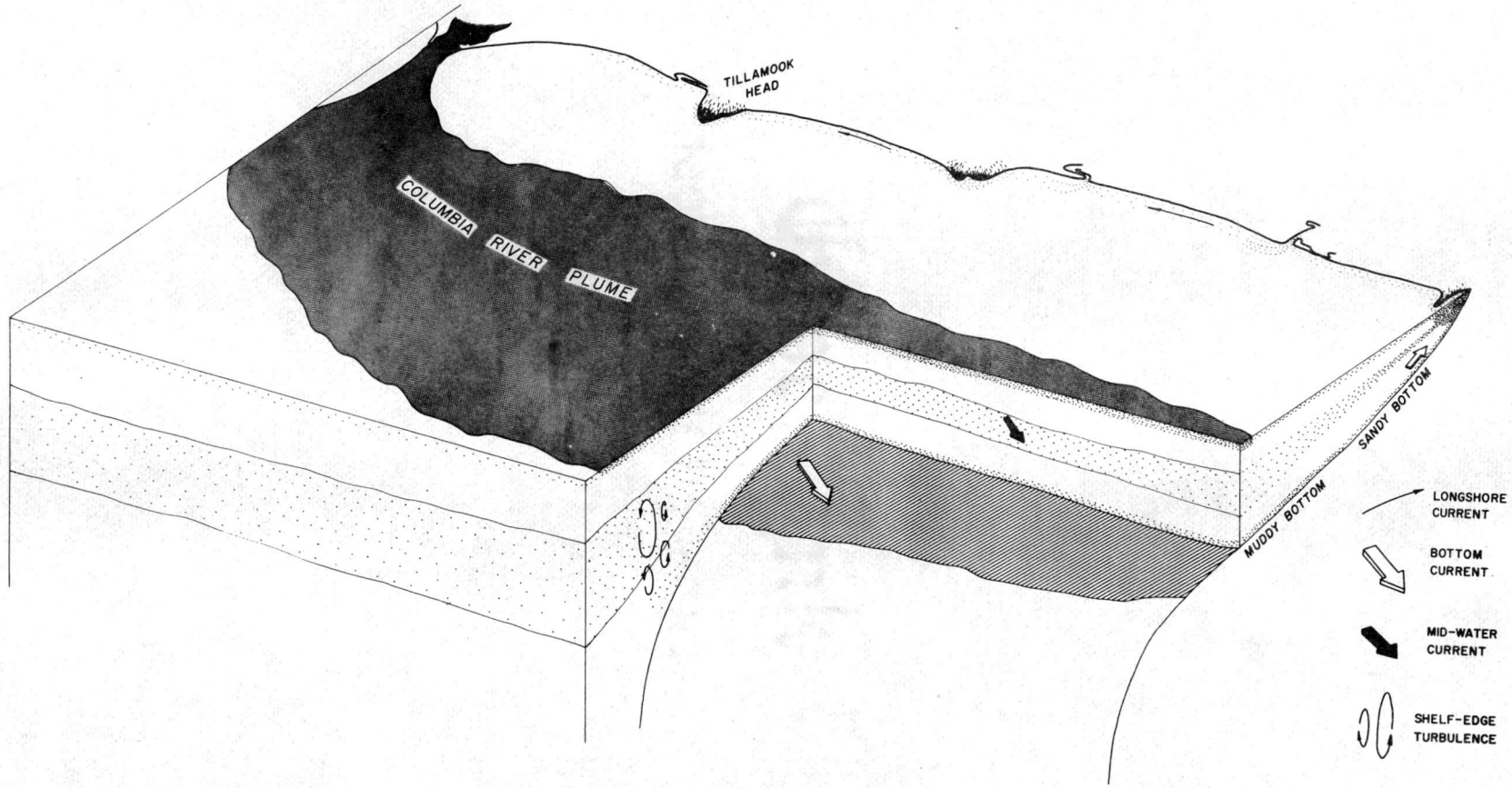

Figure 42. Model for sediment transport on the northern Oregon continental shelf.

dominant source of fine sediments on the northern shelf. Its plume distributes particles horizontally in the surface layer to the south. These particles gradually sink or are mixed into the waters below and ultimately are deposited on the outer continental shelf and lower slope. The large area of fine sediments on the outer shelf south of the Columbia River attests to the importance of the surface layer in transporting fine sediment. This area of fines does not extend beyond the shelf edge, while its eastern boundary runs nearly north-south, parallel to the coastline. The trends of the boundaries are indicative of current patterns which are confining the fine sediment to its present location.

The greatest contribution to the mid-water layer is from diffusion of fine materials from the nearshore zone. Sediments derived from coastal streams, from erosion of coastal landforms, and from onshore transport by waves are transported by the longshore current. As the coarse sediments are transported, abrasion occurs, and the resulting fine particles diffuse seaward from the surf zone. When wave activity becomes more intense, the amount and the grain size of sediment being transported will increase. The mid-water layer at the permanent pycnocline is sub-parallel to the bottom over the continental shelf, but at the shelf edge it continues seaward in the upper part of the water column, with the result that the shelf edge and upper slope are bypassed by the suspended sediment. This at least partially

accounts for the relatively low sedimentation rate on the upper slope. Spigai (1970) determined that the sedimentation rate on the upper slope of southern Oregon was one fifth that on the lower slope. This indicates that away from the stratified water of the continental shelf, the mid water layer sinks or is mixed, and the sediment transported in it is deposited on the upper slope and on the continental rise.

Material in the bottom layer is derived from erosion of the bottom by bottom currents, from sinking from the water column above, and from diffusion from the near shore zone. The fine material in the bottom layer is periodically winnowed by bottom currents generated in response to large surface waves. This material is transported into the surf zone where it is mixed vertically. Some of this material diffuses seaward in the surface layer and in the mid-water layer. These layers do not contribute to the sedimentation on the inner shelf. Since bottom transport caused by surface waves is depth dependent, this winnowing results in the well sorted nearshore sand facies.

Seaward of the depth of frequent surface wave influence, the bottom layer thins and thickens in response to decreasing and increasing bottom current strength. Over a hydrodynamically rough bottom, the thickening may be due to erosion of the bottom. Thickening of the bottom layer over a smooth bottom is due to vertical mixing of the sediment as a result of increased turbulence. Transport of sediments takes place over a circuitous path toward the southwest. At the shelf

edge, the bottom layer becomes somewhat diffuse. The bottom layer flows around topographic highs, depositing sediments in the low areas and in the lee of banks. Concentration of the bottom layer during quiescent periods may allow low-density flows to iniate.

It is tempting to try to establish the relative amount of material being transported seaward at each of the three levels. If the same particle size distribution existed in each of the layers, this might be done. However, this assumption is difficult to justify in view of the different settling rates of different sized particles. Therefore, one should not conclude that if the surface layer transmissibility is lower than the transmissibility at the bottom, the concentration of particulate matter is greater in the surface layer.

This model of continental shelf sedimentation should be accurate for any open shelf. The processes affecting sedimentation are in no way unique to this area. The most important feature of the model is probably the means by which sediment bypasses the shelf and upper slope. This method of transport should exist in any shelf region where the water is well stratified.

BIBLIOGRAPHY

Bagnold, R. A. 1963. Beach and nearshore processes. Mechanics of marine sedimentation. In: The Sea, ed. by M. N. Hill. Vol. III. New York, Interscience. p. 507-528.

Burt, W. V. and B. Wyatt. 1964. Drift bottle observations of the Davidson Current off Oregon. In: Studies on oceanography, a collection of papers dedicated to Kaji Hidaka. Seattle, University of Washington Press. p. 156-165.

Byrne, J. V. 1963. Coastal erosion, northern Oregon. In: Essays in marine geology in honor of K. O. Emery. Los Angeles, University of Southern California Press. p. 11-33.

Cacchione, D. A. and J. B. Southard. 1970. Laboratory studies of shoaling internal gravity waves. (Abstract). Transactions, American Geophysical Union. 51:313.

Chambers, D. M. 1968. Holocene sedimentation and potential placer deposits on the continental shelf off the Rogue River, Oregon. Master's thesis. Corvallis, Oregon State University. 102 numb. leaves.

Chow, Ven Te. 1964. Handbook of applied hydrology. New York, McGraw-Hill.

Collins, C. A. 1967. Description of measurements of current velocity and temperature over the Oregon continental shelf, July 1965 - February 1966. Ph.D. thesis. Corvallis, Oregon State University. 154 numb. leaves.

Costin, J. M. 1970. Visual observations of suspended-particle distribution at three sites in the Caribbean Sea. Journal of Geophysical Research. 75:4144-4150.

Curl, H. Jr. and L. F. Small. 1965. Variations in photosynthetic assimilation ratios in natural, marine phytoplankton communication. Limnology and Oceanography. Alfred C. Redfield Anniversary Volume (Supplement in Volume 10) November R67-R73.

Curray, J. R. 1960. Sediments and history of Holocene transgression, continental shelf, northwest Gulf of Mexico. In: Recent sediments, northwest Gulf of Mexico. ed. by F. P. Shepard, F. B. Phleger, and Tj. H. van Andel. Tulsa, American Association of Petroleum Geologists. p. 221-266.

Curray, J. R. 1964. Transgressions and regressions. In: Papers in marine geology, Shepard commemorative volume. ed. by R. L. Miller. New York, Macmillan Company. p. 175-201.

Draper, L. 1967. Wave activity at the sea bed around northwestern Europe. Marine Geology. 5:133-140.

Duxbury, A. C. 1965. The union of the Columbia River and the Pacific Ocean - general features. Ocean Science and Ocean Engineering. Transactions of the Joint Conference, Marine Technology Society and American Society of Limnology and Oceanography. Washington, D. C. June 1965. p. 914-922.

Einstein, H. A. 1950. The bedload function for sediment transportation in open channel flows. U. S. Department of Agriculture, Technical Bulletin 1026. 70 p.

Einstein, H. A. and R. B. Krone. 1962. Experiments to determine modes of cohesive sediment transport in salt water. Journal of Geophysical Research. 67:1451-1461.

Emery, K. O. 1952. Continental shelf sediments off southern California. Geological Society of America, Bulletin 53:1105-1108.

Ewing, M. and E. Thorndyke. 1965. Suspended matter in deep ocean water. Science. 147:1291-1294.

Gaul, R. D., J. M. Snodgrass and D. J. Cretzler. 1963. Some dynamical properties of the Savonious rotor current meter. In: Marine sciences instrumentation. Vol. 2. Proceedings of the Symposium on Transducers for Oceanic Research, San Diego, California, 1962. New York, Plenum. p. 35-47.

Heezen, B. C., C. D. Hollister, and W. F. Ruddiman. 1966. Shaping of the continental rise by deep geostrophic contour currents. Science. 152:502-508.

Hickson, R. E. 1960. Open river channel improvements. Unpublished report, U. S. Army Corps of Engineers, Portland, Oregon.

Inman, D. L. 1963. Sediments: physical properties and mechanics of sedimentation. In: Submarine Geology, ed. by F. P. Shepard. New York, Harper and Row. p. 101-151.

Kachel, N. B. and R. W. Sternberg. 1971. Transport of bedload as ripples during an ebb current. Marine Geology. 10:229-244.

Korgen, B. J. 1969. Temperature and velocity fields near the deep ocean floor west of Oregon. Ph.D. thesis. Corvallis, Oregon State University. 155 numb. leaves.

Kuenen, Ph. H. 1965. Experiments in connection with turbidity currents and clay-suspension. Proceedings of the Symposium of the Colston Research Society. 17:47-74.

Lyall, A. K., D. J. Stanley, H. N. Giles, and A. Fischer, Jr. 1971. Suspended sediment and transport at the shelf-break and on the slope, Wilmington Canyon area, Eastern U.S.A. Marine Technology Society Journal. 5:15-27. Jan.-Feb, 1971.

Longuet-Higgins, M. S. 1953. Mass transport in water waves. Philosophical Transactions of the Royal Society, London. Series A. 245:535-581.

Maloney, N. J. 1965. Geology of the continental terrace off the central coast of Oregon. Ph.D. thesis. Corvallis, Oregon State University. 233 numb. leaves.

Maughan, P. M. 1963. Observations and analysis of ocean currents above 250 meters off the Oregon coast. Master's thesis. Corvallis, Oregon State University. 49 numb. leaves.

McCave, I. N. 1970. Deposition of fine-grained suspended sediment from tidal currents. Journal of Geophysical Research. 75: 4151-4159.

McManus, D. A. and C. S. Smyth. 1970. Turbid bottom water on the continental shelf of the northern Bering Sea. Journal of Sedimentary Petrology. 40:869-873.

Moore, D. G. 1970. Reflection profiling studies of the California continental borderland structure and Quaternary turbidite basins. Geological Society of America, Special Paper 107, 142 p.

Mooers, C. N. K. and R. L. Smith. 1968. Continental shelf waves off Oregon. Journal of Geophysical Research. 73:549-557.

Mooers, C. N. K. 1970. The interaction of an internal tide with the frontal zone in a coastal upwelling region. Ph. D. thesis. Corvallis, Oregon State University. 480 numb. leaves.

Morse, B. A. and N. McGary. 1963. Graphic representative of the salinity distribution near the Columbia River south. Ocean Science and Ocean Engineering. Transactions of the Joint Conference, Marine Technology Society and American Society of Limnology and Oceanography. Washington, D. C. June 1965. p. 923-942.

National Marine Consultants, 1961. Wave statistics for three deep-water stations along the Oregon-Washington coast. U. S. Army, Corps of Engineers, District Seattle, Washington, Portland, Oregon, bulletin. 17 pp.

Neudeck, R. H. 1971. Photographic investigation of sediment transport mechanics on the Oregon continental margin. Master's thesis. Corvallis, Oregon State University. (In preparation).

Pak, H. 1969. The Columbia River as a source of marine light scattering particles. Ph. D. thesis. Corvallis, Oregon State University. 110 numb leaves.

Pak, H., G. F. Beardsley, Jr., and R. L. Smith. 1970. An optical and hydrographic study of a temperature inversion off Oregon during upwelling. Journal of Geophysical Research. 75:629-638.

Partheniades, E., R. H. Cross, III, and A. Ayora. 1969. Further results on the deposition of cohesive sediments. In: Proceedings of Eleventh Conference on Coastal Engineering, London. p. 723-742.

Phillips, O. M. 1966. The dynamics of the upper ocean. London, Cambridge University Press. 261 p.

Pillsbury, R. D., R. L. Smith and J. G. Pattulo. 1970. A compilation of observations from moored current meters. Vol. III: Oregon continental shelf, May-June 1967, April-September 1968. 102 numb. leaves. (Oregon State University, Department of Oceanography. Data report 40 on National Science Foundation grants GA 1435, GA 295 and Office of Naval Research contracts 1286(10) and N00014-67-A-0369-0007, Project 083-102).

Postma, H. 1967. Sediment transport and sedimentation in the estuarine environment. In: Estuaries. ed. by G. H. Lauff, American Association for the Advancement of Science. Washington, D. C. p. 158-179.

Pyrkin, Yu. G. 1966. Measurement of the velocity distribution of bottom currents in the Atlantic Ocean. Isvestya, Atmospheric and Oceanic Physics 2:1316-1317.

Robinson, A. 1970. Research Assistant. Oregon State University, Department of Oceanography. Personal communication. Corvallis, Oregon.

Roush, R. C. 1970. Sediment textures and internal structures: A comparison between central Oregon continental shelf sediments and adjacent coastal sediments. Master's thesis. Corvallis, Oregon State University. 75 numb. leaves.

Runge, E. J. 1966. Continental shelf sediments, Columbia River to Cape Blanco, Oregon. Ph.D. thesis. Corvallis, Oregon State University. 143 numb. leaves.

Smith, R. L., J. G. Pattulo, and R. K. Lane. 1966. An investigation of the early stage of upwelling along the Oregon coast. Journal of Geophysical Research. 71:1135-1140.

Smith, R. L. 1968. Upwelling. In: Oceanography and marine biology annual review. ed. by H. Barnes. New York, Hafner Publishing Company. p. 11-46.

Southard, J. B., D. A. Cacchione, and R. D. Flood. 1971. Experiments on bottom sediment movement by breaking internal waves. (Abstract). Transactions, American Geophysical Union. 52:258.

Spigai, J. J. 1970. Marine Geology of the continental margin off southern Oregon. Ph.D. thesis. Corvallis, Oregon State University. 214 numb. leaves.

Sternberg, R. W. 1971. Measurements of incipient motion of sediment particles in the marine environment. Marine Geology. 10:113-119.

Stevenson, M. R. 1966. Subsurface currents off the Oregon coast. Ph. D. thesis. Corvallis, Oregon State University. 140 numb. leaves.

Union Carbide Corporation. 1968. "Eveready" battery applications and engineering data. New York. Unitech Division of Associated Educational Services Corporation. 706 p.

Vernon, J. W. 1966. Shelf sediment transport system. Doctoral dissertation. Los Angeles, University of Southern California. 135 numb. leaves.

Wildharber, J. L. 1966. Suspended sediment over the continental shelf off southern California. Master's thesis. Los Angeles, University of Southern California. 159 numb. leaves.

Wolf, S. C. 1970. Coastal currents and mass transport of surface sediments over the shelf regions of Monterey Bay, California. Marine Geology. 8:321-336.

APPENDIX

APPENDIX I. Station locations and weather conditions

CRUISE	DATE	LATITUDE	LONGITUDE	DEPTH	WIND	SWELL
Y 7002 C	2/24/70	45° 03.3'N	124° 38.6'W	354 m.	070 12 kts	1-2m 8 sec
C 7004 C	4/28/70	45° 48.5'N	124° 14.5'W	124 m.	-	-
C 7006 B	6/13/70	44° 39.8'N	124° 33.3'W	175 m.	-	-
		44° 39.9'N	124° 26.6'W	100 m.	-	-
C 7008 D	8/16/70	44° 40.9'N	124° 33.6'W	176 m.	000 13 kts	1-2m -
C 7012 D	12/16/70	44° 49.0'N	124° 12.5'W	90 m.	-	-
C 7102 A	2/1/71	44° 39.1'N	124° 06.6'W	36 m.	315 7 kts	1 m.
		44° 38.8'N	124° 15.0'W	76 m.	315 15 kts	1 m.
Y 7102 A	2/8/71	45° 11.2'N	124° 19.4'W	274 m.	200 8 kts	1 m. 8 sec
		45° 10.9'N	124° 17.3'W	186 m.	180 16 kts	2 m. 10 sec
	2/9/71	45° 11.0'N	124° 14.7'W	165 m.	175 18 kts	2 m. 10 sec
		45° 11.0'N	124° 12.2'W	146 m.	180 18 kts	2 m. 10 sec
		45° 11.0'N	124° 10.7'W	128 m.	180 18 kts	2 m. 10 sec
		45° 10.7'N	124° 09.0'W	110 m.	180 18 kts	2 m. 8 sec
		45° 10.9'N	124° 07.3'W	91 m.	180 24 kts	2 m. 8 sec
		45° 11.0'N	124° 04.9'W	74 m.	180 20 kts	1-2m 5 sec
		45° 11.0'N	124° 03.0'W	55 m.	180 22 kts	1-2m 6 sec

APPENDIX I (Continued)

CRUISE	DATE	LATITUDE	LONGITUDE	DEPTH	WIND	SWELL
Y 7102 A	2/9/71	45° 11.0'N	124° 00.1'W	37 m.	180 20 kts	1-2m. 6 sec
	2/11/71	44° 39.3'N	124° 33.4'W	165 m.	080 10 kts	2-3m. 11 sec
		44° 39.2'N	124° 32.9'W	146 m.	100 14 kts	2m. 11 sec
		44° 39.1'N	124° 30.9'W	125 m.	100 12 kts	2m. 11 sec
		44° 38.8'N	124° 28.7'W	110 m.	100 10 kts	2m. 11 sec
		44° 38.6'N	124° 26.5'W	91 m.	100 14 kts	2m. 11 sec
	2/12/71	44° 39.5'N	124° 15.7'W	73 m.	210 6 kts	2m. 10 sec
		44° 39.4'N	124° 10.3'W	55 m.	145 6 kts	2m. 10 sec
C 7103 F	3/24/71	45° 11.0'N	124° 14.0'W	36 m.	-	2-4m 10 sec
Y 7104 C	4/27/71	44° 46.3'N	124° 14.1'W	90 m.	250 8 kts	1m. 8 sec
		44° 46.1'N	124° 31.2'W	165 m.	270 12 kts	1-2m 8 sec
		44° 49.7'N	124° 26.8'W	160 m.	300 10 kts	1-2m 8 sec
		44° 49.0'N	124° 25.4'W	165 m.	315 4 kts	1-2m 8 sec
	4/28/71	44° 44.2'N	124° 27.0'W	125 m.	310 8 kts	1m. 8 sec
Y 7105 A	5/5/71	45° 59 2'N	124° 11.3'W	92 m.	285 10 kts	1m. 7 sec
		45° 59.4'N	124° 36.2'W	165 m.	300 14 kts	1m. 7 sec
		45° 59.0'N	124° 00.5'W	28 m.	270 10 kts	1m. 7 sec
		45° 59.0'N	124° 02.9'W	55 m.	270 10 kts	1m. 7 sec

APPENDIX I (Continued)

CRUISE	DATE	LATITUDE	LONGITUDE	DEPTH	WIND	SWELL
Y 7105 A	5/5/71	45° 59.0'N	124° 04.8'W	70 m.	270 10 kts	1m. 7 sec
		45° 59.2'N	124° 11.5'W	88 m.	285 10 kts	1m. 7 sec
		45° 58.9'N	124° 14.7'W	112 m.	295 6 kts	1m. 7 sec
		45° 59.0'N	124° 19.1'W	132 m.	280 8 kts	1m. 7 sec
		45° 58.6'N	124° 25.3'W	146 m.	280 8 kts	1m. 7 sec
		45° 59.4'N	124° 49.6'W	165 m.	300 14 kts	1m. 7 sec
		45° 59.1'N	124° 38.4'W	182 m.	300 16 kts	1m. 7 sec
		45° 59.4'N	124° 43.5'W	280 m.	300 14 kts	1m. 7 sec
	5/7/71	45° 59.0'N	124° 20.0'W	130 m.	000 16 kts	1m. 7 sec
		45° 58.8'N	123° 59.5'W	19 m.	320 14 kts	1m. 6 sec
		45° 59.0'N	124° 02.5'W	40 m.	320 16 kts	1m. 6 sec
		45° 59.1'N	124° 03.6'W	60 m.	320 14 kts	1m. 6 sec
		45° 59.1'N	124° 05.5'W	76 m.	320 16 kts	1m. 6 sec.
		45° 58.5'N	124° 11.8'W	98 m.	320 18 kts	1m. 6 sec
		45° 58.7'N	124° 16.6'W	115 m.	320 16 kts	1m. 6 sec
		45° 58.6'N	124° 20.3'W	135 m.	320 21 kts	1m. 6 sec
		45° 59.5'N	124° 28.6'W	150 m.	320 20 kts	1m. 6 sec

APPENDIX I (Continued)

CRUISE	DATE	LATITUDE	LONGITUDE	DEPTH	WIND	SWELL
Y 7105 A	5/7/71	45° 59.3'N	124° 36.3'W	179 m.	320 18 kts	1m. 7 sec
		45° 59.2'N	124° 39.5'W	183 m.	330 18 kts	1m. 7 sec
		45° 59.3'N	124° 43.5'W	275 m.	330 22 kts	1m. 7 sec